YILDIRIM BEYAZIT UNIVERSITY

GRADUATE SCHOOL OF NATURAL AND APPLIED SCIENCES

THE MODELING AND SIMULATION OF INTERSATELLITE LASER COMMUNICATION SYSTEMS

M.Sc. THESIS by
Mustafa PANCAR

Department of Electronics and Communication Engineering

ANKARA, 2014

THE MODELING AND SIMULATION OF INTERSATELLITE LASER COMMUNICATION SYSTEMS

A Thesis Submitted to the

Graduate School of Natural and Applied Sciences of Yıldırım Beyazıt University

In Partial Fulfillment of the Requirements for the Degree of Master of Science in Electronics and Communication Engineering, Department of Electronics and Communication Engineering

by

Mustafa PANCAR

June, 2014

ANKARA

M.Sc. THESIS EXAMINATION RESULT FORM

We have read the thesis entitled "THE MODELING AND SIMULATION OF INTERSATELLITE LASER COMMUNICATION SYSTEMS" completed by MUSTAFA PANCAR under supervision of PROF.DR. ŞERAFETTIN EREL and we certify that in our opinion it is fully adequate, in scope and in quality, as a thesis for the degree of Master of Science.

.....

Prof.Dr. Şerafettin EREL

Supervisor

.....

Prof.Dr. Fatih V. ÇELEBİ

(Jury Member)

.....

Assoc.Prof.Dr. Haldun GÖKTAŞ

(Jury Member)

Prof.Dr. Fatih V. ÇELEBİ

Director

Graduate School of Natural and Applied Sciences

ACKNOWLEDGEMENTS

I wish to express my sincere gratitude to my thesis supervisor Prof.Dr. Şerafettin EREL, for his supervision, generous support, encouragement, and guidance through the M.Sc. process.

I would like to thank my thesis committee members, Prof.Dr. Fatih V. ÇELEBİ, and Assoc.Prof.Dr. Haldun GÖKTAŞ, for their helpful suggestion, insightful comments, and hard questions.

I would also like to thank former Chief of the TGS SATCOM Col. Seyit GÜVENÇ, current Chief of the TGS SATCOM Lt. Col. Cem Sinan BARIM and Recep ARSLAN for their encouragement and support.

I expand my thanks to Laleser FİLİZ for her encouragement and patience during the M.Sc. process.

Last but not least, I would like to thank to my late mother and my father for everything.

June, 2014 Mustafa PANCAR

CONTENTS

Page

ABBREVIATIONS

ASE	Amplified Spontaneous Emission
ASK	Amplitude Shift Keying
APD	Avalanche Photodiode
BPSK	Binary Phase Shift Keying
BER	Bit Error Rate
CW	Continuous Wave
EDFA	Erbium Doped Fiber Amplifier
FSO	Free Space Optical
GEO	Geosynchronous Orbit
IOL	Inter Orbital Link
ISL	Inter Satellite Link
LEO	Low Earth Orbit
LPF	Low Pass Filter
MEO	Medium Earth Orbit
NRZ	Non Return to Zero
OOK	On-Off Keying
OWC	Optical Wireless Channel
PSK	Phase Shift Keying
PIN	Positive Intrinsic Negative Photodiode
PRBS	Pseudo Random Bit Sequence
RF	Radio Frequency
RZ	Return to Zero
SNR	Signal to Noise Ratio

LIST OF TABLES

LIST OF FIGURES

LIST OF SYMBOLS

A	Attenuation
α	Insertion loss
$B_N(s)$	Nth-order Bessel polynomial
B_r	Bit rate
β	Spontaneous emission factor
c_f	Fall time coefficient
c_r	Rise time coefficient
Γ	Mode confinement factor
D_R	Receiver telescope diameter
D_T	Transmitter telescope diameter
$\Delta\theta$	Phase difference
$\Delta\emptyset$	Signal phase change
$extrat$	Extinction ratio
ε	Gain compression factor
η_{int}	Internal quantum efficiency
n_l	Number of leading zeros
η_R	Optics efficiency of the receiver
n_t	Trailing zeros
η_T	Optics efficiency of the transmitter
f_c	Filter cutoff frequency
G_T	Geometrical gain
G_R	Receiver telescope gain
h	Planck's constant
$H(s)$	Transfer function for Bessel filter
θ_R	Receiver azimuth pointing error angle
θ_T	Transmitter azimuth pointing error angle (divergence angle)
$i(t)$	Electrical current
i_d	Additive dark current
i_{dm}	Dark current
$i_s(t)$	Optical signal
$i_{sh}(t)$	Shot noise current

$i_{th}(t)$	Thermal noise current
k	Ionization ratio
λ	Wavelength
L_R	Receiver pointing loss factor
L_P	Pointing loss factor
L_T	Transmitter pointing loss factor
M	Gain
$Modulation(t)$	Electrical input signal
N	Parameter order
N_G	Number of bits generated
$\mathrm{N_t}$	Carrier density at transparency
P_R	Received optical power
P_T	Transmitter optical power
σ_g	Differential gain coefficient
r	Responsivity
SF	Symmetry factor
T	Bit period
T_T	Transmission factors for the transmitter
T_R	Transmission factors for the receiver
T_w	Time window
τ_p	Photon lifetime
τ_n	Carrier lifetime
V	Active layer volume
v_g	Group velocity
ν	Optical frequency
w_b	3 dB bandwidth
Z	Distance between the transmitter and the receiver (Range)

THE MODELING AND SIMULATION OF INTERSATELLITE LASER COMMUNICATION SYSTEMS

ABSTRACT

Free Space Optical (FSO) Communication Systems are alternatives to Radio Frequency (RF) communication systems due to the high data rate, high bandwidth capacity, smaller size, and weight, less power consumption, high security, resistance to interference etc. There are many manufactured satellites orbiting around the earth and RF technique, which is a conventional communication method for satellite systems, is used in order for them to communicate with each other. It is possible to send several Gbps data to thousands kilometers distances with laser communication. This is done by means of adopting optical wireless communication technology into space technology; hence, intersatellite optical wireless communication is developed. In this thesis, detailed literature survey about free space optical communication system has been done. The importance of laser systems for free-space communication has been discussed and the status of laser techniques for intersatellite communication has been examined. The functions of the each basic component such as laser source, photodetector, modulation type, telescope used in a typical system have been examined. The intersatellite link has been modeled and simulated by means of Optiwave Software for the various link configurations and the system performance (BER/Q-Factor) has also been analyzed in terms of each basic parameter such as transmitted power, wavelength, data rate, range and telescope diameter in order to achieve minimum BER. APD type and PIN type photodetector comparison has been performed. Moreover, Erbium Doped Fiber Amplifier (EDFA) has been used for the intersatellite link to recognize its effect on the link quality. It has been shown that communication performance of the system can be improved by choosing the most appropriate component in terms of communication requirements.

Key Words: Intersatellite Laser Communication, Free Space Optical Communication, Optical Wireless Channel, Bit Error Rate, Q Factor.

UYDULARARASI LAZER HABERLEŞME SİSTEMLERİNİN MODELLENMESİ VE SİMÜLASYONU

ÖZET

Serbest Ortam Optiksel Haberleşme Sistemleri; yüksek veri hızı, geniş bant genişliği kapasitesi, küçük boyut ve hafiflik, düşük güç tüketimi, yüksek güvenlik ve girişime karşı dirençli olma gibi özelliklerinden dolayı radyo frekanslı haberleşme sistemlerine alternatif sistemlerdir. Dünya yörüngesinde, çok sayıda insan yapımı uydu bulunmakta ve bu uyduların birbirleriyle haberleşmelerinde geleneksel radyo frekanslı haberleşme teknikleri kullanılmaktadır. Lazer haberleşmesi ile veri birkaç Gb/s hızında binlerce kilometre uzaklığa gönderilebilmektedir. Bu yetenek, optiksel kablosuz haberleşme teknolojisinin uzay teknolojisine adapte olmasını sağlamış ve böylece uydulararası optiksel kablosuz haberleşme sistemleri gelişmiştir. Bu tez çalışmasında, serbest ortam optiksel haberleşme sistemleri ile ilgili detaylı literatür taraması yapılmıştır. Lazer sistemlerinin serbest ortam haberleşmesindeki önemi ve uydulararası haberleşmede lezer tekniğinin kullanılma durumu incelenmiştir. Lazer haberleşme sistemlerindeki; lazer kaynağı, foto dedektör, modülasyon tipi, anten gibi temel bileşenlerin fonksiyonları incelenmiştir. Optiwave yazılımı kullanılarak değişik link konfigürasyonlarına göre uydulararası haberleşme linki modellenmiş ve simüle edilmiştir. Sistem performansı (BER/Q faktör); verici gücü, dalga boyu, veri hızı, mesafe, anten çapı gibi temel parametrelere göre en düşük BER değerini elde etmek amacıyla analiz edilmiştir. Aynı sistem konfigürasyonunda APD ve PIN tipi fotodiyot kullanılarak karşılaştırmaları yapılmıştır. Ayrıca uydulararası haberleşme linkinde erbium katkılı fiber yükselteç (EDFA) kullanılarak link kalitesine etkisi incelenmiştir. Yapılan modelleme ve simülasyonlardan, haberleşme gereksinimlerine göre en uygun bileşen kullanılarak sistem performansının arttırılabileceği gösterilmiştir.

Anahtar Kelimeler: Uydulararası Lazer Haberleşmesi, serbest ortam optiksel haberleşme, optiksel kablosuz kanal, bit hata oranı, Q faktör.

CHAPTER ONE

INTRODUCTION

Free Space Optical (FSO) Communication Systems are alternatives to Radio Frequency (RF) communication systems due to the high data rate, high bandwidth capacity, smaller size and weight, less power consumption, high security, resistance to interference and etc.

The reason to use Optical Wireless Communication System over RF communication system is the very large difference between their wavelengths. The optical spectrum wavelength is much smaller compared to RF, conversely frequency is much higher compared to RF, therefore the beamwidth obtained using optical spectrum is narrower than that of the RF system and bandwidth capacity achieved using optical spectrum is greater than that of the RF system. Additionally, optical wireless system has many advantages over RF communication system such as reducing the antenna size, hence reducing the weight of the satellite, decreasing the power used, and offering higher data rate. All of these reasons are very important in a satellite system, because it can reduce the payloads size and consequently reducing costs [1-4].

The Free Space Optical Communication System is based on the usage of lasers as signal carriers. This is considered to be the technology for realizing a high speed and large capacity satellite communication [3]. Wavelengths used for Free Space Optical Communications are in the optical region in electromagnetic spectrum. Electromagnetic spectrum is shown in Figure 1.1 below [5].

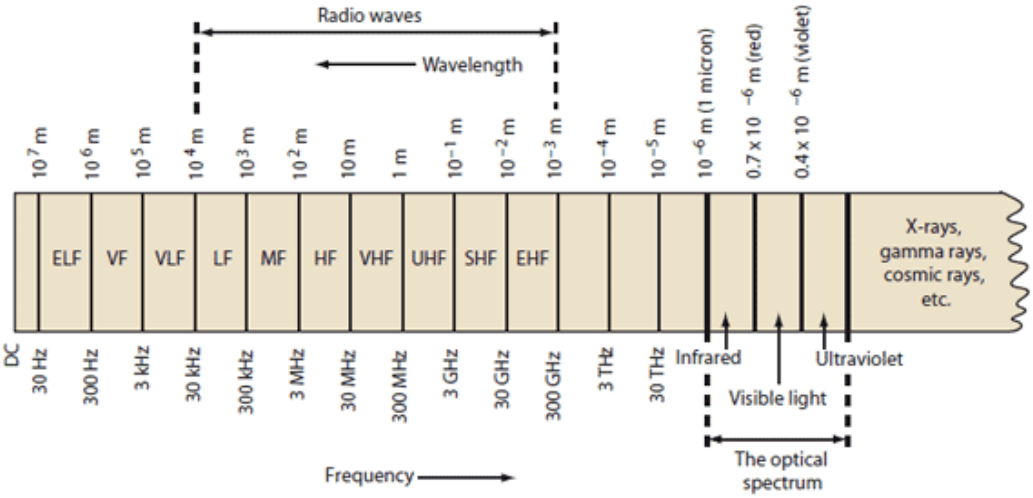

Figure 1.1 Electromagnetic spectrum.

Different wavelengths in optical domain can be used for FSO communication depending on laser source. In this thesis, analysis of 850 nm and 1550 nm wavelengths have been performed due to the compatibility with current technology and devices [6]. On the other hand, performance comparisons have been done for different wavelengths.

Laser communication technology is able to send several Gbps data to the distance of thousands kilometers apart. This caused to adapt optical wireless communication technology into space technology; hence, inter-satellite optical wireless communication is developed [7].

Figure 1.2 shows a general block diagram of The Free Space Optical Communication System.

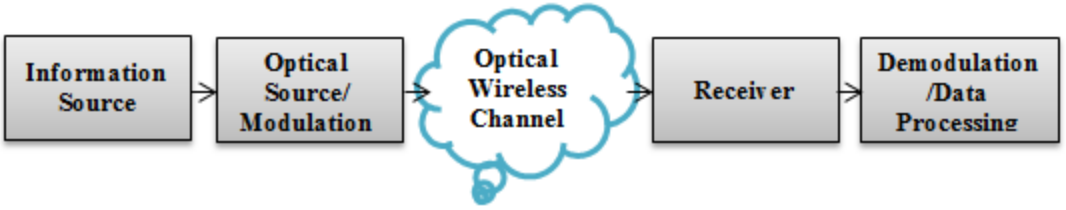

Figure 1.2 General block diagram of FSO.

1.1 Satellite Orbits

There are essentially three types of orbits. These are Low Earth Orbit (LEO), Medium Earth Orbit (MEO), and High Earth & Geosynchronous Orbit (GEO). The height of the orbit, or distance between the satellite and Earth's surface, determines how quickly the satellite moves around the Earth. An Earth-orbiting satellite's motion is mostly controlled by Earth's gravity. As satellites get closer to Earth, the pull of gravity gets stronger, and the satellite moves more quickly [8]. Figure 1.3 shows the Earth satellite orbits [8].

Figure 1.3 Earth satellite orbits.

Low Earth Orbit (LEO) is the closest orbit to Earth with altitude of 180 km to 2,000 km. The period is in the order of one and a half hours. With near 90° inclination, this type of orbit guarantees worldwide long term coverage as a result of the combined motion of the satellite and earth rotation. This is the reason for choosing this type of orbit for observation satellites (for example, the SPOT satellite: altitude 830 km, period 101 minutes). A constellation of several tens of satellites in low altitude circular orbits can provide worldwide real-time communication. For instance the GLOBALSTAR constellation incorporates 48 satellites at 1414 km and IRIDIUM constellation with 66 satellites at 780 km [8,9].

The Medium Earth Orbit (MEO) is from 2.000 km to 35.780 km altitude and the orbital period is 6 hours. With constellations of about 10 to 15 satellites, continuous

coverage of the Earth is guaranteed, allowing worldwide real-time communications [8, 9].

The Geosynchronous Earth Orbit (GEO) is the most popular earth orbit; the satellite orbits around the earth in the equatorial plane according to the earth rotation at an altitude of 35 786 km. The period is equal to that of the rotation of the earth. The satellite thus appears as a point fixed in the sky and ensures continuous operation at the fixed coverage area [8, 9].

Inter Satellite Links (ISL) can be considered as individual beams of multibeam satellites; the beams in this case are directed towards other satellites not in the direction of the earth. Two beams are necessary for bidirectional communication between satellites, one for transmission and the other for reception. Three classes of inter-satellite link can be distinguished [3, 9]:

- Links between GEO and LEO satellites (GEO–LEO links) also called Inter Orbital Links (IOL),
- Links between geostationary satellites (GEO–GEO),
- Links between low orbit satellites (LEO–LEO).

The scenarios for inter-satellite links are summarized in Figure 1.4 [10].

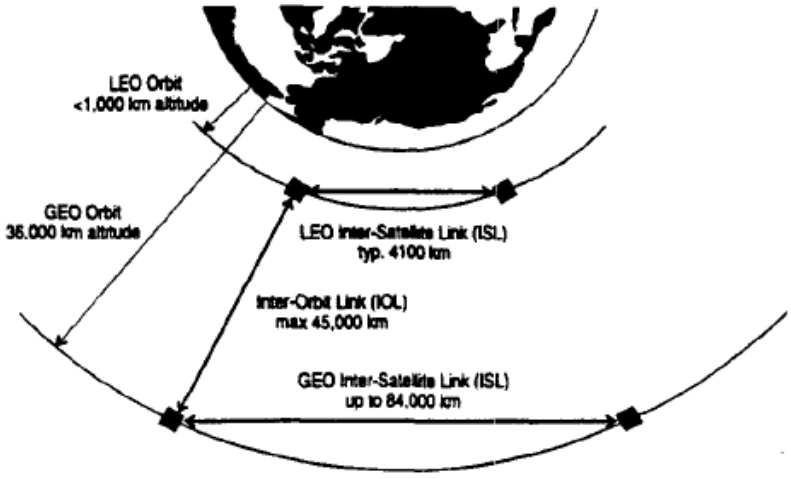

Figure 1.4 Inter-satellite link scenarios.

In this thesis, analysis has been done for LEO to LEO, LEO to GEO and GEO to GEO links and ranges have been set up in accordance with these link distances.

Inter-satellite links make the following configurations and advantages possible [9]:

- Extending the coverage area,
- Geostationary satellites can be used as a relay for permanent links between low orbit satellites and earth stations,
- Increasing system capacity by combining the capacities of several geostationary satellites,
- The planning of systems with a higher degree of flexibility,
- Consideration of systems providing a permanent link and worldwide coverage using low orbit satellites as an alternative to systems using geostationary satellites,
- Reducing the constraints on orbital position.

1.2 Transmitters

In inter-satellite optical wireless communications, lasers are used as optical source for transmitters. The laser is an oscillator to optical frequencies which is composed of an optical resonant cavity, optical feedback, population inversion and a gain mechanism to compensate the optical losses [11, 12]. The light emitted from a laser is monochromatic, directional and coherent. Active medium, excitation mechanism, high reflectance mirror, partially transmissive mirror are the common components of all lasers. Laser output can be continuous or pulsed [12]. There are many types of lasers for different applications. Lasers are often described by the kind of lasing medium they use - solid state, gas, excimer, dye, or semiconductor. Types of lasers can be used for communication are given in Table 1.1 [13].

Table 1.1 Types of laser source for FSO communication systems.

Laser Type	Component
Gas	CO_2 He-Ne
Solid State	Nd:YAG NdYLF Nd:YAP
Semiconductor (laser diode)	GaAlAs InGaAs InGaAsP

There are many considerations in designing a transmitter. The laser used should not only be powerful enough to transmit the necessary beam over a specified distance, but it must pass a screening test designed to select lasers with acceptable operating temperature, narrow linewidths, acceptable optical properties, reasonable FM responses, and prospects for long life [14]. A laser must qualify for space usage in a satellite crosslink system. For example gas lasers (CO_2, He-Ne) are not practical in space due to their relatively low efficiency and large size [15]. Solid state laser's advantages are their stability and have narrow spectral width and also producing ultrashort pulses of extremely high peak power. However, solid-state lasers are optically pumped with flash lamps and life times of flash lamps are relatively short compared to long time satellite communication. And also external modulator (electro-optic or acousto-optic) should be used for modulation [13].

Semiconductor lasers are of interest for the FSO industry, because of their relatively small size, compact, architectural simplicity, high power conversion efficiency, and cost efficiency [6, 11]. Many of these lasers are used in optical fiber systems with high availability. Table 1.2 summarizes the materials commonly used in semiconductor lasers [6].

Table 1.2 Materials used in semiconductor laser with wavelengths that are relevant for FSO communication systems.

Material	**Wavelengths (nm)**
GaAlAs	620-895
GaAs	904
InGaAsP	1100-1650 1550

Additionally, specific data rate, modulation type, bandwidth, output power, wavelength parameters are also important factors in order to make the most appropriate choice. Laser Specifications are given Table 1.3 below [13].

Table 1.3 Laser specifications for FSO communication systems.

Type	Compounds	Wavelength (nm)	Data Rate	Peak Power
Solid State Pulsed	Nd:YAG Nd:YLF Nd:YAP	1064 1047 or 1053 1080	<10 Mbps	10-100 W
Solid State CW	Nd:YAG Nd:YLF Nd:YAP	1064 1047 or 1053 1080	> Gbps	1-5 Watt
Semiconductor Pulsed	GaAlAs InGaAs	780-890 890-980	1-2 Gbps 1-2 Gbps	200 mW 1 W
Semiconductor CW	GaAlAs InGaAs InGaAsP	780-890 890-980 1300 or 1500	1-2 Gbps 1-2 Gbps > Gbps	200 mW 1 W < 50 mW

There are different methods of modulation of the laser beam which can be used to send information in the beam. The optical carrier can be modulated in its frequency, amplitude, phase, and polarization. The most commonly used schemes are amplitude modulation with direct detection and phase modulation in combination with a homodyne or heterodyne receiver due to their simple implementation [16].

In communication systems, technically the simplest digital modulation scheme is Amplitude Shift Keying (ASK). Provision of it in optical systems is On-Off Keying (OOK). OOK is an intensity modulation scheme where the light source is turned on to transmit a logic ”1” and turned off to transmit a ”0”. In its simplest form this modulation scheme is called Non Return to Zero (NRZ) -OOK. Moreover NRZ also

other codes exist. The most common one besides NRZ is Return to Zero (RZ) coding [16].

Coherent modulation systems are also used in optical communications. Usually, a binary coherent modulation scheme is used. For instance Binary Phase Shift Keying (BPSK), where the phase of the coherent laser light is shifted between two states [16].

An OOK system is more robust regarding atmospheric distortion than a coherent modulation system. This is because in OOK the information is only encoded in intensity while Phase Shift Keying (PSK) uses intensity and phase coding. Both the intensity and the phase of a beam are disturbed in atmospheric propagation. Further, OOK has mainly been used in optical fiber communications due to its low complexity. As a result of it more reliable and cost effective components are available in the market, which is important for the development of FSO communication system. Consequently, OOK systems are commonly preferred for optical links [11, 16-18]

In this thesis, direct detection with OOK has been used for modeling and analysis.

1.3 Receivers

Optical communications receivers can be classified into two basic types. These are non-coherent receivers (direct detection) and coherent receivers (coherent detection) [11, 19]. With direct detection, the incident photons are converted into electrons by a photodetector. The resulting baseband electric current at the output of photodetector is amplified then detected by a matched filter. With coherent detection, the optical signal field associated with the incident photons is mixed with the signal from a local oscillator. The subsequent optical field is converted into a bandpass

electric current by a photodetector and is afterwards amplified by an intermediate frequency amplifier. The demodulator detects the convenient signal either by envelope detection or by coherent demodulation [9]. The block diagram of the direct detection system and coherent detection system are shown in Figure 1.5 and Figure 1.6, respectively [9].

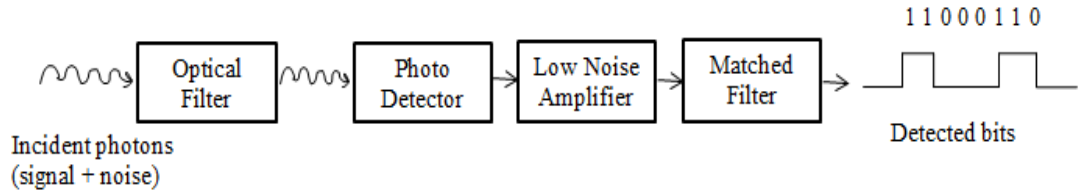

Figure 1.5 Optical direct detection receiver.

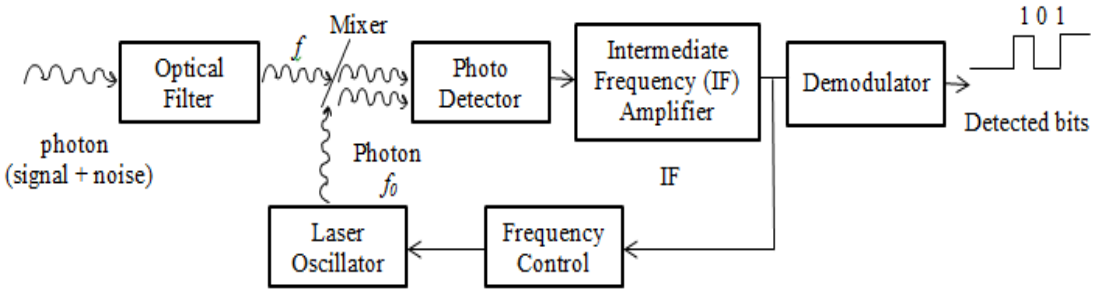

Figure 1.6 Optical coherent detection receiver.

The coherent mixing process requires that the local beam to be aligned with the beam received in order to get efficient mixing. This can be implemented in two different ways; if the frequency of signal and local oscillator are different and are uncorrelated, it is called heterodyne detection; if the frequencies of the signal and local oscillator are the same and correlated the processes is referred to as homodyne detection. The block diagram of the heterodyne detection system and homodyne detection system are shown in Figure 1.7 and Figure 1.8, respectively [11]. Due to the mixing process, coherent receivers are theoretically more sensitive than direct detection receivers. In terms of sensitivity, the coherent communications systems with phase modulation theoretically have the best performance of all. Sensitivity is the number of photons per bit required to get a given probability of error [11].

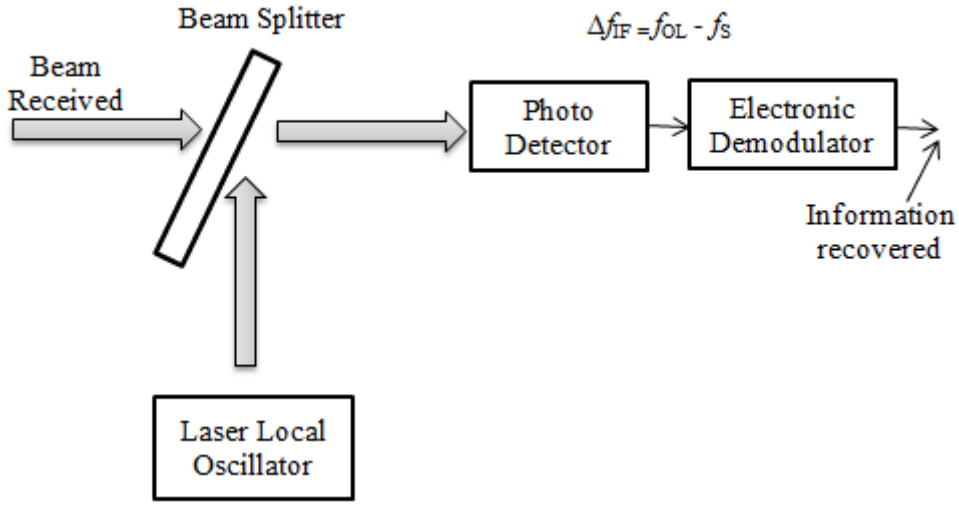

Figure 1.7 Optical heterodyne receiver.

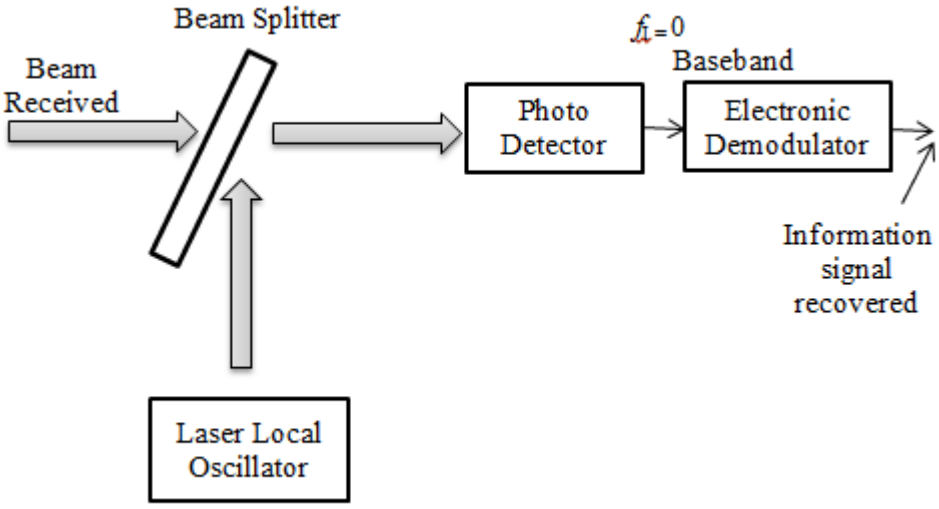

Figure 1.8 Optical homodyne receiver.

As with laser, detectors play a key role in the design of the system. The optical signals must be converted to the electrical signal at the receiver. This conversion is made by the photodetectors. There are two main types of photodetectors, Positive Intrinsic Negative Photodiode (PIN) and Avalanche Photodiode (APD). The main parameters that characterize the photodetectors in communications are spectral response, photosensitivity, quantum efficiency, dark current, noise equivalent power,

response time and bandwidth. The photodetection is achieved by the response of a photosensitive material to the incident light to produce free electrons. These electrons can be directed to form an electric current when applied an external potential. A photodiode is designed to operate in reverse bias [11, 14, 20, 21]. Table 1.4 shows the detector type for FSO communication systems [13].

Table 1.4 Detector type for FSO communication systems.

Application	**Detector Type**	**Materials**
Communication	APD PIN CCD PMT	Silicon, InGaAs, InGaAsP Silicon, InGaAs, InGaAsP Silicon Solid state silicon photo cathode
Acquisition	CCD CID QAPD QPIN	Silicon Silicon Silicon Silicon, InGaAs
Tracking	CCD CID QAPD QPIN	Silicon Silicon Silicon Silicon, InGaAs

In this thesis, APD type and PIN type of photodiodes are used for modeling and analysis.

1.4 Thesis Outline

In this thesis;

- Detailed literature survey about free space optical communication system has been done,
- The importance of laser systems for free-space communication has been discussed and the status of laser techniques for inter-satellite communication has been examined,
- The functions of each basic component such as laser source, photo detector, modulation type, telescope used in a typical system have been examined,
- The inter-satellite link has been modeled and simulated for the various link configurations with using Optiwave Software,
- APD type and PIN type photodetector comparison has also been done,
- Erbium Doped Fiber Amplifier (EDFA) has been used for the inter-satellite link to recognize its effect on the link quality.
- The system performance (BER/Q-Factor) has been analyzed in terms of each basic parameter such as transmitted power, wavelength, data rate, range and telescope diameter in order to achieve minimum BER.

CHAPTER TWO

MODELING

Optiwave's Optisystem Software version 12 and MATLAB are used for system modeling and analyzing. Inter-satellite Laser Communication System consists of Transmitter, Optical Wireless Channel (OWC), and Receiver. System design model is shown in Figure 2.1.

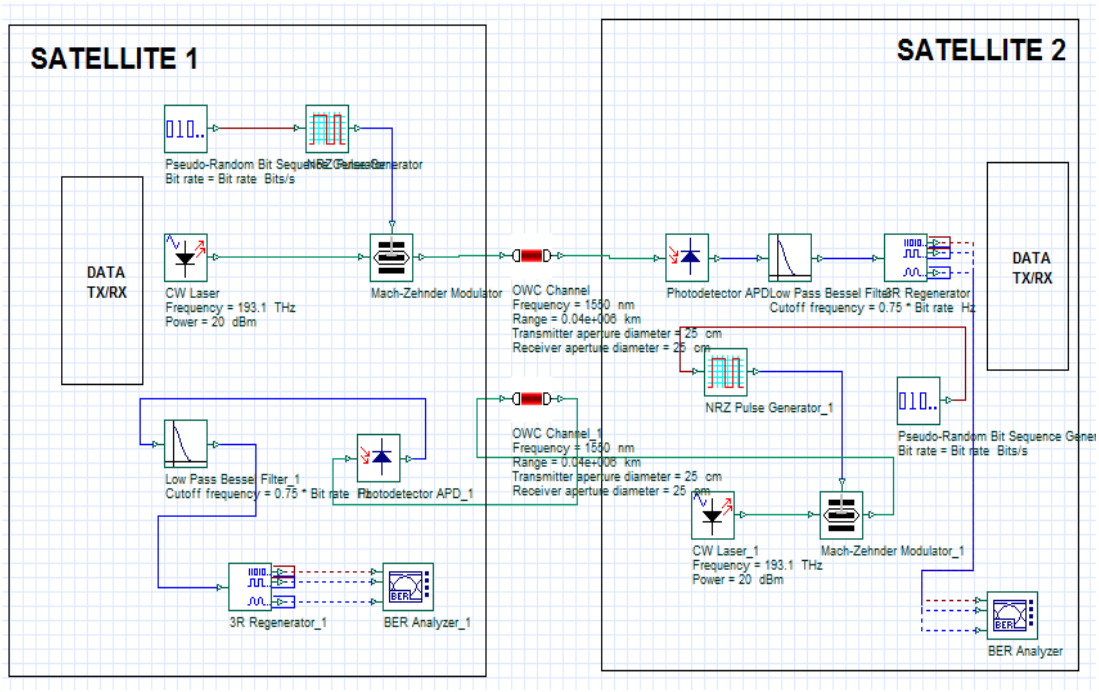

Figure 2.1 System design model for full duplex inter-satellite laser communication system between two satellites.

The transmitter includes data source, Non Return to Zero (NRZ) Pulse Generator, a laser source, modulator and a telescope. The receiving module includes a telescope, photodetector, filter and a demodulator. The transmitter converts the electrical signals into optical signals by using the laser. The transmitter telescope collimates the laser radiation in the receiver satellite direction, using data from the tracking system. The tracking system directs the receiver telescope in the direction of the transmitter satellite. Component's, which are used modeling and simulations,

specifications have been taken from the component library of the Optisystem Optical Communication System Design Software.

2.1 Transmitter in Modeling

In this model transmitter consists of four subsystems. These are Pseudo Random Bit Sequence (PRBS) Generator, Non Return to Zero (NRZ) Pulse Generator, Continuous Wave (CW) Laser, Mach-Zehnder Modulator.

2.1.1 Pseudo Random Bit Sequence (PRBS) Generator

PRBS generates a pseudo random binary sequence according to different operation modes [22]. This subsystem represents the information or data that will be transmitted. In this thesis, PRBS generator with order k is used to generate a sequence with period of 2^k-1 [23]. The bit sequence is designed to approximate the characteristics of random data.

This subsystem generates a sequence of N bits where;

$$N = T_w B_r \quad \textbf{(2.1)}$$

$$N_G = N - n_l - n_t \quad \textbf{(2.2)}$$

T_w is the global parameter time window and B_r is the parameter bit rate.

N_G is the number of bits generated. n_l and n_t are the number of leading zeros and the number of trailing zeros. Figure 2.2. depicts the bit sequence illustration.

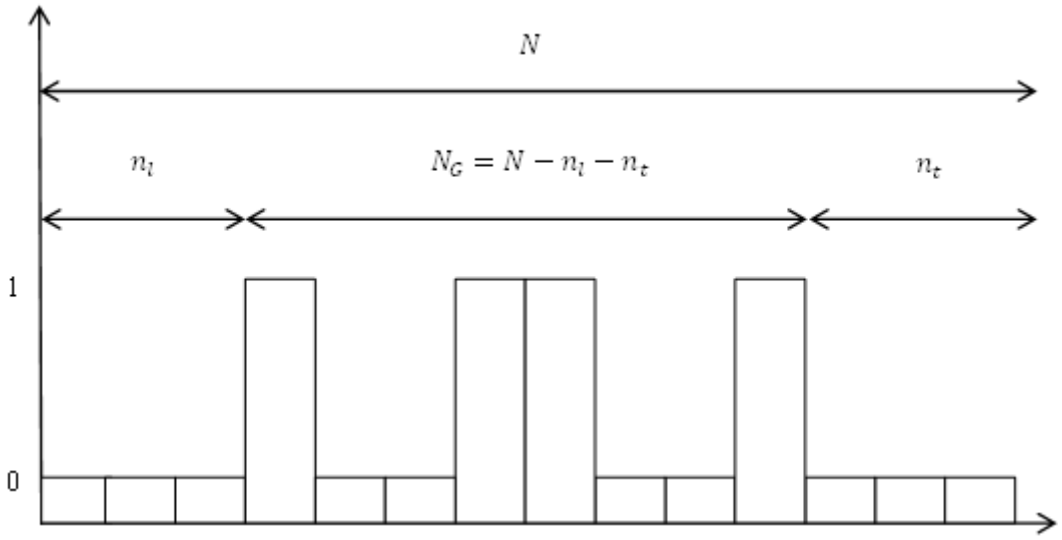

Figure 2.2 Bit sequence illustration.

2.*1.2 Non Return to Zero (NRZ) Pulse Generator*

A non-return-to-zero (NRZ) code is a binary code in which 1's are represented by a positive voltage and 0's are represented by a negative voltage [24] [25]. Due to the fact that there is no negative light in optical communications, the terms NRZ are used differently, NRZ means that a bit of logical value 1 (a pulse of light) changes its value (from light on to light off or vice versa) at the boundaries of the bit period [25]. Figure 2.3 illustrates the NRZ encoding technique.

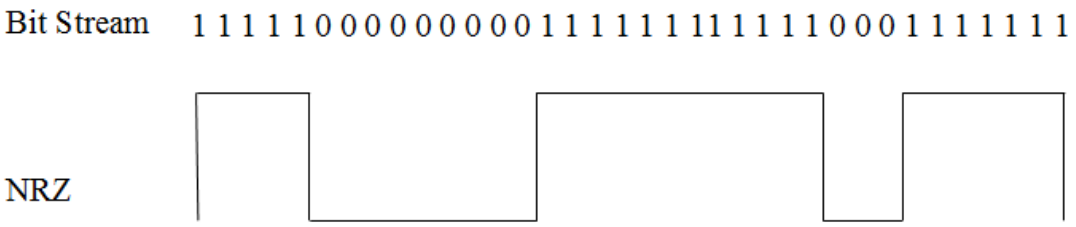

Figure 2.3 NRZ encoding format.

NRZ pulse generator generates a non-return to zero coded signals. This subsystem encodes the data from the pseudo random bit sequence generator using the non-return zero encoding technique. This subsystem produce pulses with different edge shapes according to the parameter rectangle shape (exponential, Gaussian, linear, sine).

Exponential:

$$E(t) = \begin{cases} 1 - e^{-\left(\frac{t}{c_r}\right)}, 0 \leq t < t_1 \\ 1, t_1 \leq t < t_2 \\ e^{-\left(\frac{t}{c_f}\right)}, t_2 \leq t < T \end{cases} \quad \textbf{(2.3)}$$

Gaussian:

$$E(t) = \begin{cases} 1 - e^{-\left(\frac{t}{c_r}\right)}, 0 \leq t < t_1 \\ 1, t_1 \leq t < t_2 \\ e^{-\left(\frac{t}{c_f}\right)^2}, t_2 \leq t < T \end{cases} \quad \textbf{(2.4)}$$

Linear:

$$E(t) = \begin{cases} t/c_r, 0 \leq t < t_1 \\ 1, t_1 \leq t < t_2 \\ t/c_f, t_2 \leq t < T \end{cases} \quad \textbf{(2.5)}$$

Sine:

$$E(t) = \begin{cases} \sin(\pi.\frac{t}{c_r}), 0 \leq t < t_1 \\ 1, t_1 \leq t < t_2 \\ \sin(\pi.\frac{t}{c_f}), t_2 \leq t < T \end{cases} \quad \textbf{(2.6)}$$

where c_r is the rise time coefficient and c_f is the fall time coefficient. t_1 and t_2, together with c_r and c_f are numerically determined to generate pulses with the exact values of the parameters rise time and fall time, and T is the bit period.

2.1.3 Continuous Wave (CW) Laser

This component generates a continuous wave (CW) optical signal. The behavior of a semiconductor laser diode is modeled by three rate equations which describe the relation between the carrier density $N(t)$, photon density $S(t)$, and output optical power P [26,27].

$$\frac{dN(t)}{dt} = \frac{I(t)}{q.V} - \frac{N(t)}{\tau_n} - v_g \,.\sigma_g \,.(N(t) - N_t).\frac{1}{\left(1 + \varepsilon.S(t)\right)} \,.S(t) \qquad (\mathbf{2.7})$$

$$\frac{dS(t)}{dt} = \Gamma \,.v_g \,.\sigma_g \,.(N(t) - N_t).\frac{1}{\left(1 + \varepsilon.S(t)\right)} \,.S(t) - \frac{S(t)}{\tau_p} + \frac{\Gamma.\beta.\mathrm{N(t)}}{\tau_n} \qquad (\mathbf{2.8})$$

$$P = \frac{S \,.\, V.\, \eta_{int} \,.h \,.\nu}{2 \,.\, \Gamma\, \tau_p} \qquad \mathbf{(2.9)}$$

Where,

σ_g : Differential gain coefficient

v_g : Group velocity

ε : Gain compression factor

N_t : Carrier density at transparency

β : Spontaneous emission factor

Γ : Mode confinement factor

V : Active layer volume

τ_p : Photon lifetime

τ_n : Carrier lifetime

η_{int} : Internal quantum efficiency

h : Planck's constant

ν : Optical frequency

2.1.4 Mach-Zehnder Modulator

The Mach-Zehnder modulator is the electro-optic modulator based on an interferometric principle that functions is to vary intensity of the light source from the laser according to the output of the NRZ pulse generator. It consists of two 3 dB couplers which are connected by two waveguides of equal length shown in Figure 2.4. When an input laser beam is launched at the input of the modulator, it splits into two equal parts, one of which has a phase modulator. By means of an electro-optic effect, an externally applied voltage which comes from NRZ pulse generator varies the refractive indices in the waveguide branches. The different paths can lead to constructive and destructive interference at the output, depending on the applied voltage. Then the output intensity can be modulated according to the voltage. [28].

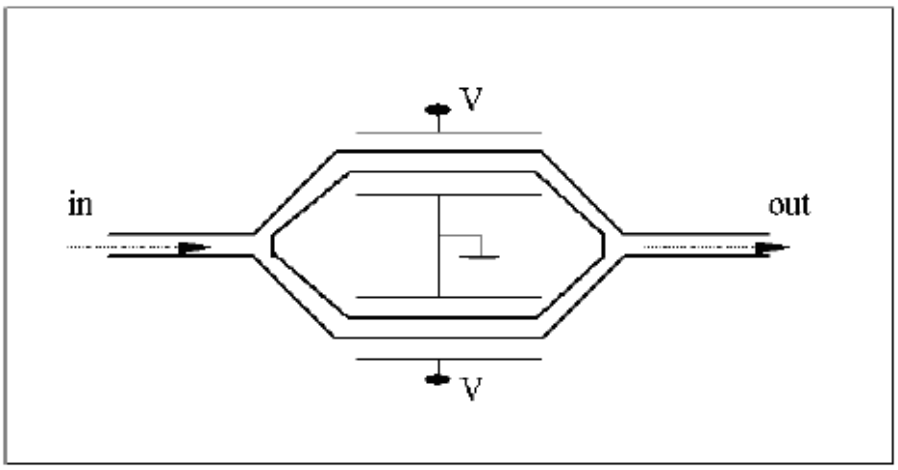

Figure 2.4 Mach-Zehnder modulator varies the light intensity according to voltage.

The equations below describe the behavior of the Mach-Zehnder modulator:

$$E_{out}(t) = E_{in}(t).\cos(\Delta\theta(t)) \,.\, e^{(j.\Delta\emptyset(t))} \quad \textbf{(2.10)}$$

$\Delta\theta$ is the phase difference between the two branches and is defined as:

$$\Delta\theta(t) = \frac{\pi}{2}.(0.5 - ER.(Modulation(t) - 0.5)) \quad \textbf{(2.11)}$$

$$\mathrm{ER} = 1 - \frac{4}{\pi}.\tan^{-1}(\frac{1}{\sqrt{extrat}}) \quad \textbf{(2.12)}$$

$\Delta\emptyset$ is the signal phase change defined as:

$$\Delta\emptyset(t) = SC.\Delta\theta(t).(1 + SF)/(1 - SF) \quad \textbf{(2.13)}$$

where the parameter SC is –1 if negative signal chirp is true, or 1 if negative signal chirp is false. $extrat$ is the extinction ratio, SF is the symmetry factor, and $Modulation(t)$ is the electrical input signal.

2.2 Optical Wireless Channel (OWC) in Modeling

This subsystem models an optical wireless communication (OWC) channel. It is a subsystem of two telescopes and the wireless communication channel between them.

Free space optical links are simulated with using this subsystem. The component is a subsystem of transmitter telescope, optical wireless communication channel and receiver telescope. The received optical power is given by [18, 28-38].

$$P_R = P_T\eta_T\eta_R(\frac{\lambda}{4\pi Z})^2 G_T G_R L_T L_R \quad \textbf{(2.14)}$$

P_T : Transmitter optical power

η_T : Optics efficiency of the transmitter

η_R : Optics efficiency of the receiver

λ : Wavelength

Z : Distance between the transmitter and the receiver (Range)

G_T : Transmitter telescope gain

G_R : Receiver telescope gain

L_T : Transmitter pointing loss factor

L_R : Receiver pointing loss factor

The term in parentheses is the free-space loss. $\eta_T L_T$ can be expressed by T_T and named transmission factors for the transmitter similarly $\eta_R L_R$ can be expressed by T_R and named transmission factors for the receiver.

Geometrical gain can be expressed by:

$$G_T \approx (\frac{\pi D_T}{\lambda})^2 \quad \textbf{(2.15)}$$

D_T is the transmitter telescope diameter. Similarly, the receiver telescope gain that can be expressed by:

$$G_R \approx (\frac{\pi D_R}{\lambda})^2 \quad \textbf{(2.16)}$$

D_R is the receiver telescope diameter.

Most systems use a narrow-beam-divergence angle laser transmitter and narrow field of view receiver; therefore small mispointing can cause signal loss. The approximation transmitter pointing loss factor is given by:

$$L_T = \exp(-G_T \theta_T^2) \quad \textbf{(2.17)}$$

θ_T is transmitter azimuth pointing error angle also called the divergence angle at the transmitter,

$$\theta_T \approx \frac{\lambda}{D_T} \quad \textbf{(2.18)}$$

and the approximation receiver pointing loss factor by:

$$L_R = \exp(-G_R \theta_R^2) \quad \textbf{(2.19)}$$

θ_R is receiver azimuth pointing error angle.

Attenuation(A) which is the ratio of output power to input power can be expressed as follows,

$$A = \frac{P_T}{P_R} = \frac{Z^2 \left(\frac{\lambda}{D_T}\right)^2}{{D_R}^2 T_R T_T (1 - L_P)} \quad \textbf{(2.20)}$$

This equation can be arranged by using equation 2.18,

$$A = \frac{Z^2 \, {\theta_T}^2}{{D_R}^2 T_R T_T (1 - L_P)} \quad \textbf{(2.21)}$$

L_P is the pointing loss factor.

In this analysis, the transmitter and receiver telescopes are assumed to be ideal where the optical efficiency is equal to 1 and there is no pointing error. Additional losses due to scintillation, mispointing, and others are also assumed to be zero. In

addition, by reason of the altitude of the satellites that is above the Earth's atmospheric layers, there is no attenuation due to atmospheric effects.

2.3 Receiver in Modeling

In this model receiver consist of tree subsystems. These are Photodetector, Low Pass Filter, and 3R Regenerator.

2.3.1 Photodetector

The photodetector is an optoelectronic device that receives the optical signal and converts it into electrical signal [6, 20, 21].

The incoming optical signal and noise bins are received by the photodetector. Figure 2.5 depicts the optical signal with noise in photodetector.

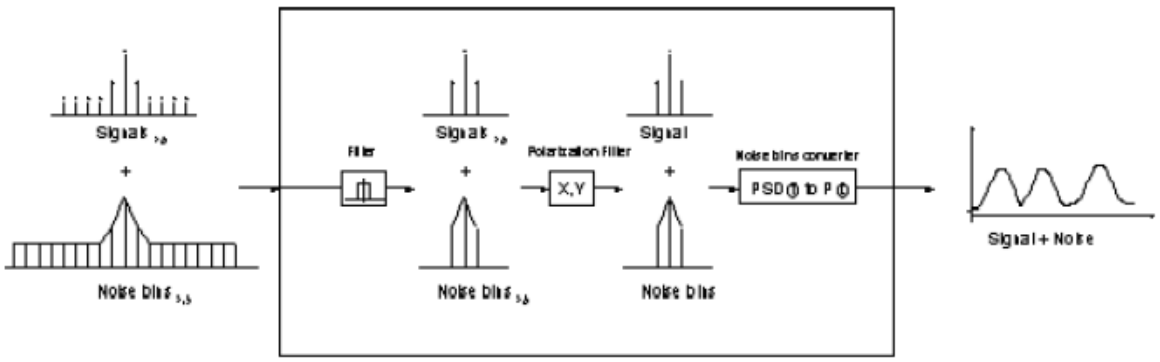

Figure 2.5 Optical signal with noise illustration in photodetector.

Optical noise bins are converted to Gaussian noise inside of the signal bandwidth. The combined optical field is then converted to optical power and the output noise and signal are combined. The optical power is converted to electrical current by;

$$i(t) = i_s(t) + i_{th}(t) + i_d + i_{sh}(t) \quad \textbf{(2.22)}$$

$i_s(t)$ is the optical signal calculated from the responsivity r and the gain M as:

$$i_s(t) = MrP_S(t) \quad \textbf{(2.23)}$$

And $i_{th}(t)$ is the thermal noise current calculated from the power spectral density and i_d is the additive dark current.

The shot noise current $i_{sh}(t)$ is calculated according to the power spectral density:

$$N_{sh}(t) = qM^2F(rP_s(t) + i_{dm}) \quad \textbf{(2.24)}$$

i_{dm} is the dark current and F depends on M:

$$F(M) = kM + (2 - \frac{1}{M})(1 - k) \quad \textbf{(2.25)}$$

k is the ionization ratio.

The responsivity of Si, Ge, and InGaAs is calculated based on the Figure 2.6 [6].

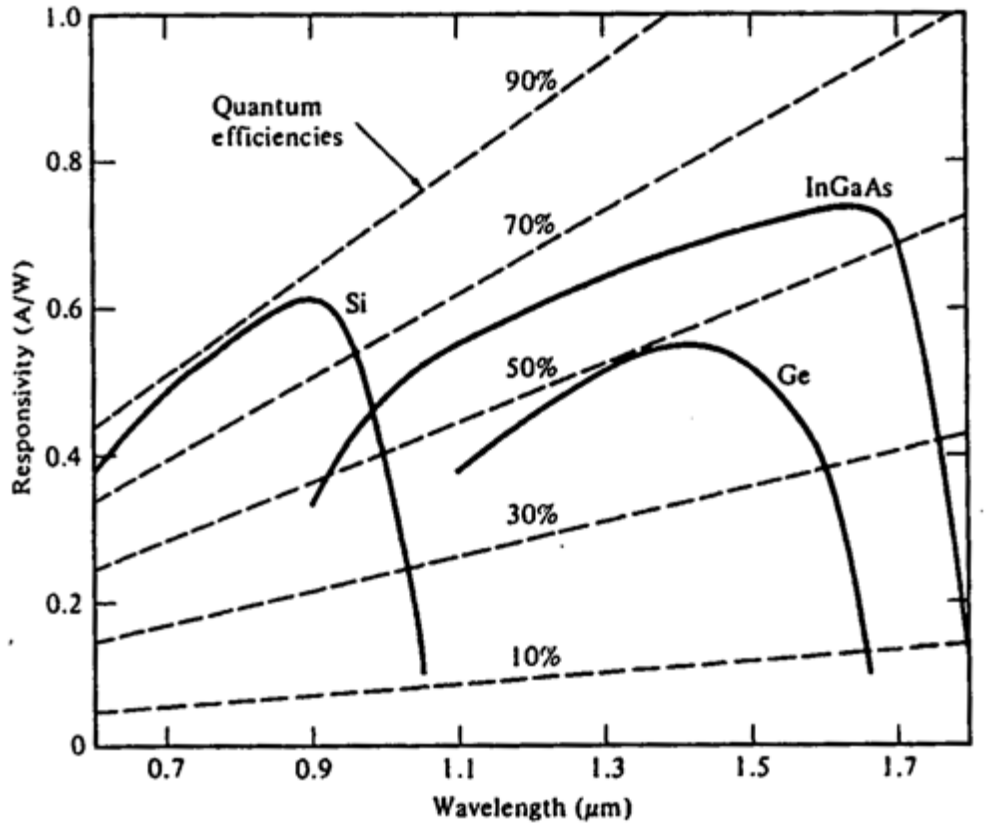

Figure 2.6 Responsivity curves for detector materials such as Si, Ge, InGaAs.

2.3.2 Low Pass Bessel Filter

Low Pass Filter (LPF) is used to remove distortion caused by noise or interference in the signal. The order of the Bessel function is 4 and 3dB cut-off frequency of filter is 0.75 x signal bit rate. Bessel filters have the following transfer function [39-43]:

$$H(s) = \alpha \frac{d_0}{B_N(s)} \tag{2.26}$$

α is the insertion loss, N is the parameter order, and,

$$d_0 = \frac{(2N)!}{2^N . N!} \quad \textbf{(2.27)}$$

being a normalizing constant and $B_N(s)$ an nth-order Bessel polynomial of the form:

$$B_N(s) = \sum_{k=0}^{N} d_k \, s^k \quad \textbf{(2.28)}$$

$$d_k = \frac{(2N-k)!}{2^{N-k} . k! \, (N-k)!} \quad \textbf{(2.29)}$$

$$s = j(\frac{f . w_b}{f_c}) \quad \textbf{(2.30)}$$

f_c is the filter cutoff frequency and $w_b$denotes the normalized 3 dB bandwidth and approximated by:

$$w_b \approx \sqrt{(2N-1) . ln2} \quad \textbf{(2.31)}$$

2.3.3 The 3R Regenerator

The 3R regenerator is the subsystem in order to regenerate electrical signal of the original bit sequence. It generates the original bit sequence, and a modulated electrical signal to be used for Bit Error Rate (BER) analysis.

CHAPTER THREE

RESULTS AND ANALYSIS

In this section, the functions of the each basic parameter such as wavelength, transmit power, range, data rate, telescope diameter, photo detector type have been changed and the system performance (BER/Q Factor) have been analyzed according to these changes.

The Q-factor can be used to analyze system performance. The Q factor is a function of the Signal to Noise Ratio (SNR) for optical systems thus provides a qualifying description of the receiver performance and offers the minimum SNR required obtaining a specific Bit Error Rate (BER) for a given signal. Figure 3.1 shows the relationship of Q-factor to BER. As can be seen in Figure 3.1 the higher the value of Q factor, the better the BER.

$$BER = \frac{1}{2} erfc(\frac{Q}{\sqrt{2}}) \quad \textbf{(3.1)}$$

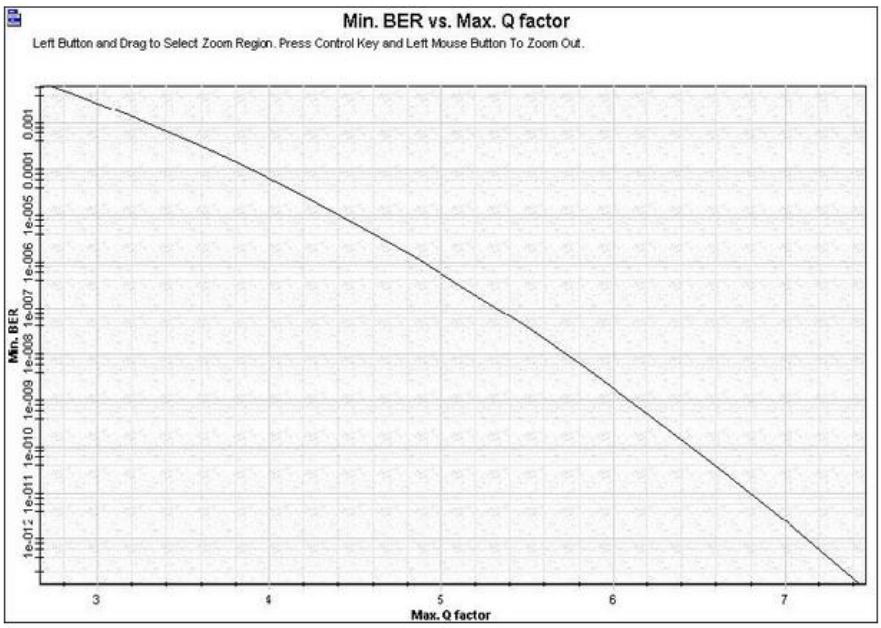

Figure 3.1 Diagram for relationship between maximum Q factor and BER.

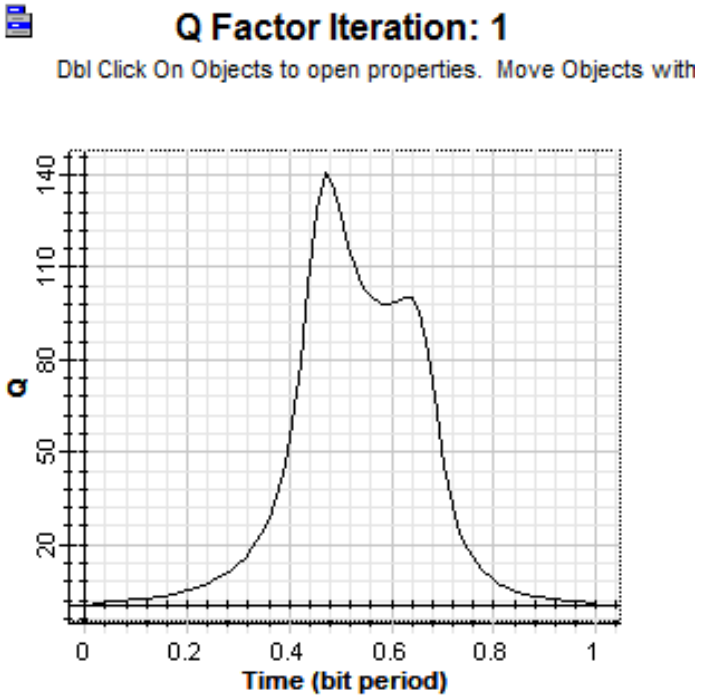

Figure 3.2 Maximum value for the Q factor versus decision instant.

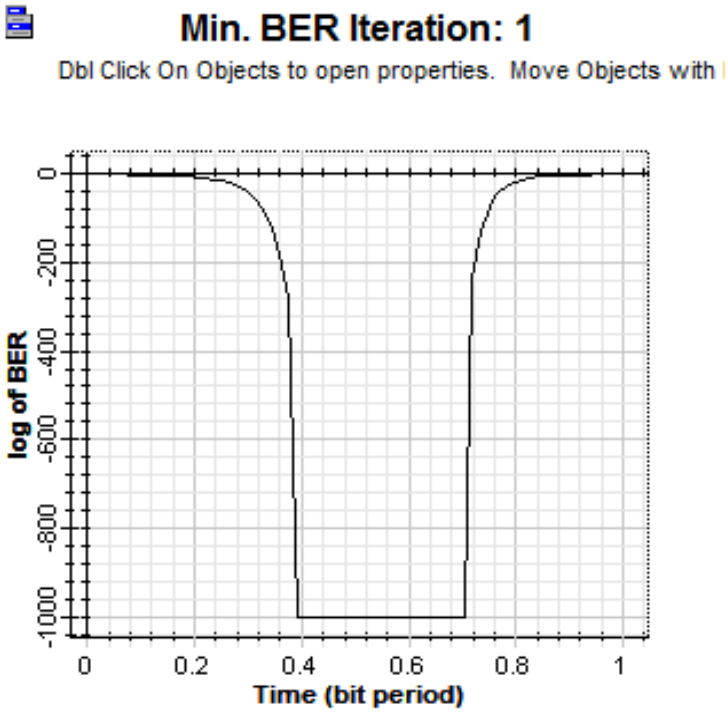

Figure 3.3 Minimum value for the BER versus decision instant.

The sensitivity of the receiver is measured as number of detected photons per bit (at peak power) necessary to achieve a BER of common requirements. Common requirements in satellite communications are 10^{-5} BER for voice and 10^{-7} BER for data [45]. In this thesis, it's aimed to obtain 10^{-9} BER, which is equal to Q factor 6, for better quality communication [17, 48].

In addition, an eye diagram has also been used to analyze system performance. An eye diagram is a common indicator of the quality of signals in high-speed digital transmissions. As can be seen in Figure 3.4, important information can be revealed by an eye diagram. It can indicate the best point for sampling, amount of jitter and distortion and divulge the SNR at the sampling point. Moreover, time variation at zero crossing can be seen in diagram, which indicates a measure of jitter [46, 47].

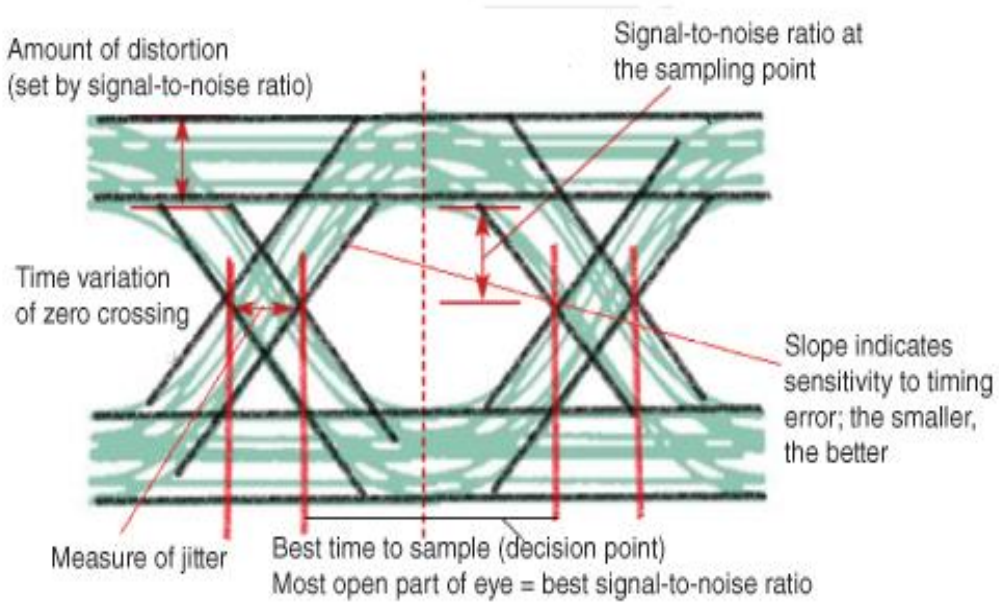

Figure 3.4 Interpretation of an eye diagram.

3.1 Relationship between Q Factor Transmit Power (Laser Type) and Wavelengths

It is mentioned in Section 1.2 that, different types of lasers can be used in inter-satellite laser communications and according to the compounds used in the laser wavelength and the peak power varies.

In this section for simulation, range has been set to a constant value of 45.000 km which is the maximum distance for LEO-GEO Inter Orbit Link (IOL) and telescope diameter has been set a constant value of 25 cm which is the diameter of world first optical satellites ARTEMIS and SPOT-4 [49]. Besides, wavelength and data rate have been set at a constant value of 1550 nm and 50 Mbps, respectively.

Firstly, the transmit power has been set at 14 levels which are 17 dBm to 30 dBm, linearly to determine the power required to achieve specific BER which is 10^{-9} in this thesis. System design model is shown in Figure 3.5.

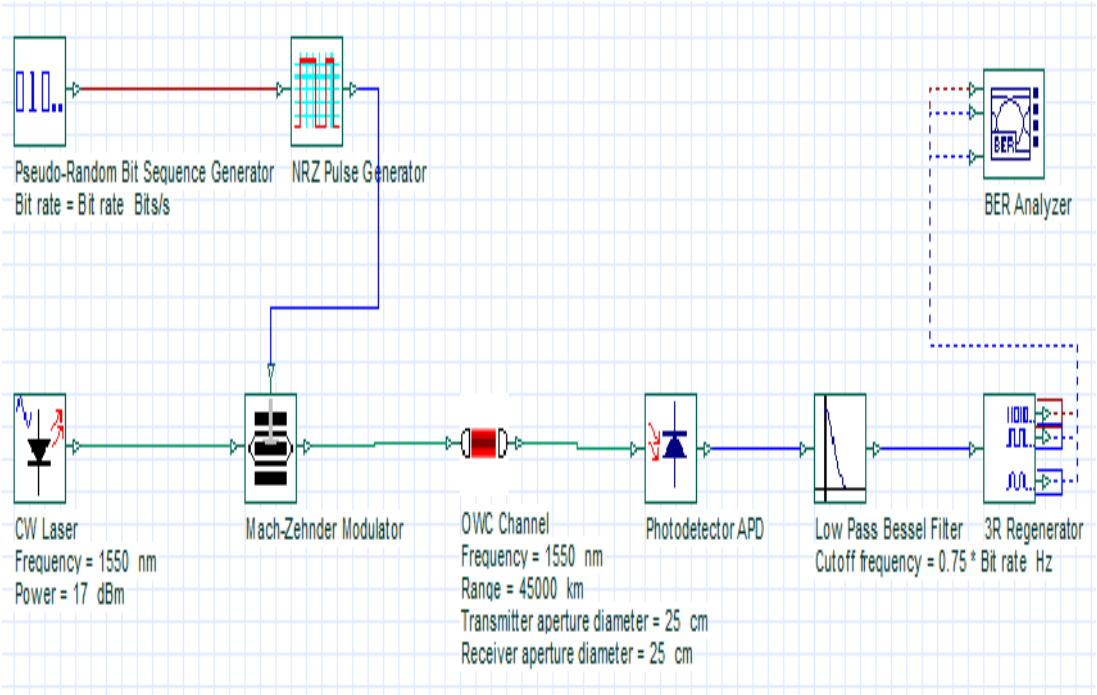

Figure 3.5 System design model for simplex inter-satellite laser communication system between two satellites.

The graph of Q-factor against transmit power has been plotted in Figure 3.6. As can be seen in this figure, link can not be established up to 25 dBm and transmit power should be at least 29 dBm to obtain with 10^{-9} BER.

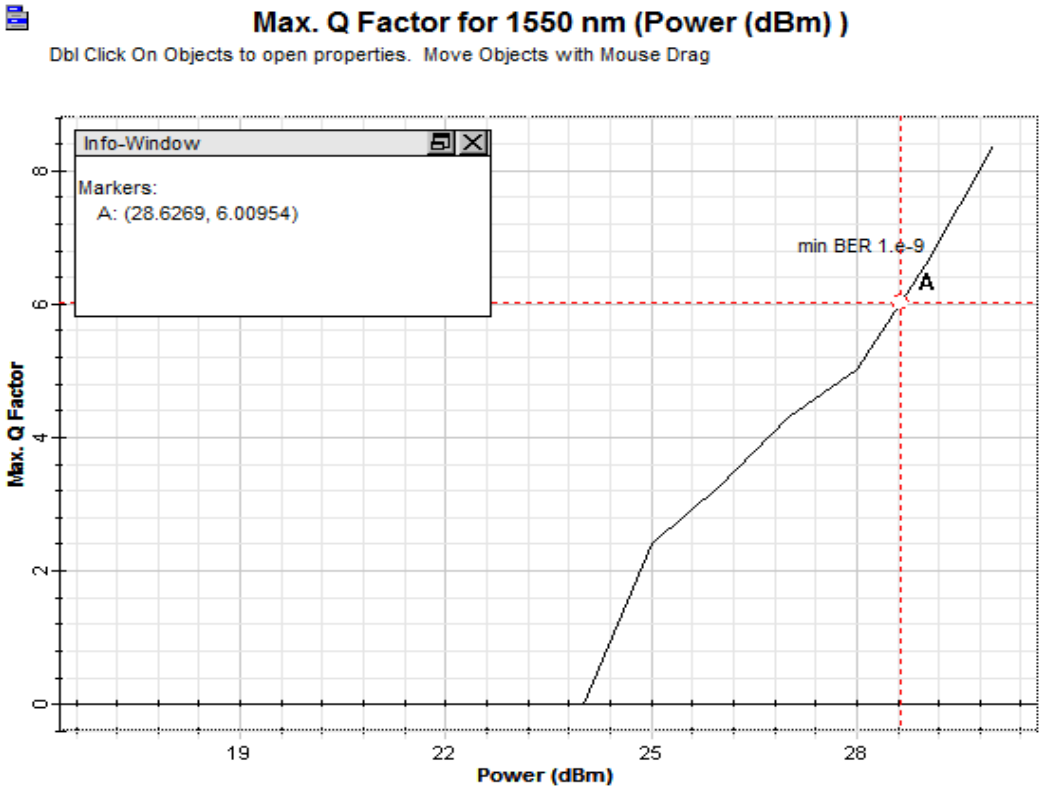

Figure 3.6 Q factor versus transmit power diagram at 1550 nm wavelength.

Maximum Q factor and minimum BER have been plotted in Figure 3.7 and Figure 3.8, respectively for each transmitted power value. Figure 3.7 indicates that Q factor is 0 for the transmitted power values less than 25 dBm.

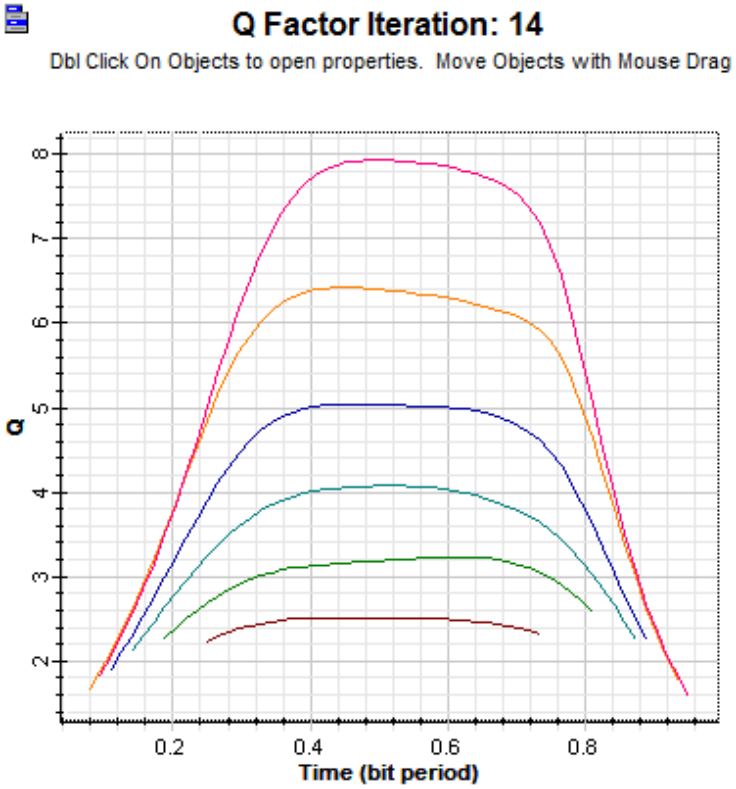

Figure 3.7 Maximum Q factor for each transmit power value.

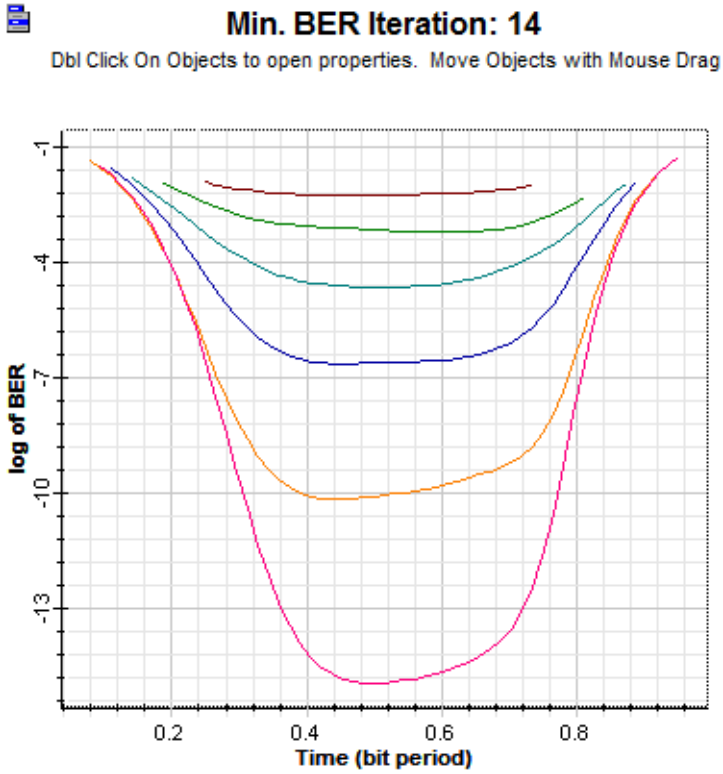

Figure 3.8 Minimum BER for each transmit power value.

Eye diagrams have been plotted for each transmit power value and shown in figures from 3.9 to 3.22. As can be seen in figures, when the transmit power increases, the eye diagram consist of less jitter and the opening of eye increases.

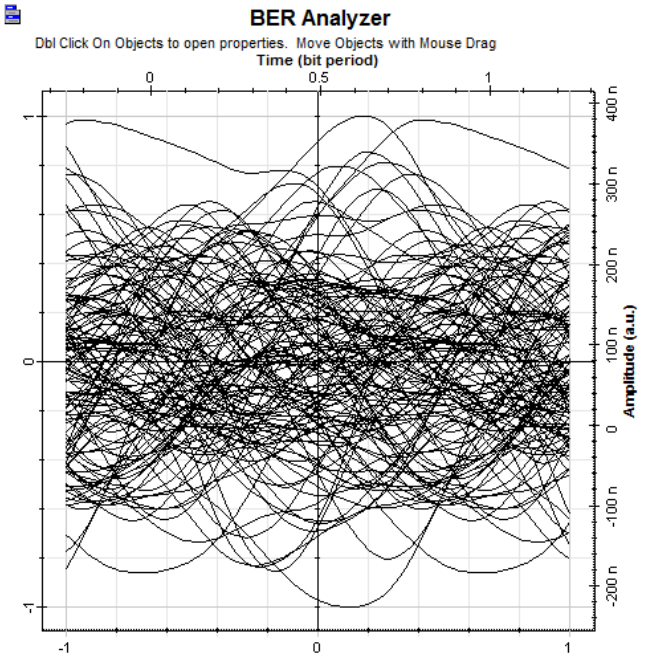

Figure 3.9 Eye diagram for 17 dBm transmit power.

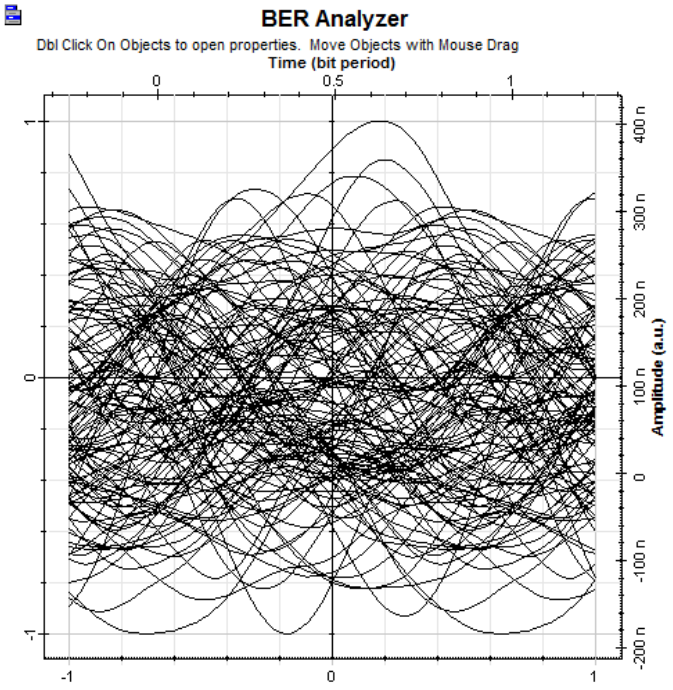

Figure 3.10 Eye diagram for 18 dBm transmit power.

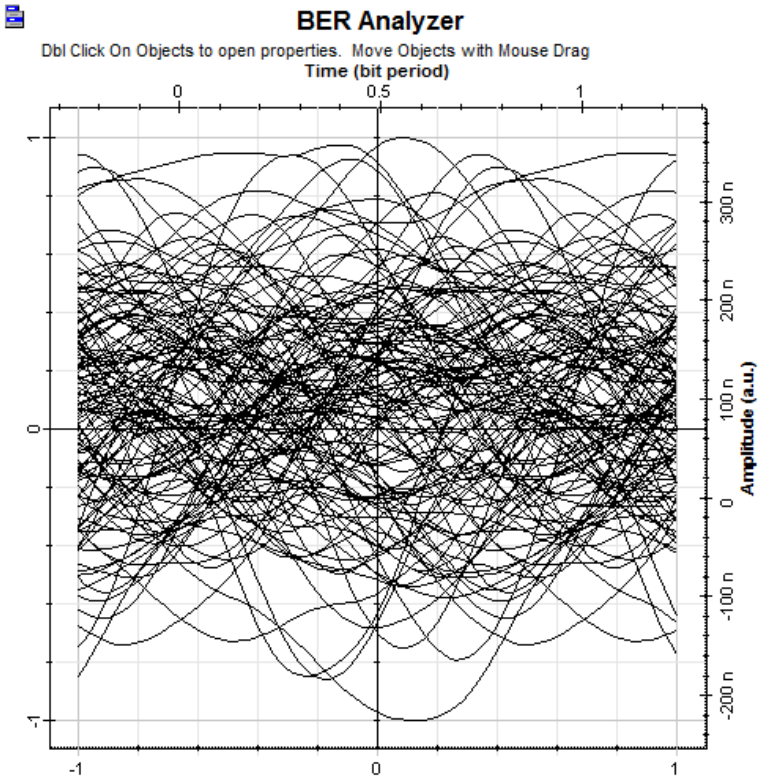

Figure 3.11 Eye diagram for 19 dBm transmit power.

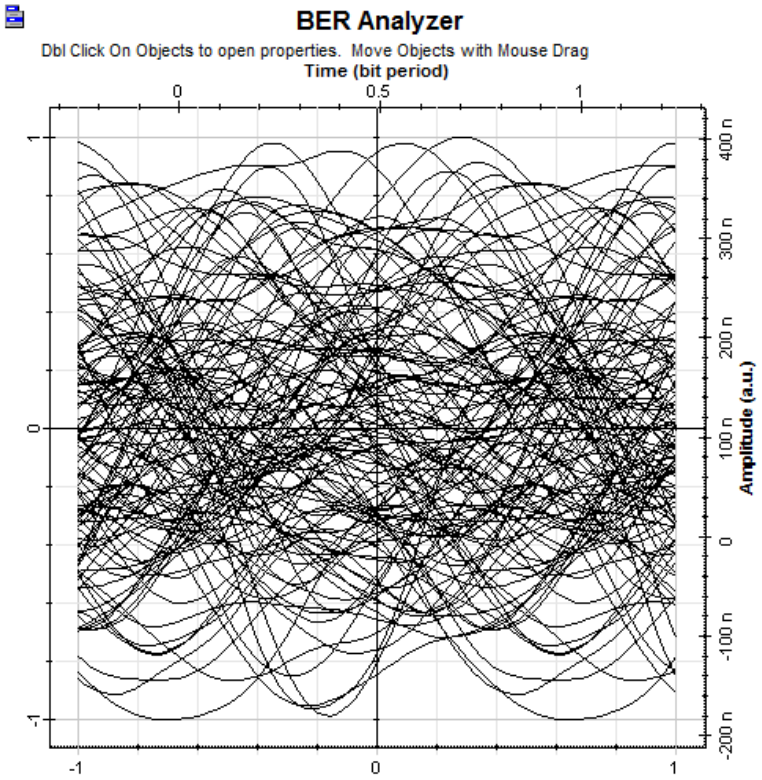

Figure 3.12 Eye diagram for 20 dBm transmit power.

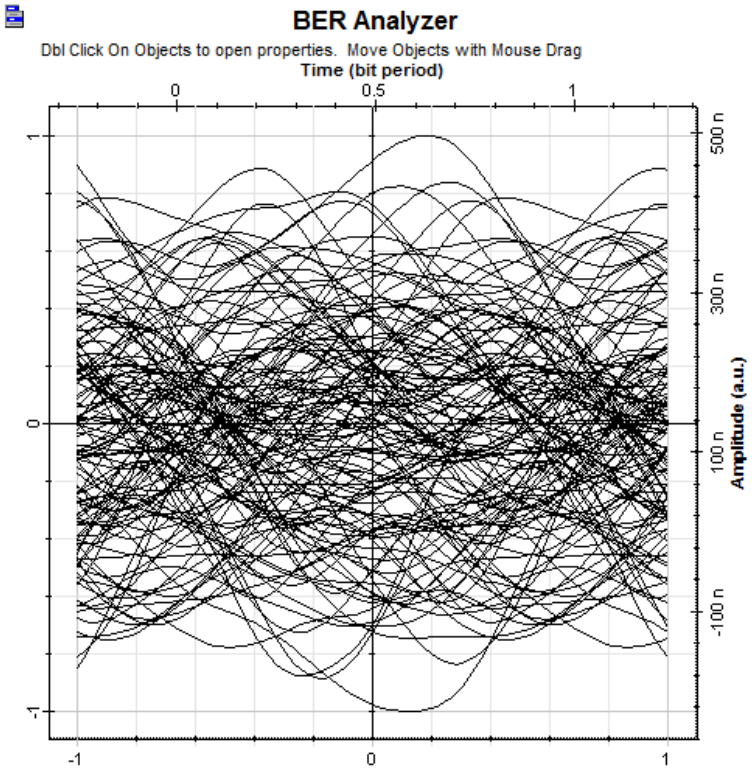

Figure 3.13 Eye diagram for 21 dBm transmit power.

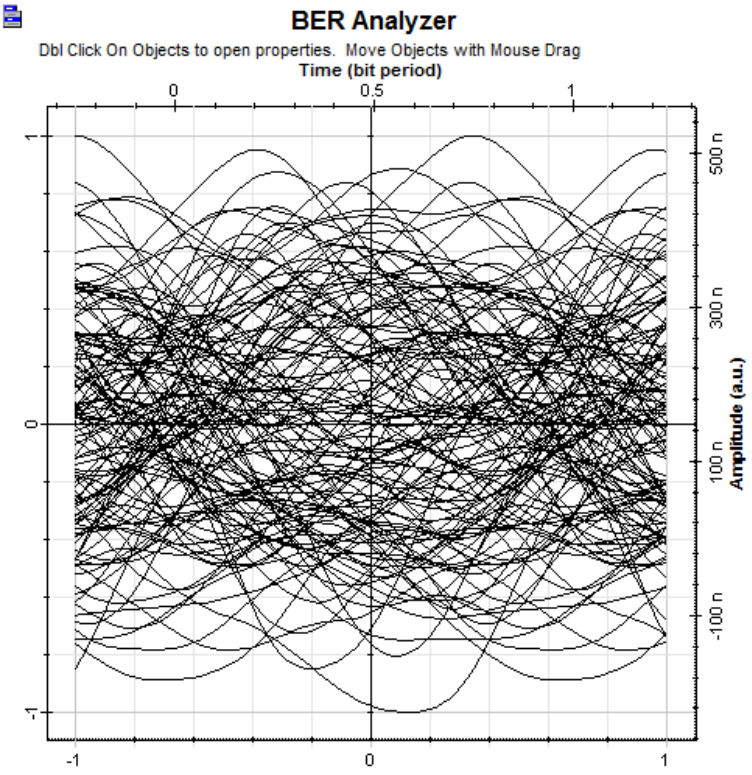

Figure 3.14 Eye diagram for 22 dBm transmit power.

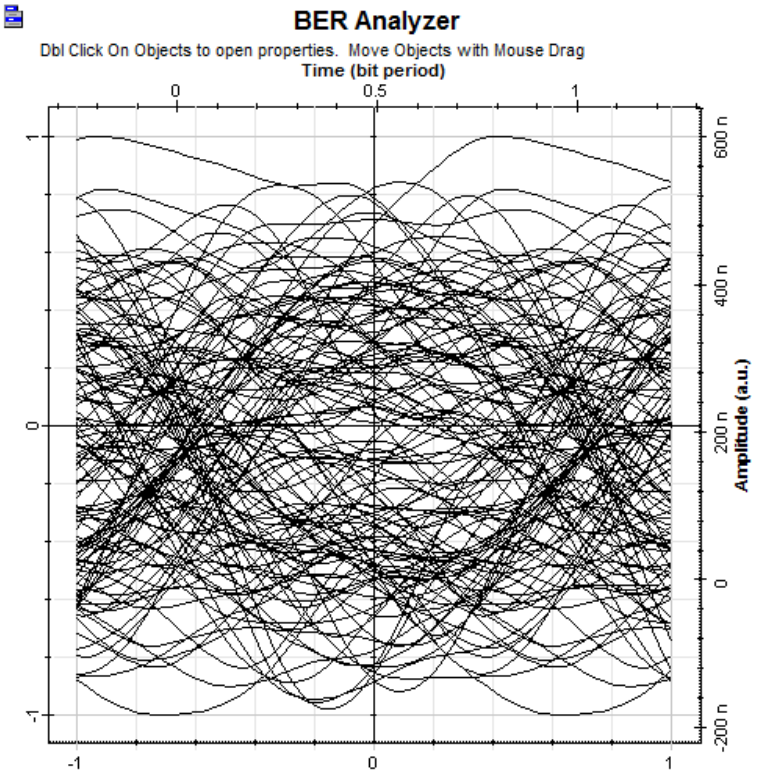

Figure 3.15 Eye diagram for 23 dBm transmit power.

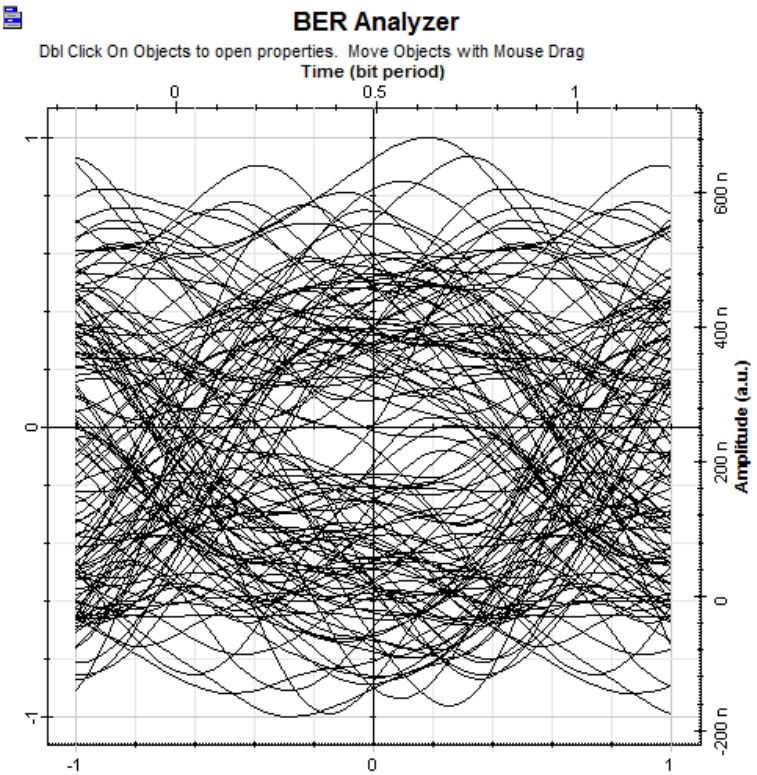

Figure 3.16 Eye diagram for 24 dBm transmit power.

As can be seen in Eye diagrams above, link can not be established by reason of 0 Q factor.

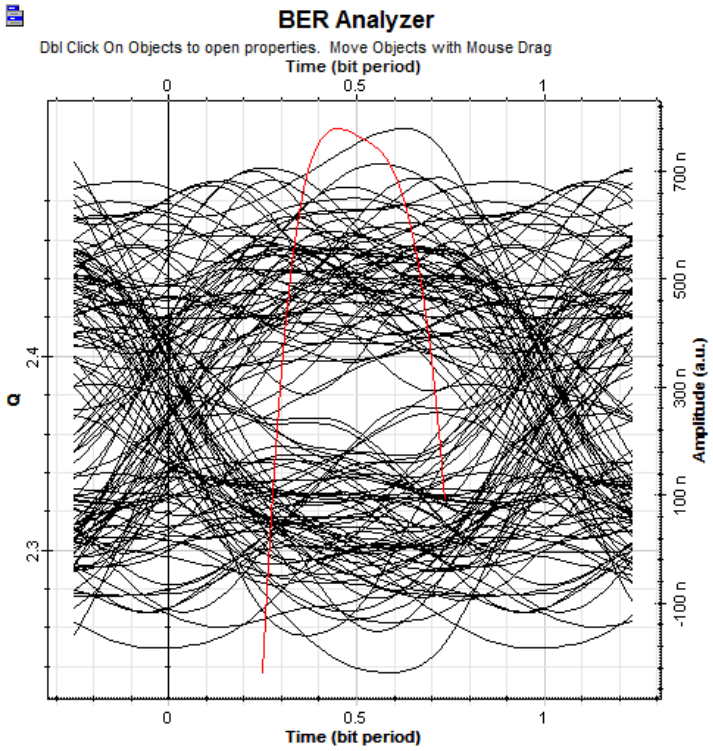

Figure 3.17 Eye diagram for 25 dBm transmit power.

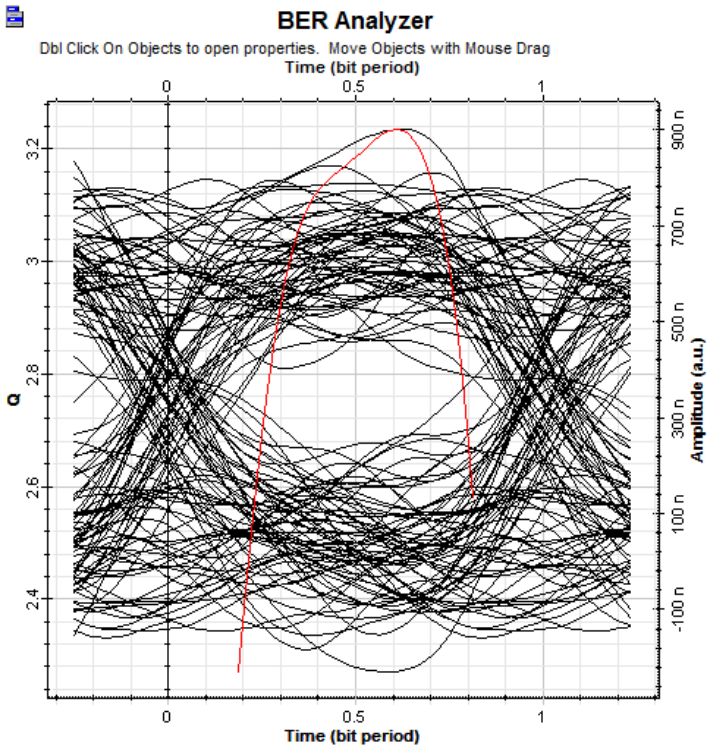

Figure 3.18 Eye diagram for 26 dBm transmit power.

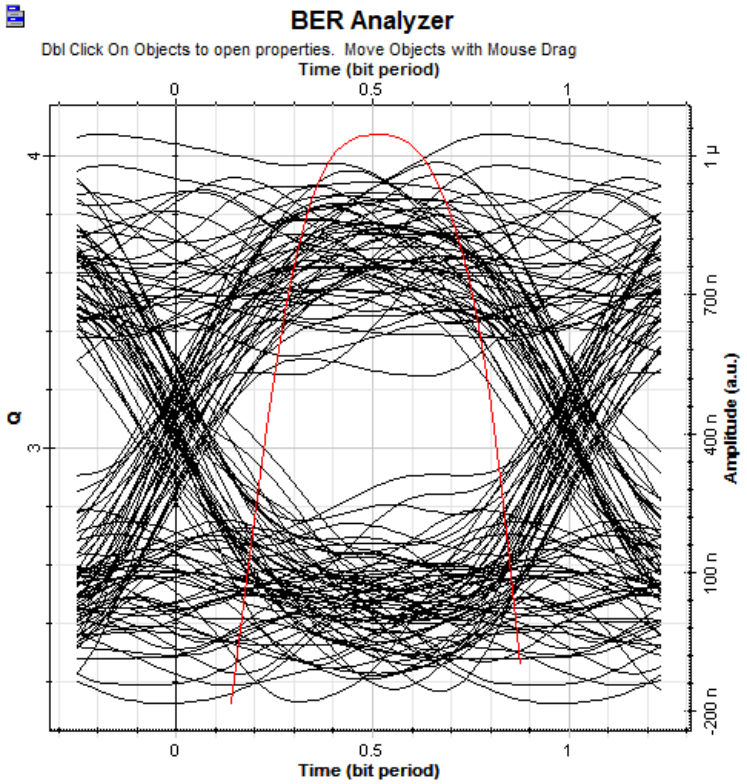

Figure 3.19 Eye diagram for 27 dBm transmit power.

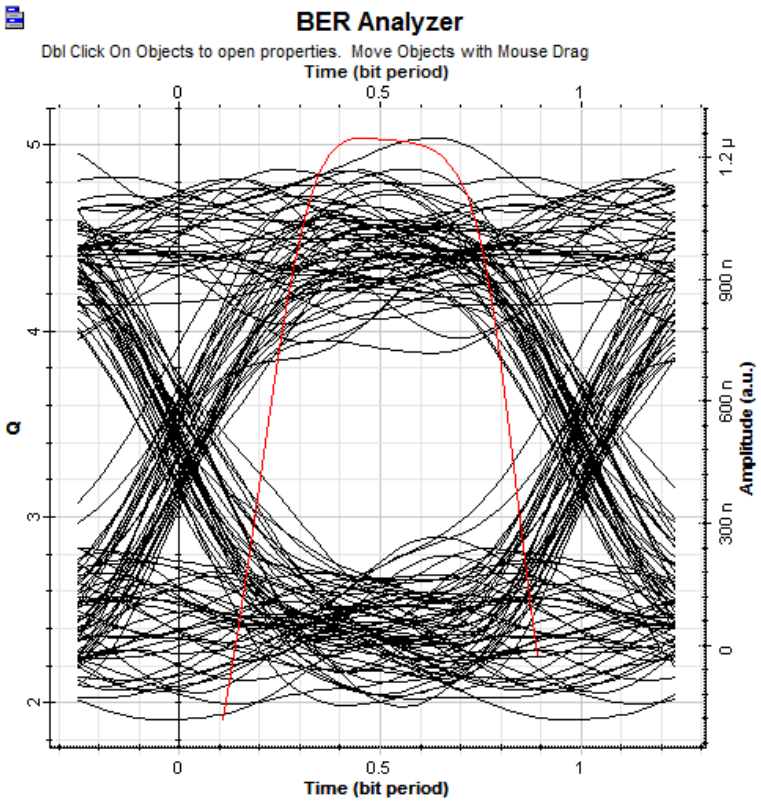

Figure 3.20 Eye diagram for 28 dBm transmit power.

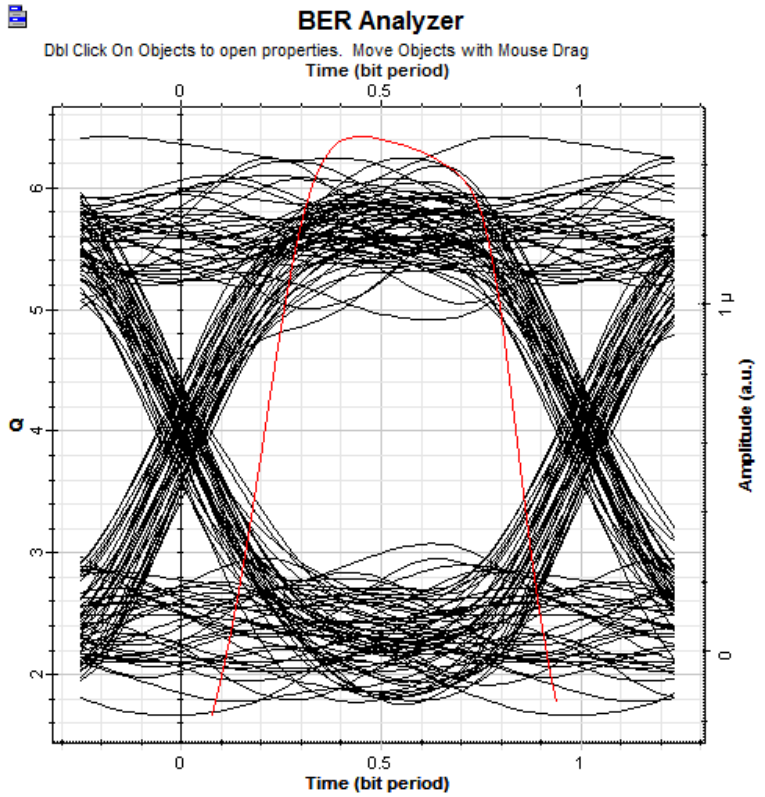

Figure 3.21 Eye diagram for 29 dBm transmit power.

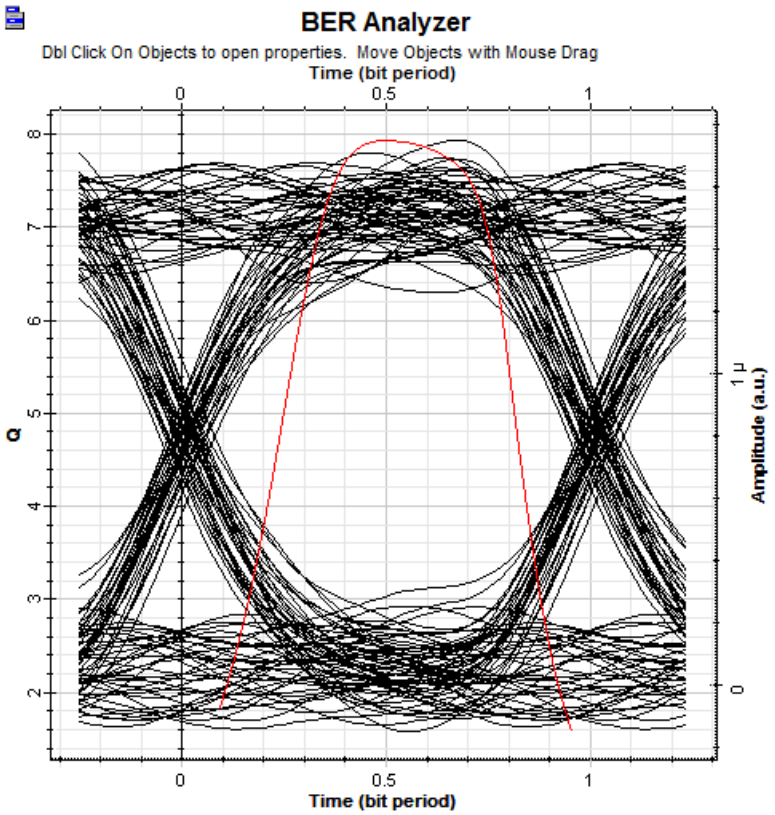

Figure 3.22 Eye diagram for 30 dBm transmit power.

Secondly, the distance, telescope diameter and data rate have been set at a constant value of 45.000 km, 25 cm and 50 Mbps, respectively as previous setup, but wavelength has been changed to 850 nm in order to understand variations in performance. The transmit power has been set at 14 levels which are from 17 dBm to 30 dBm, linearly as previous setup. As can be seen from the result of analysis, BER performance is better for 850 nm wavelength.

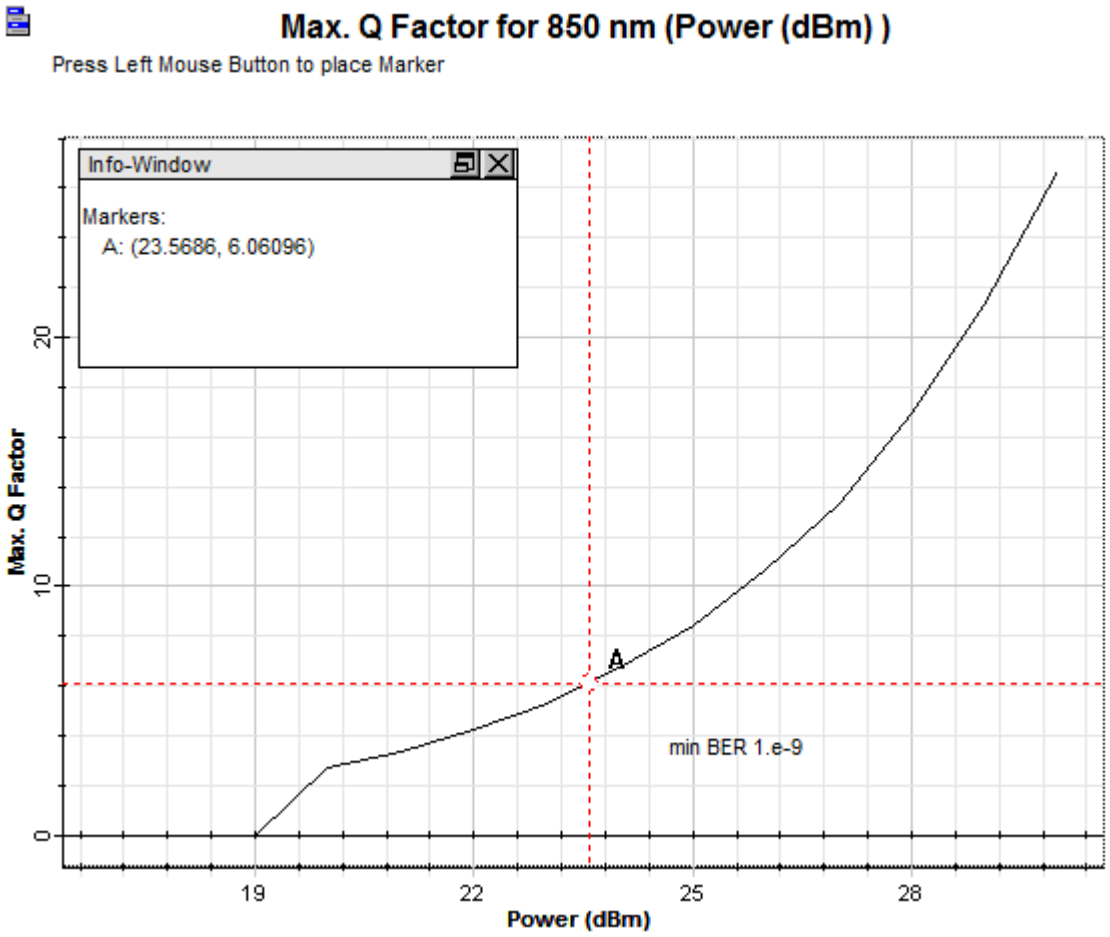

Figure 3.23 Q factor versus transmit power diagram at 850 nm wavelength.

As can be seen in Figure 3.23, Figure 3.24 and Figure 3.25, link can be establish at 19 dBm and 23 dBm transmit power is enough to obtain 10^{-9} BER for 850 nm wavelength.

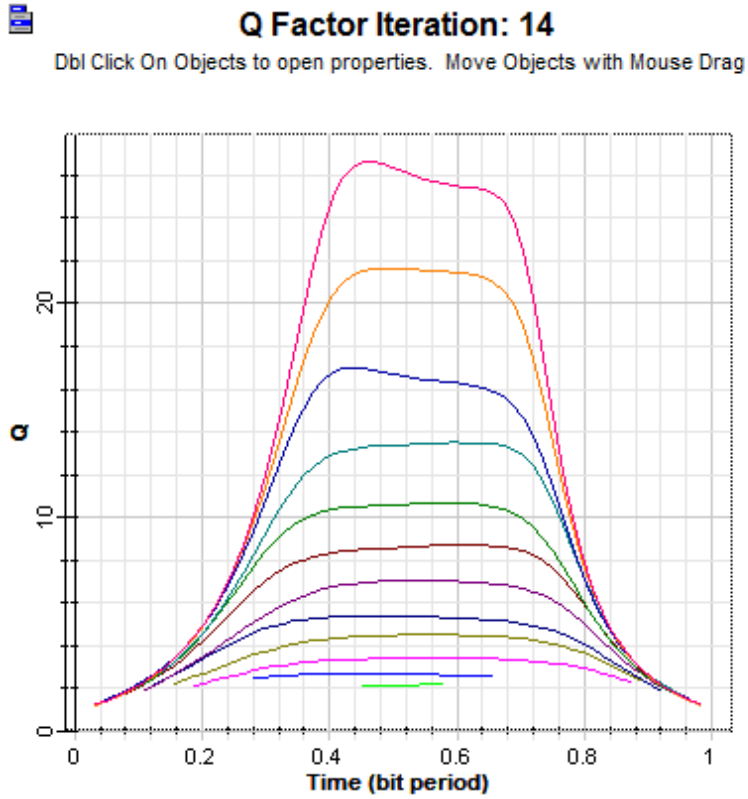

Figure 3.24 Maximum Q factor for each transmit power value.

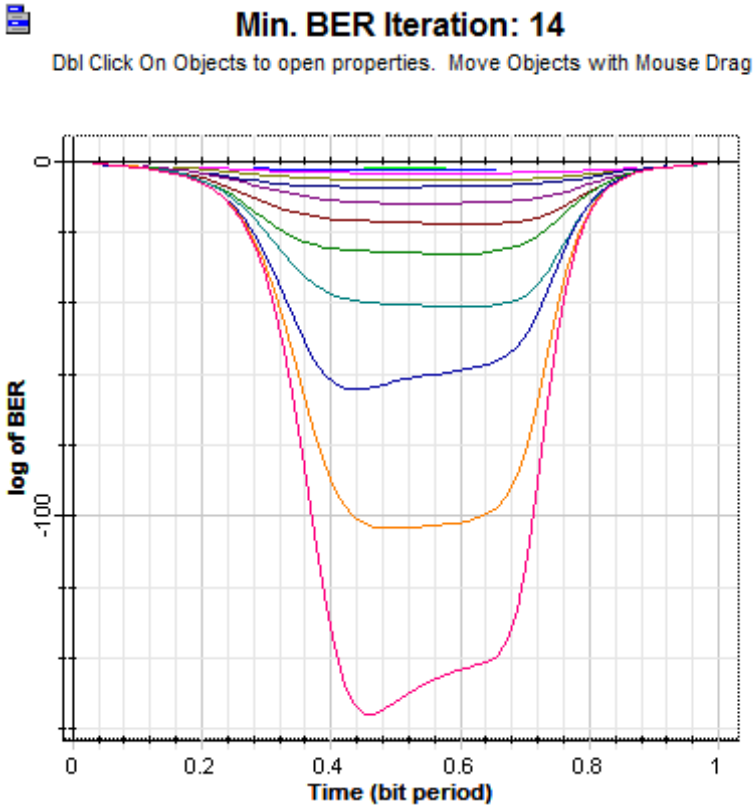

Figure 3.25 Minimum BER for each transmit power value.

Eye diagrams have been plotted for each transmit power value and shown in figures from 3.26 to 3.39. As can be seen in figures, eye diagrams have less jitter and more open than the eye diagrams of previous set up.

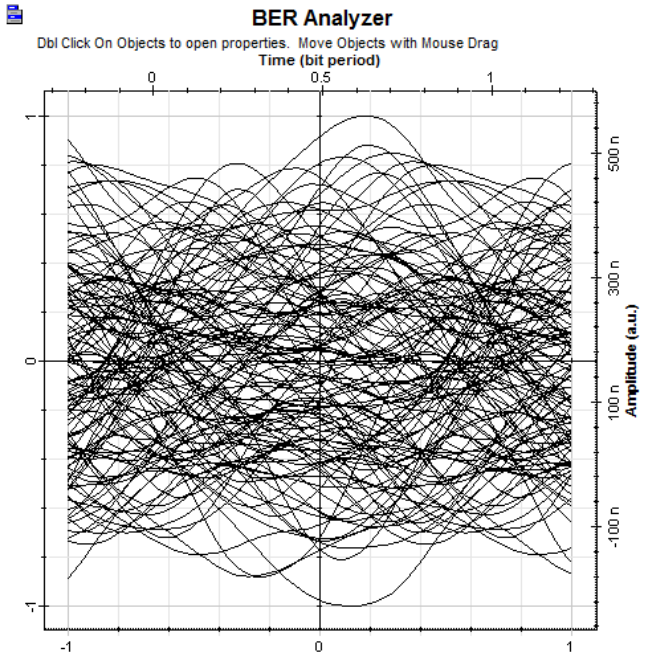

Figure 3.26 Eye diagram for 17 dBm transmit power.

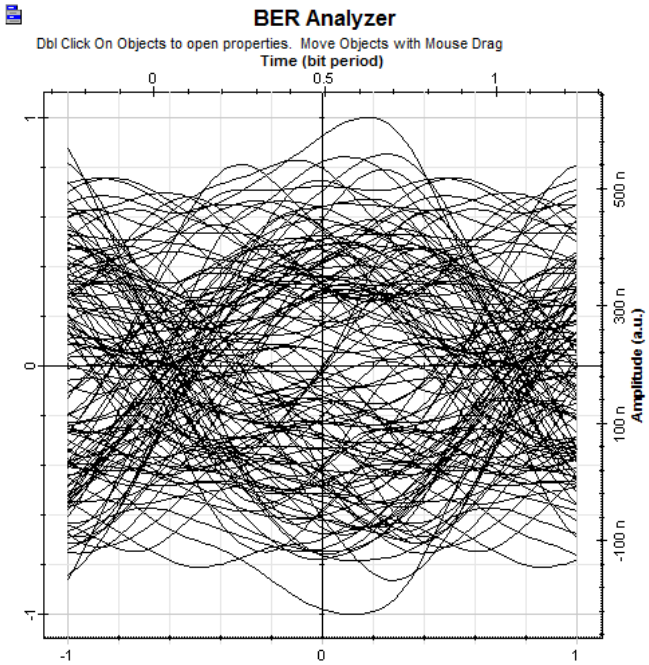

Figure 3.27 Eye diagram for 18 dBm transmit power.

As can be seen in Eye diagrams above, link can not be established by reason of 0 Q factor.

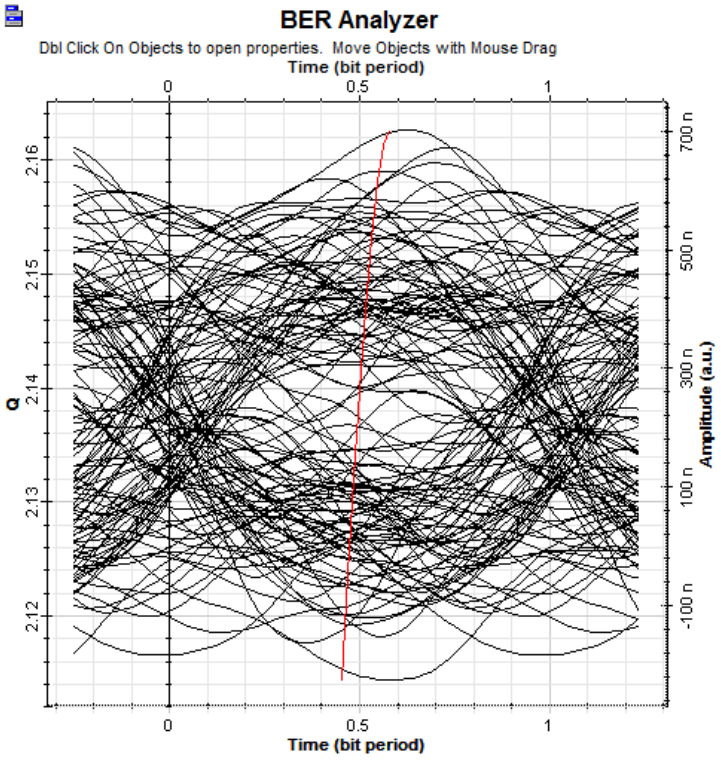

Figure 3.28 Eye diagram for 19 dBm transmit power.

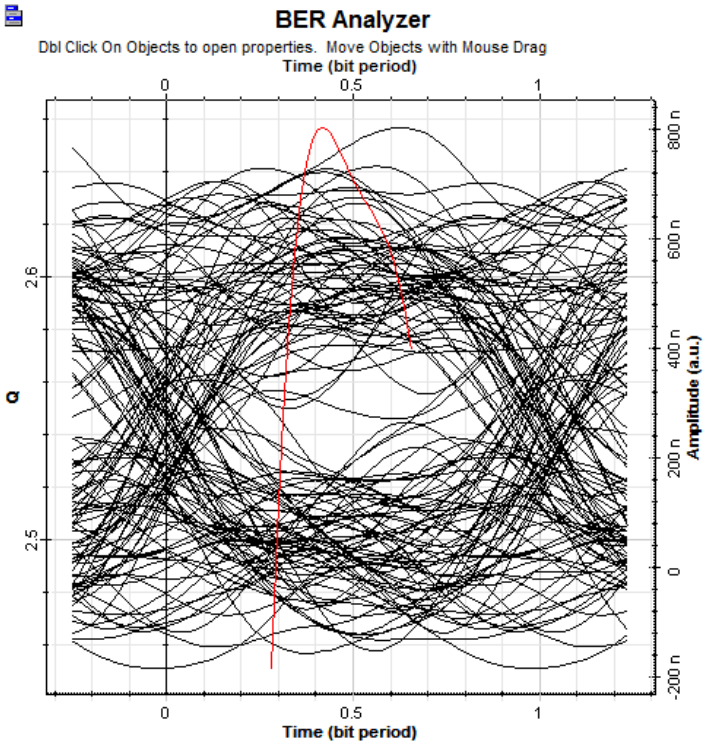

Figure 3.29 Eye diagram for 20 dBm transmit power.

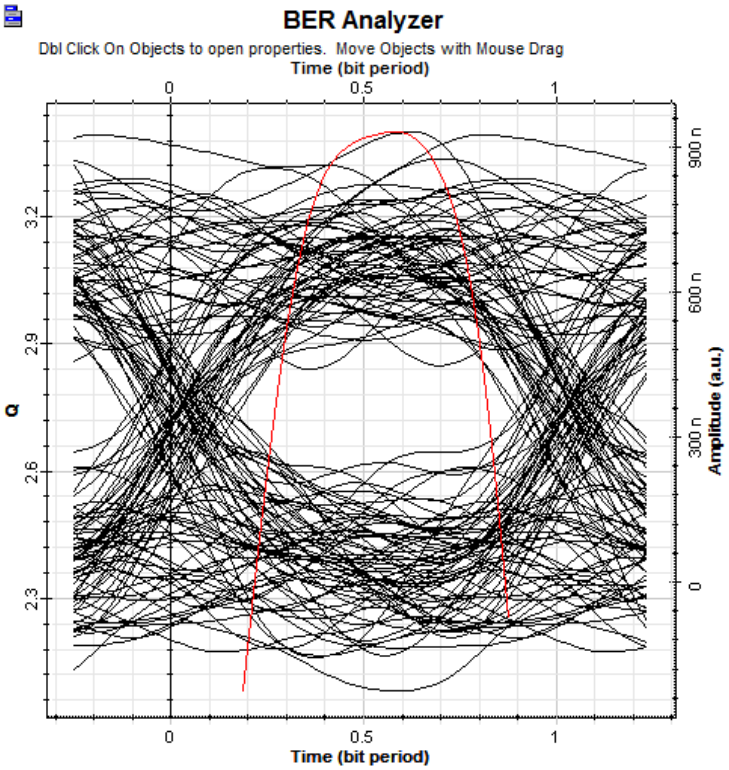

Figure 3.30 Eye diagram for 21 dBm transmit power.

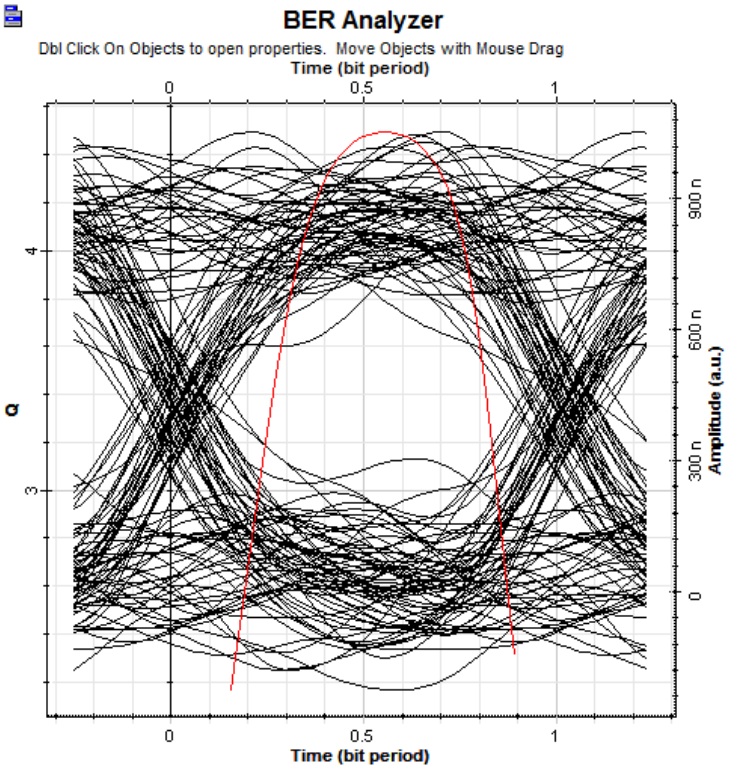

Figure 3.31 Eye diagram for 22 dBm transmit power.

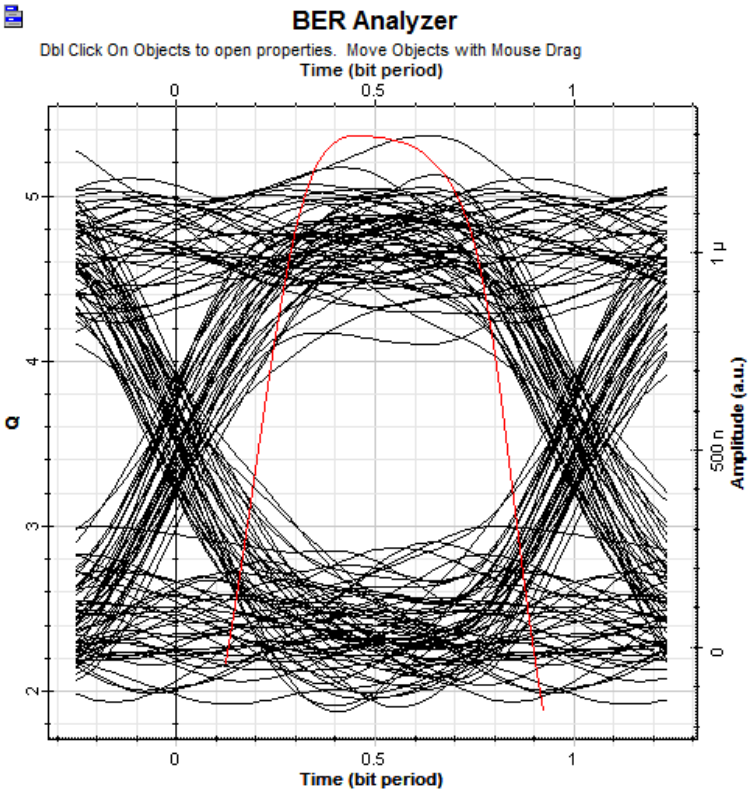

Figure 3.32 Eye diagram for 23 dBm transmit power.

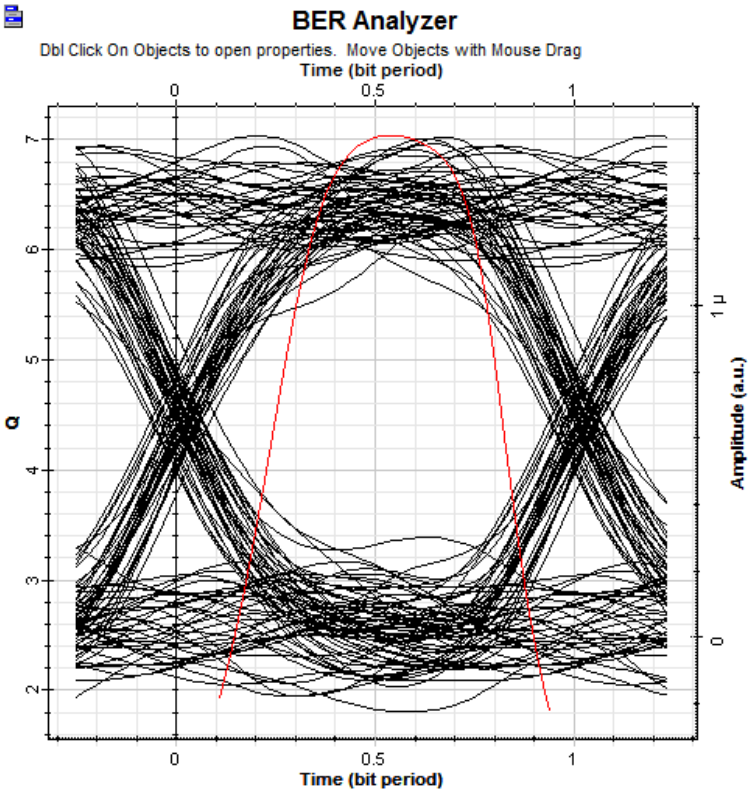

Figure 3.33 Eye diagram for 24 dBm transmit power.

As can be seen in figures below, when the transmit power increases, the eye diagram consist of less jitter and the opening of eye increases.

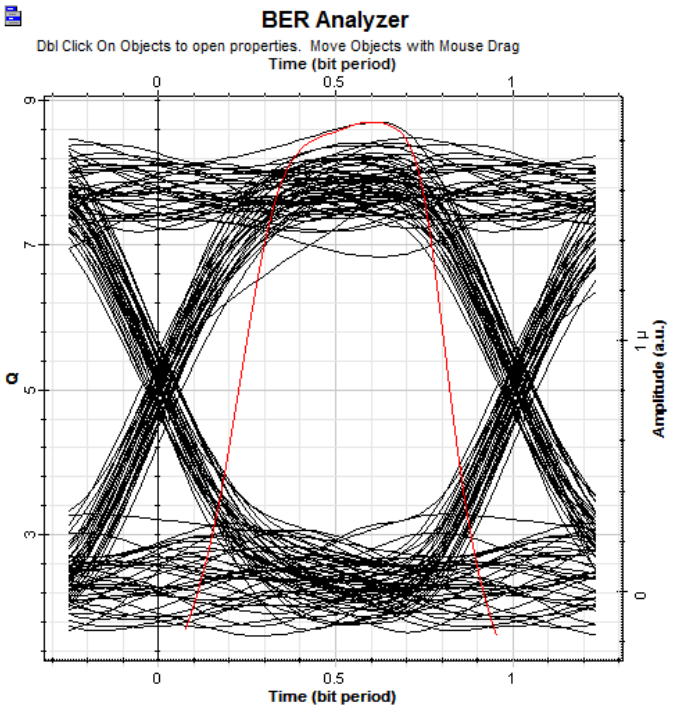

Figure 3.34 Eye diagram for 25 dBm transmit power.

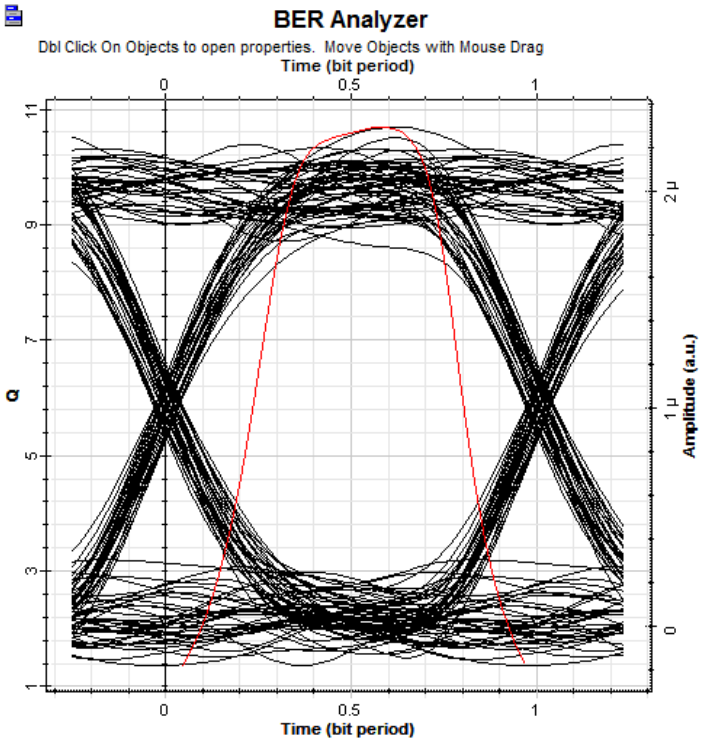

Figure 3.35 Eye diagram for 26 dBm transmit power.

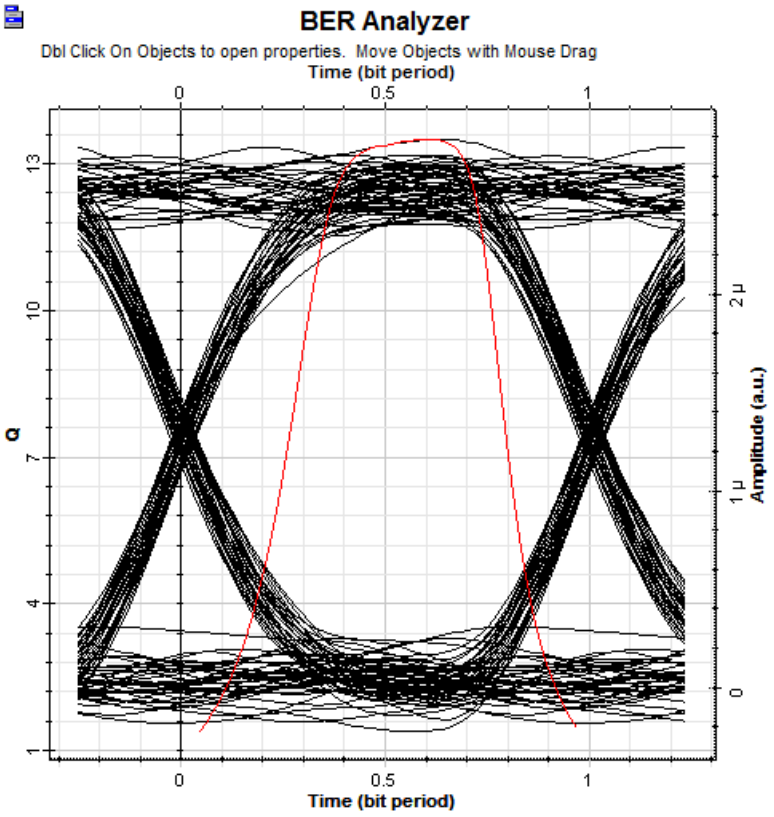

Figure 3.36 Eye diagram for 27 dBm transmit power.

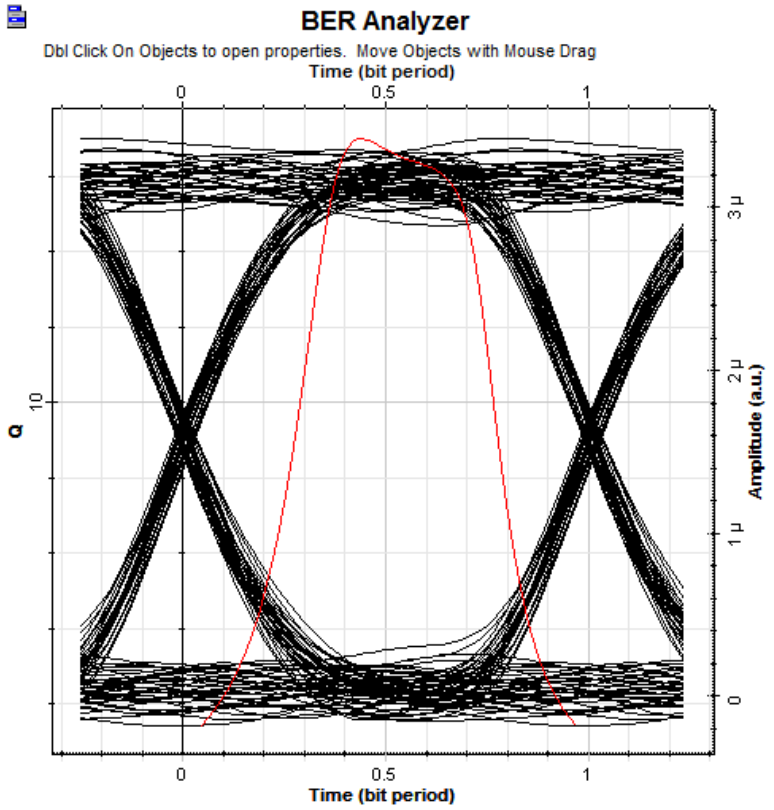

Figure 3.37 Eye diagram for 28 dBm transmit power.

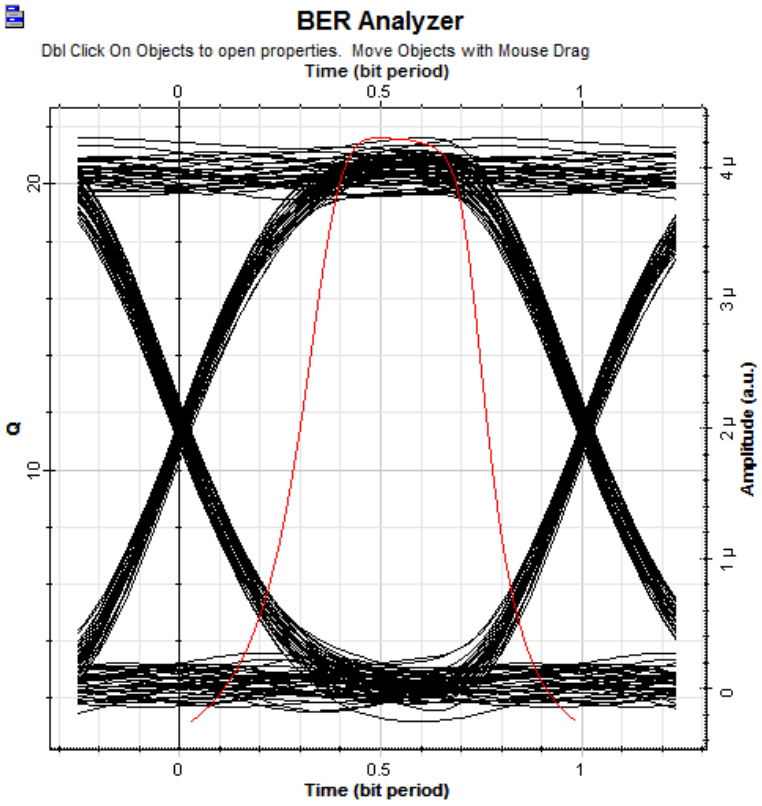

Figure 3.38 Eye diagram for 29 dBm transmit power.

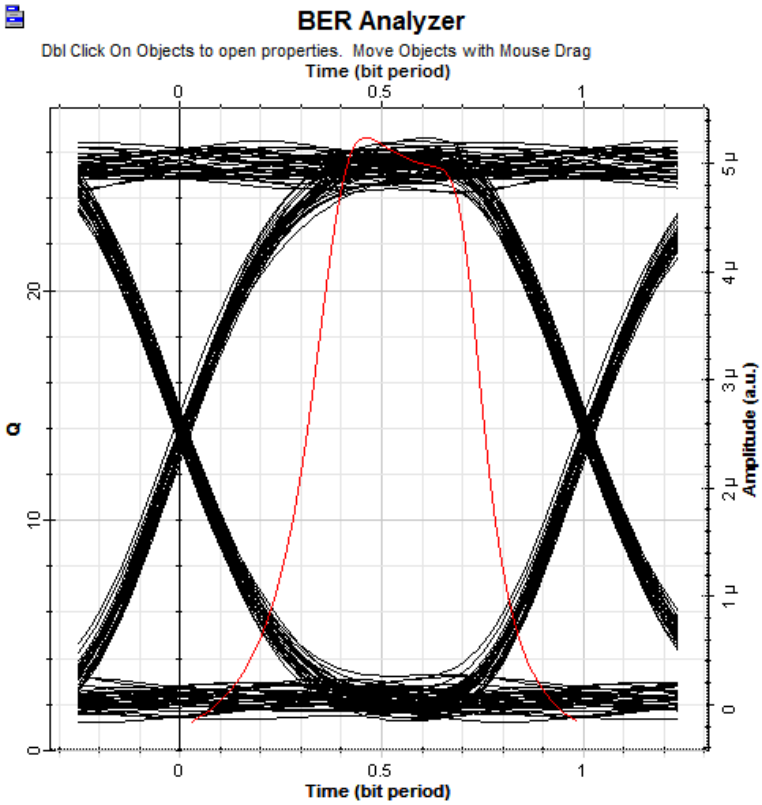

Figure 3.39 Eye diagram for 30 dBm transmit power.

In order to understand the wavelength's effect on the system performance more clearly, simulation has been performed with various wavelengths which are used for inter-satellite laser communication

The distance, telescope diameter and data rate have been set at a constant value of 45.000 km, 25 cm, 50 Mbps, respectively as previous setup. Transmit power has been set to 29 dBm, this is because the minimum power requirements for obtaining 10^{-9} BER at 1550 nm is 29 dBm.

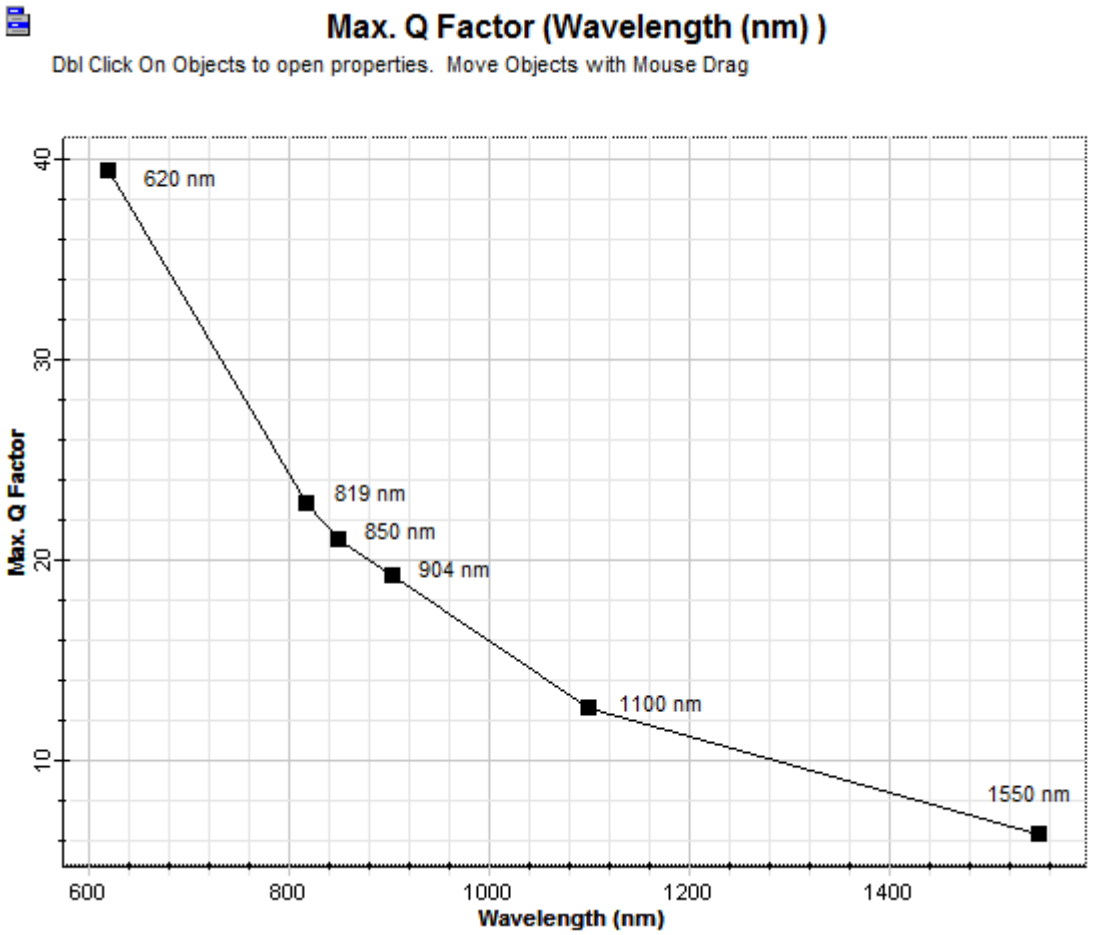

Figure 3.40 Q factor diagram at 620 nm, 819 nm, 850 nm, 904 nm, 1100 nm and 1550 nm wavelength.

Maximum Q factor and minimum BER have been plotted in Figure 3.41 and Figure 3.42, respectively for each wavelength.

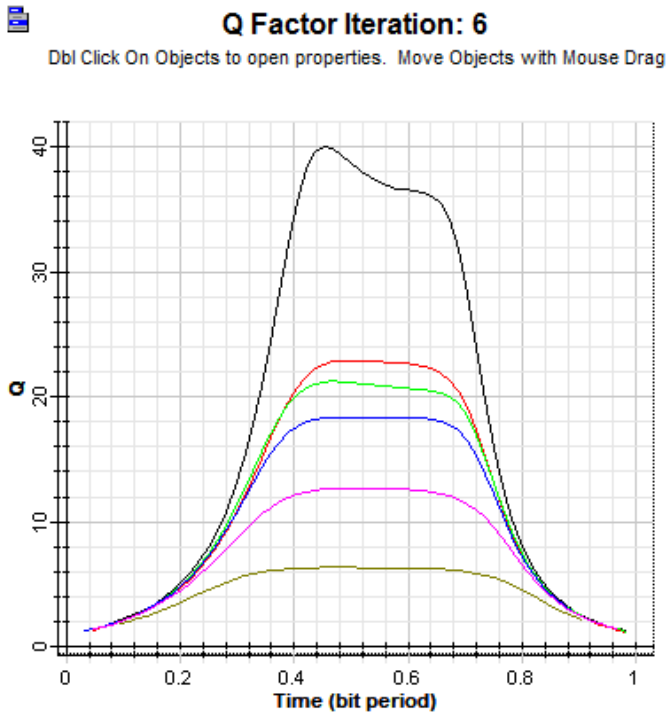

Figure 3.41 Maximum Q factor for each wavelength.

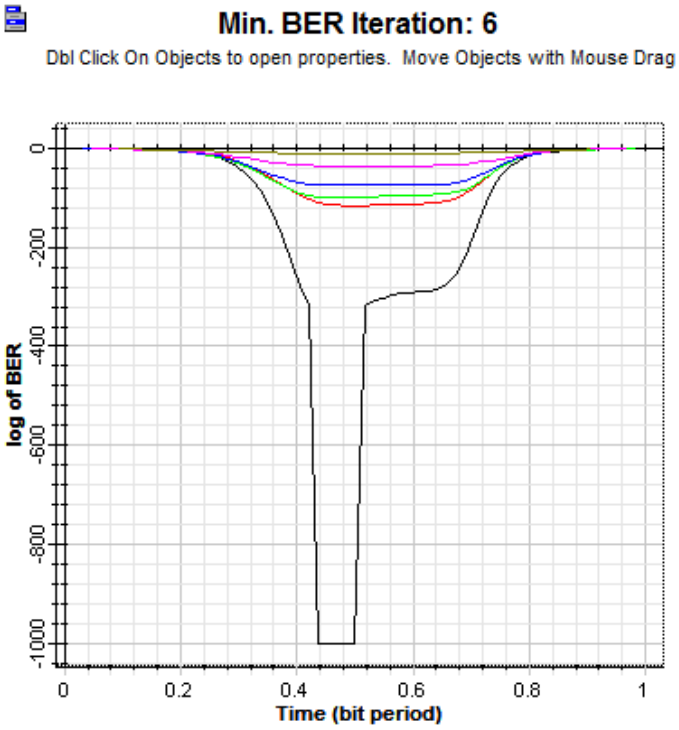

Figure 3.42 Minimum BER for each wavelength.

Eye diagrams have been plotted for each transmit power value and shown in figures from 3.43 to 3.48.

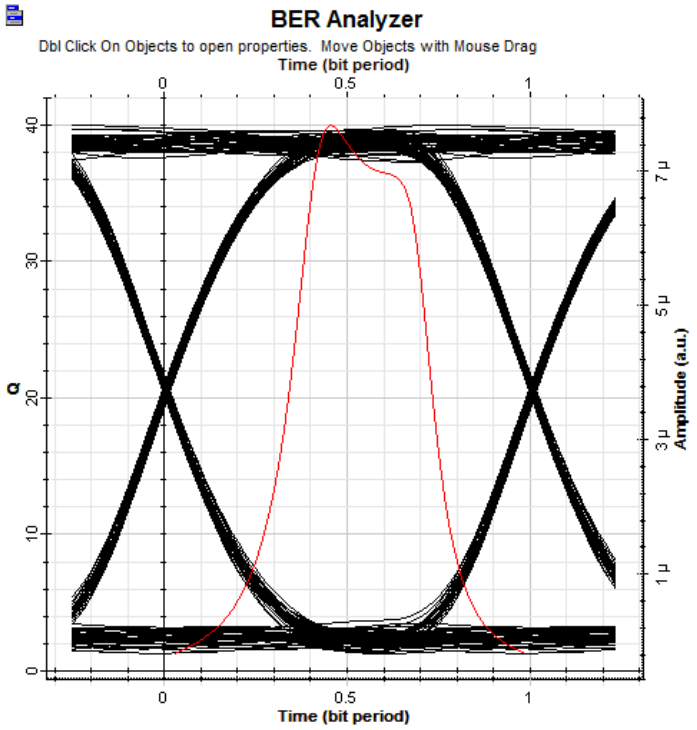

Figure 3.43 Eye diagram for 620 nm wavelength.

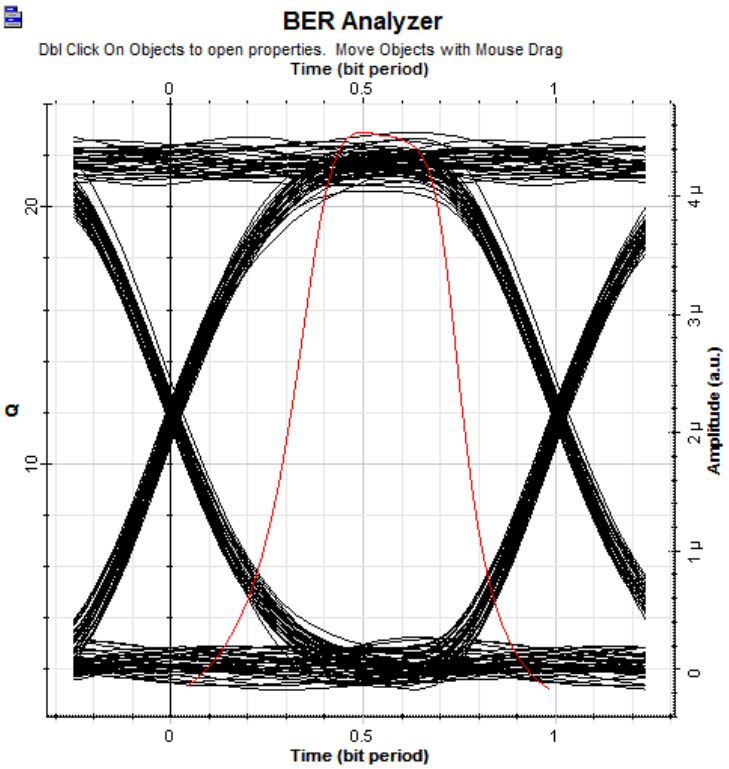

Figure 3.44 Eye diagram for 819 nm wavelength.

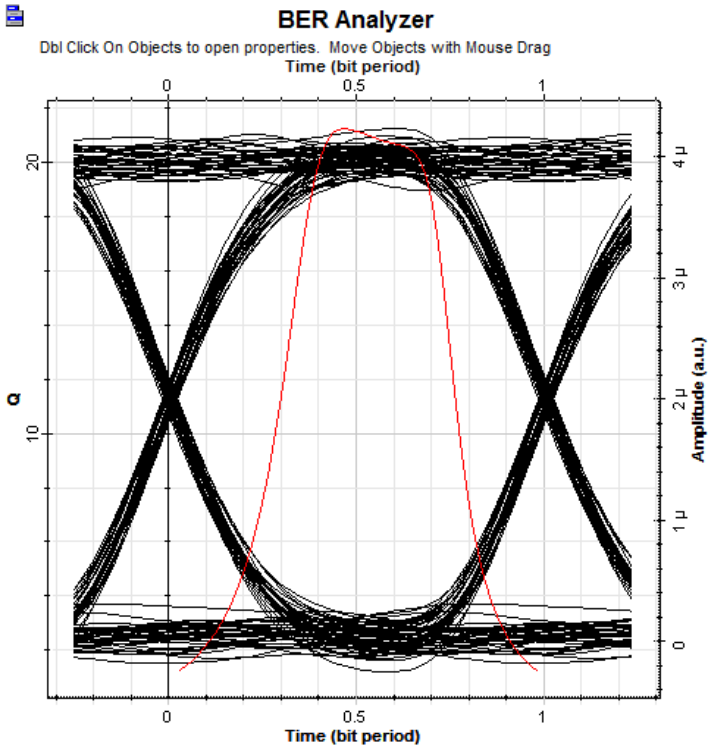

Figure 3.45 Eye diagram for 850 nm wavelength.

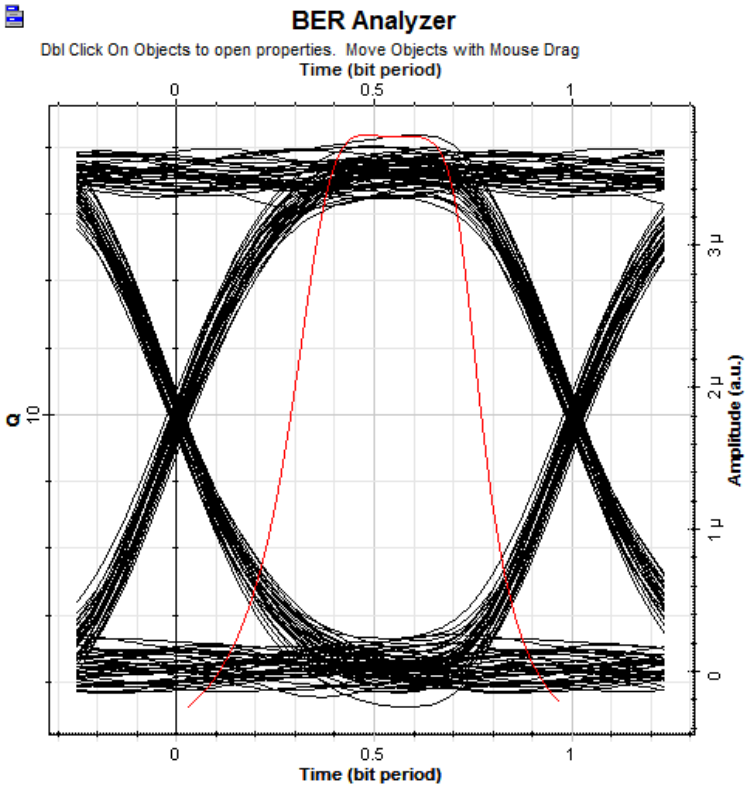

Figure 3.46 Eye diagram for 904 nm wavelength.

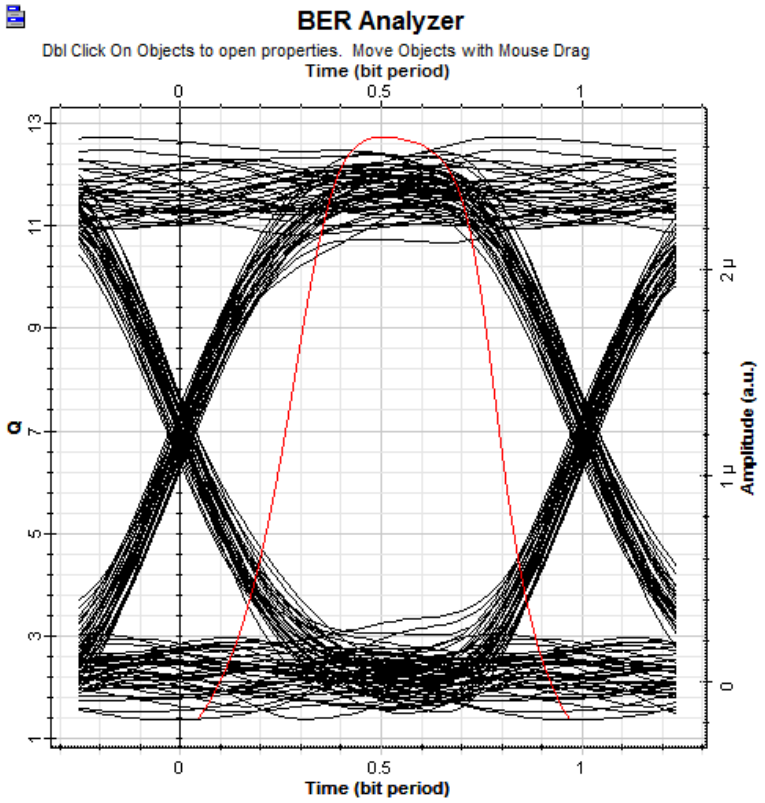

Figure 3.47 Eye diagram for 1100 nm wavelength.

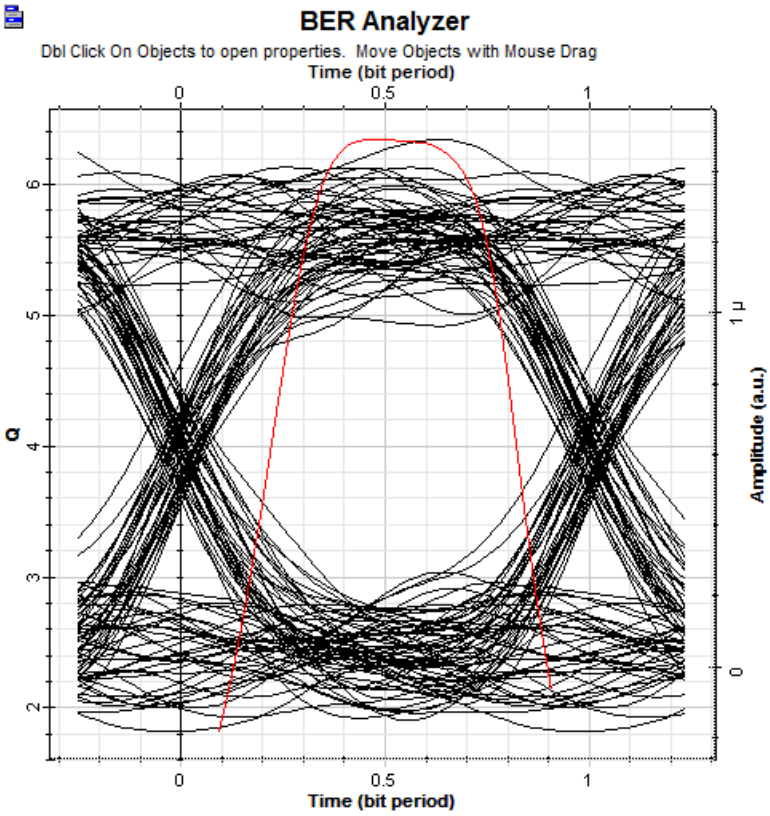

Figure 3.48 Eye diagram for 1550 nm wavelength.

Table 3.1 Maximum Q factor recorded for respective wavelengths.

Wavelength (nm)	Max Q-Factor
620	39,4296
819	22,8384
850	21,0328
904	19,187
1100	12,6371
1550	6,34252

It can be concluded from the figures between 3.40 to 3.48 and from Table 3.1 that signal qualities are better at shorter wavelengths due to bigger value of Q-factor. However, by using shorter wavelength, the effect of scattering and on account of this, attenuation will be increased. Though this problem disappears in free-space communications above the earth atmosphere, small and large particles such as space dusts and meteorites may be within the optical signal's way [3]. On the other hand, one of the most important reasons of using 1550 nm is its compatibility with current technology and devices [6].

3.2 Relationship between Q Factor, Range and Wavelength

The transmit power, wavelength, telescope diameter and data rate have been set at a constant value of 23 dBm, 850 nm, 25 cm, 50 Mbps, respectively. The distance of inter-satellite link has been set from 1000 km up to 84.000 km, linearly. This is because maximum GEO-GEO link is 84.000 km. As can be seen in Figure 3.49, 10^{-9} BER can not be achieved for distances greater than 44165 km at 850 nm wavelength.

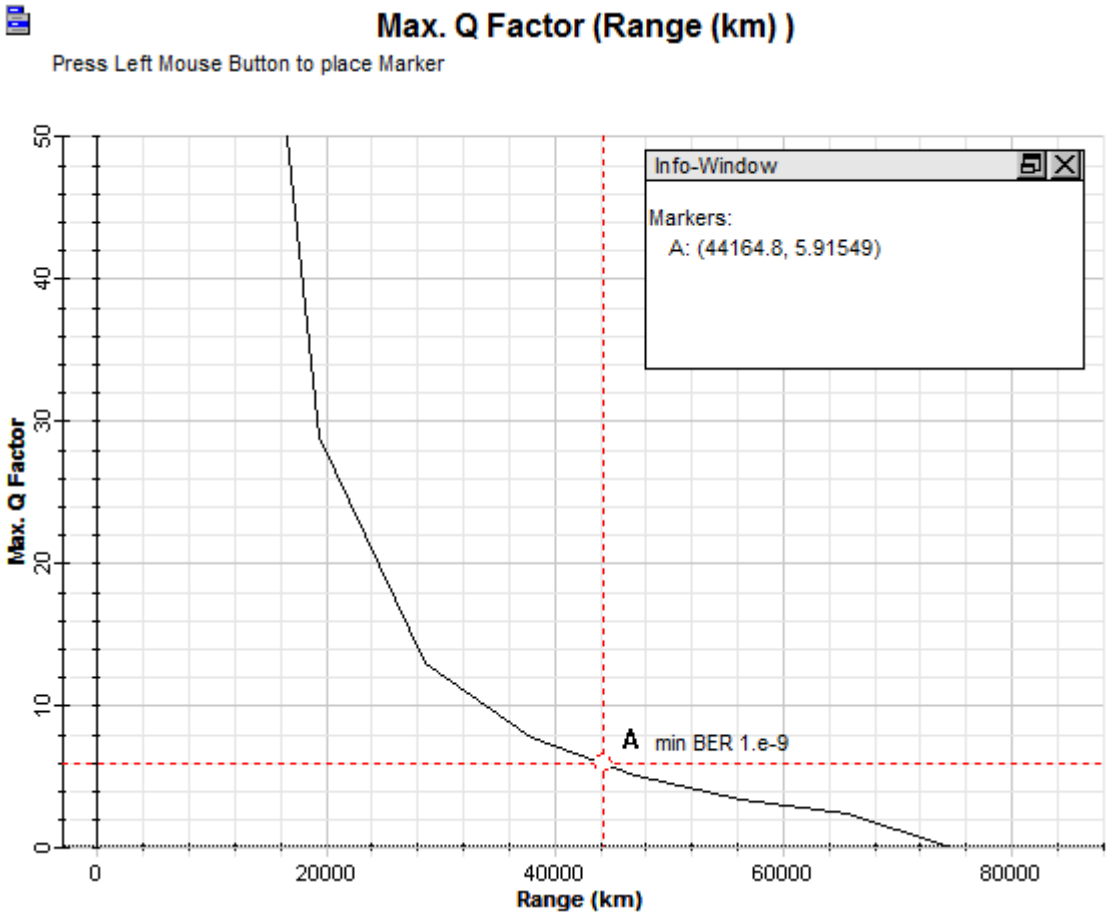

Figure 3.49 Q factor versus distance diagram at 850 nm wavelength.

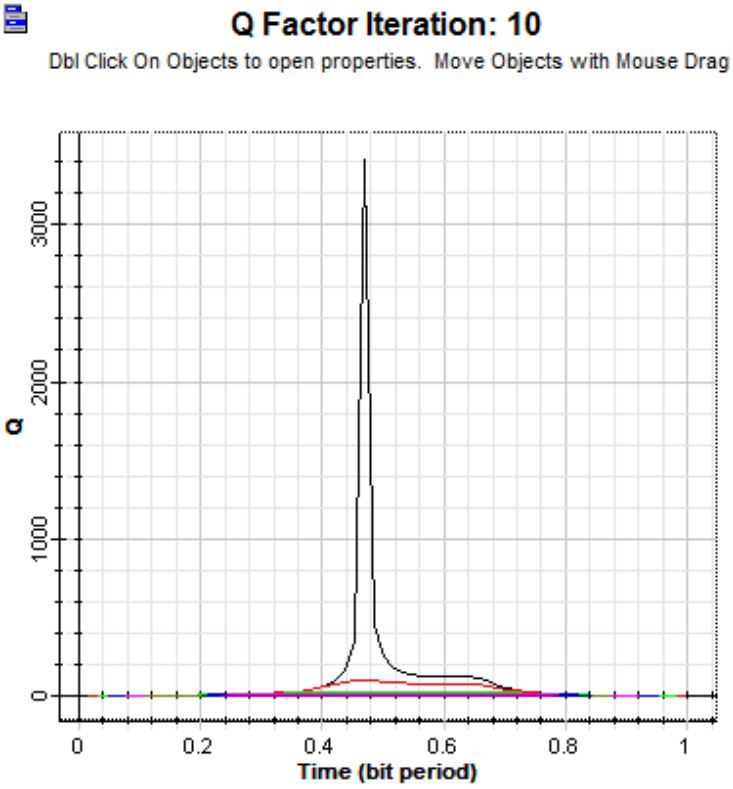

Figure 3.50 Maximum Q factor for each distance.

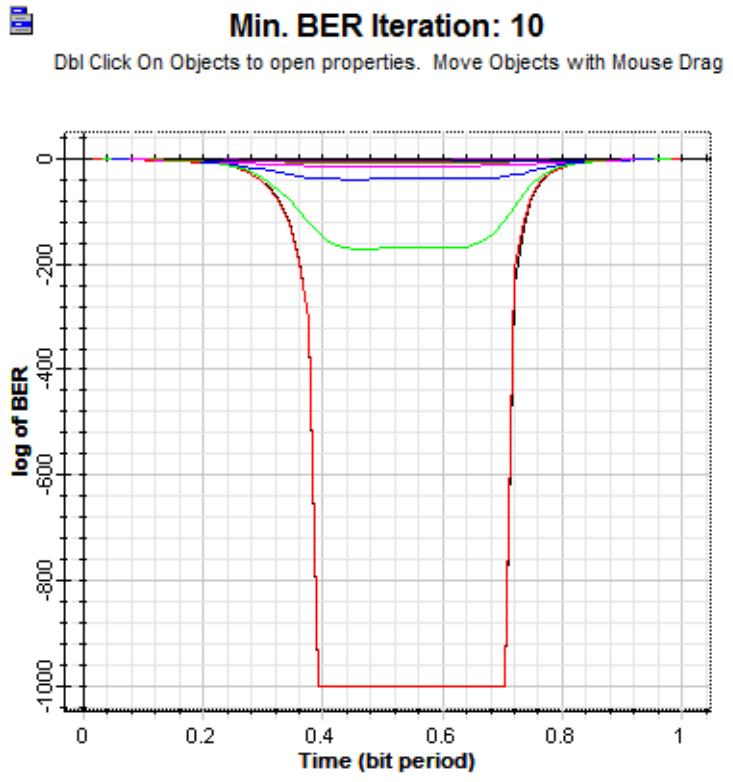

Figure 3.51 Minimum BER for each distance.

Eye diagrams have been plotted for each distance and shown in figures from 3.52 to 3.61.

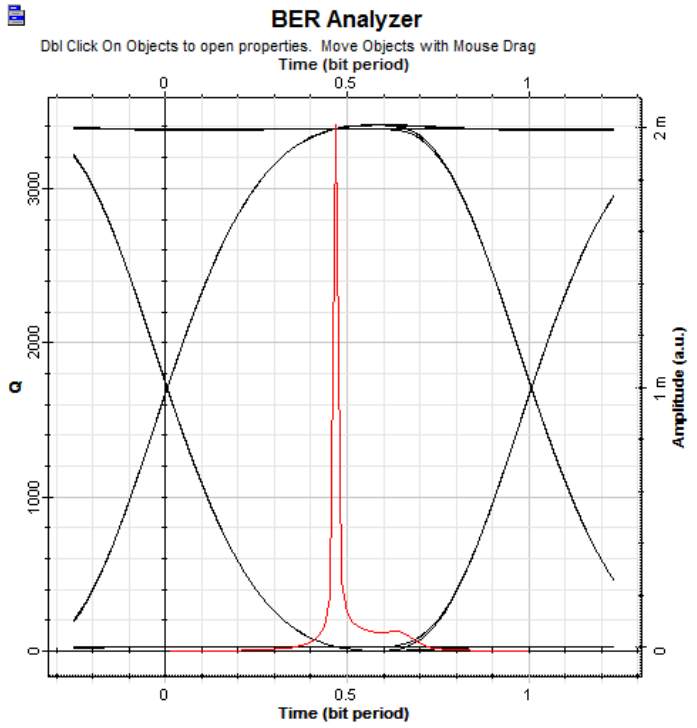

Figure 3.52 Eye diagram for 1000 km distance.

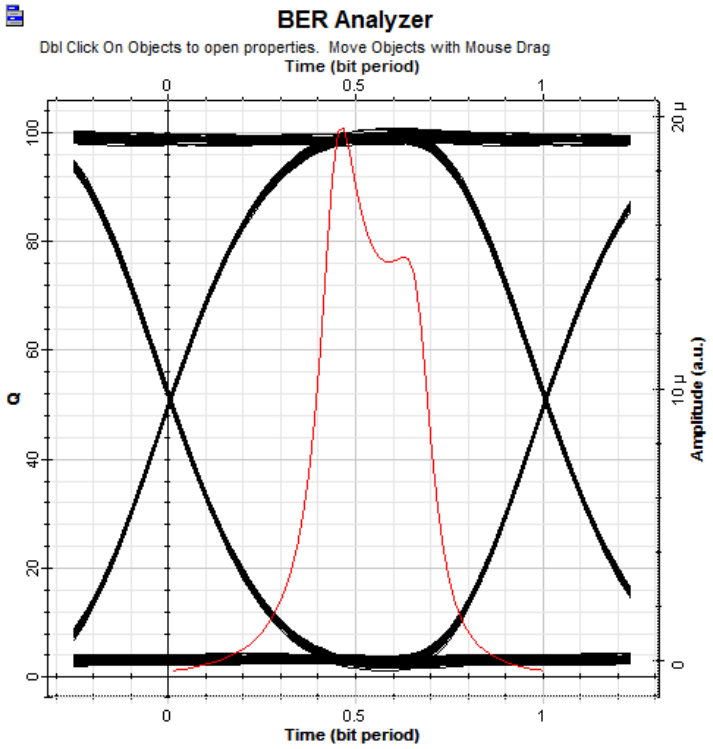

Figure 3.53 Eye diagram for 10222 km distance.

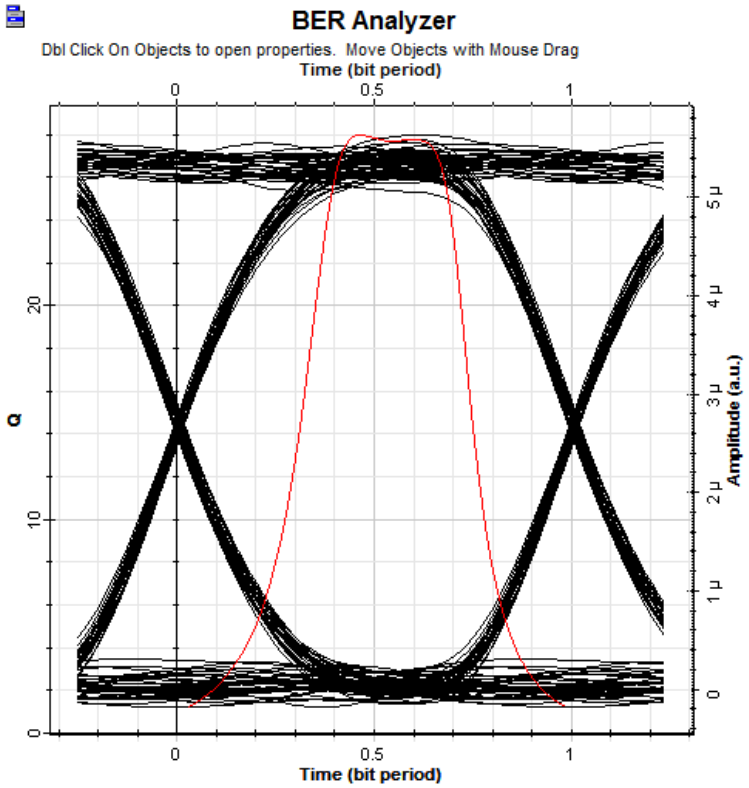

Figure 3.54 Eye diagram for 19444 km distance.

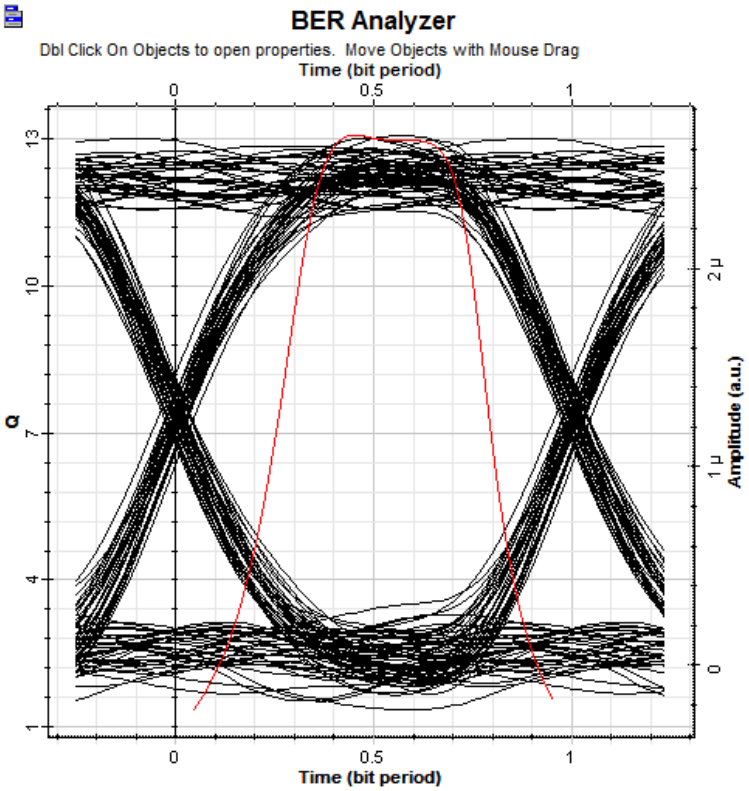

Figure 3.55 Eye diagram for 28667 km distance.

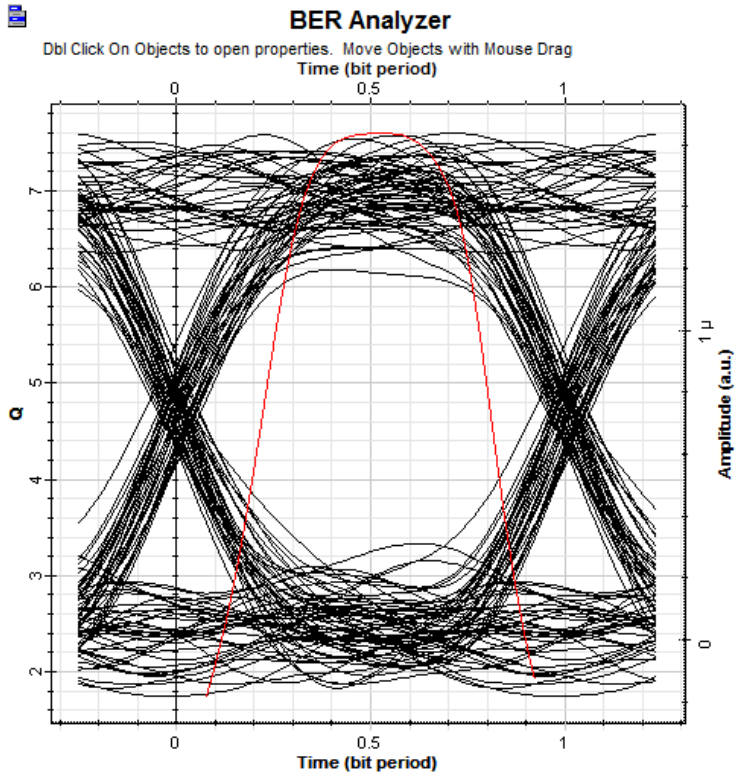

Figure 3.56 Eye diagram for 37889 km distance.

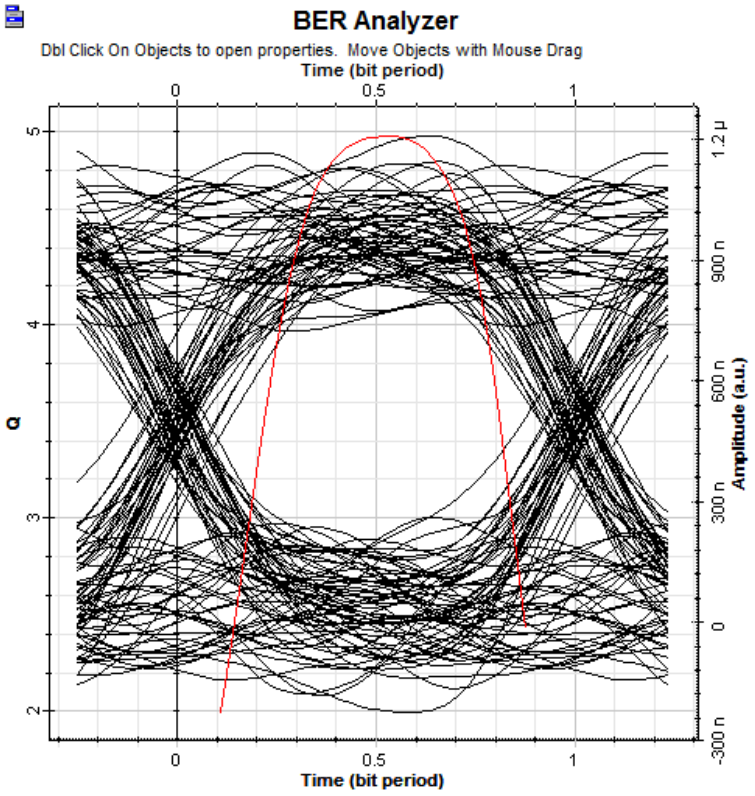

Figure 3.57 Eye diagram for 47111 km distance.

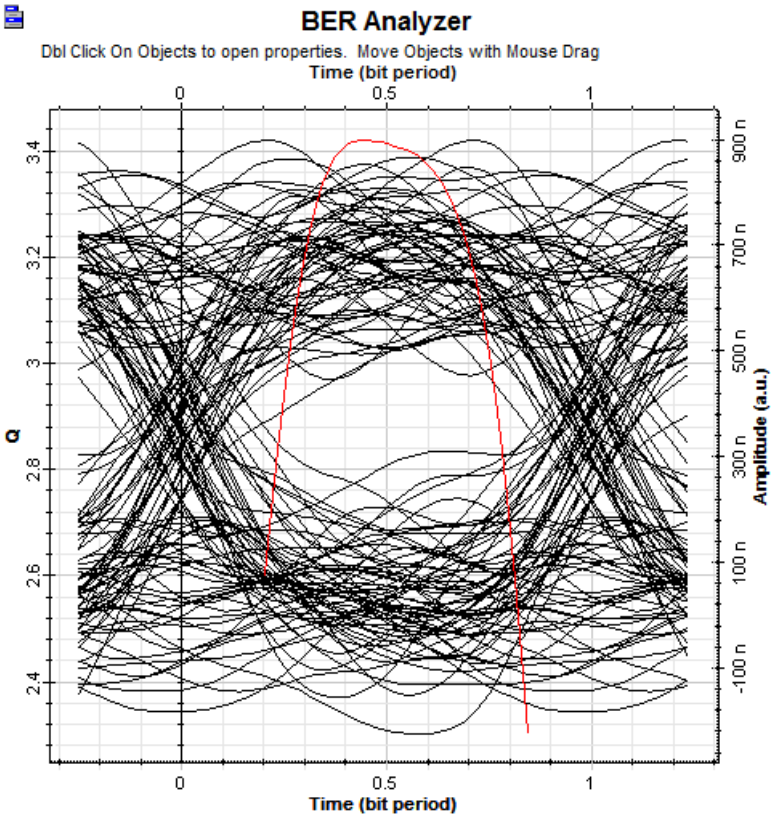

Figure 3.58 Eye diagram for 56333 km distance.

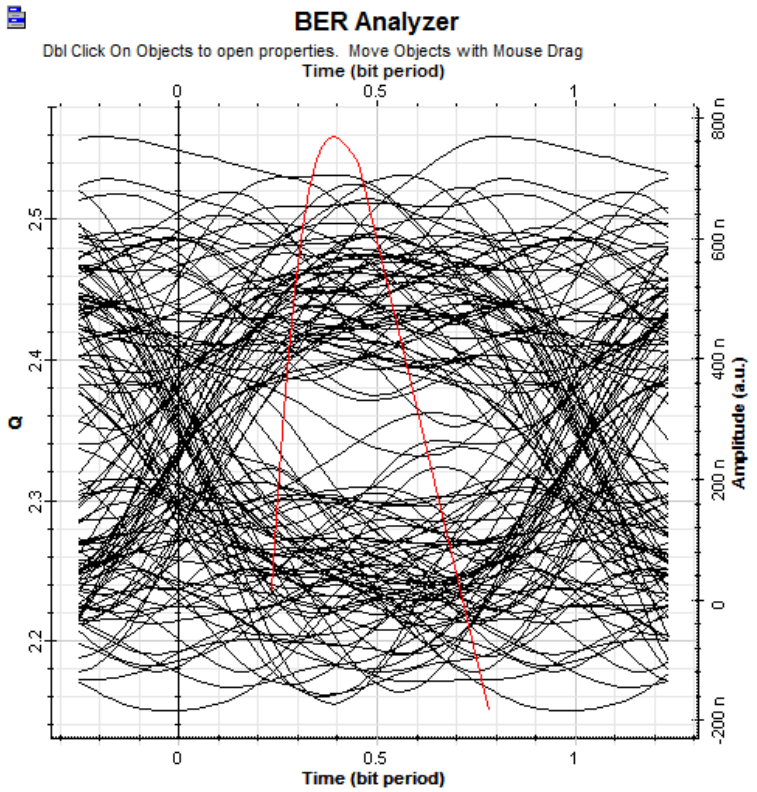

Figure 3.59 Eye diagram for 65555 km distance.

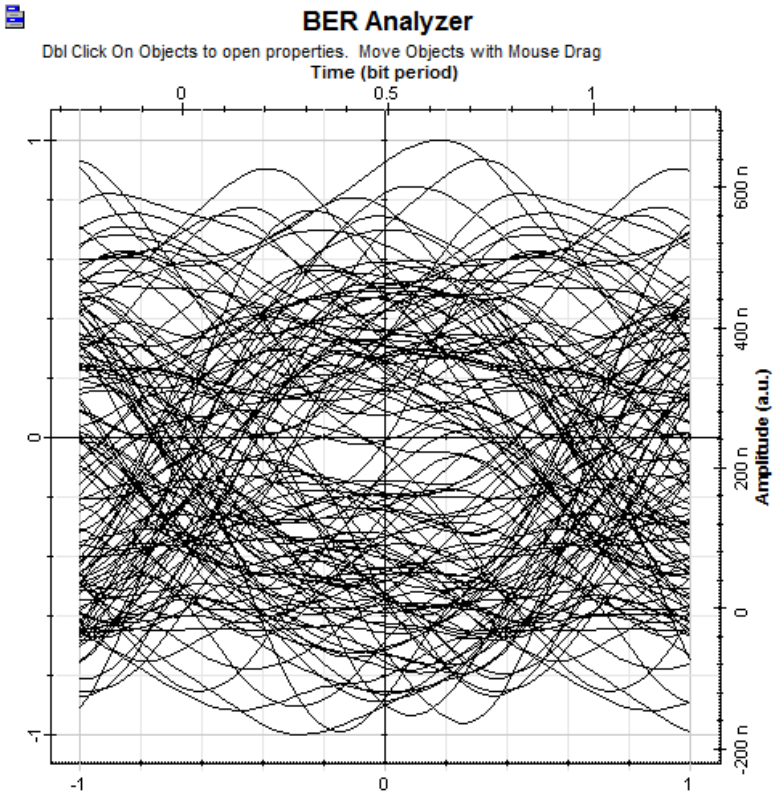

Figure 3.60 Eye diagram for 74778 km distance.

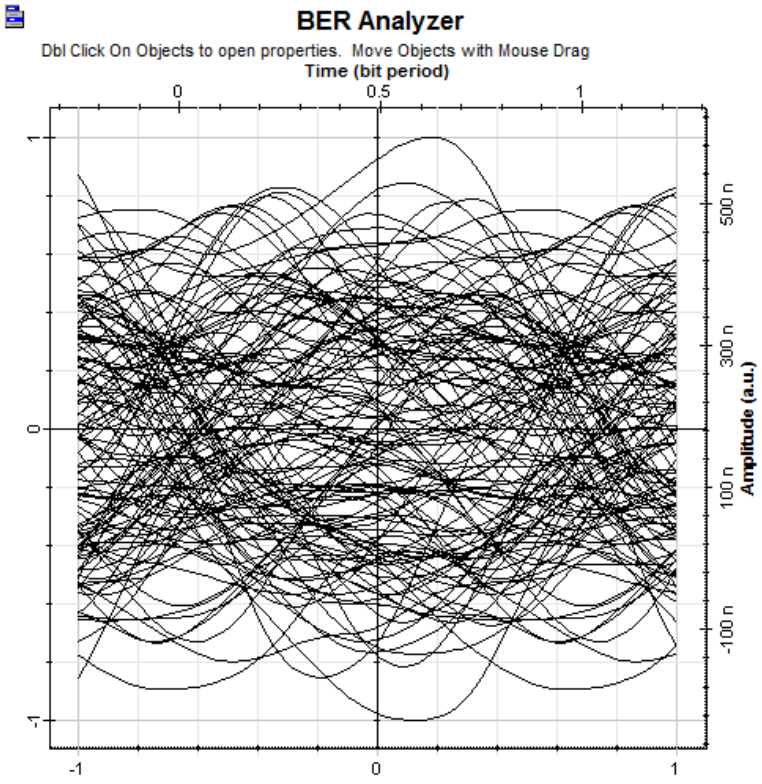

Figure 3.61 Eye diagram for 84000 km distance.

Simulation has been repeated in order to determine performance changes with different wavelengths. Transmit power, telescope diameter and data rate have been set at a constant value of 29 dBm, 25 cm, 50 Mbps, respectively. The distance has been adjusted from 1000 km up to 45.000 km and wavelength has been set to 620 nm, 819 nm, 850 nm, 904 nm, 1100 nm, 1550 nm, respectively. As can be seen in Figure 3.62 and Figure 3.63, 10^{-9} BER can be obtained for all wavelengths however signal quality is much better for shorter wavelengths. In figure 3.63, max Q factor scale has been started 6 which indicates 10^{-9} BER in order to understand graphic more clearly.

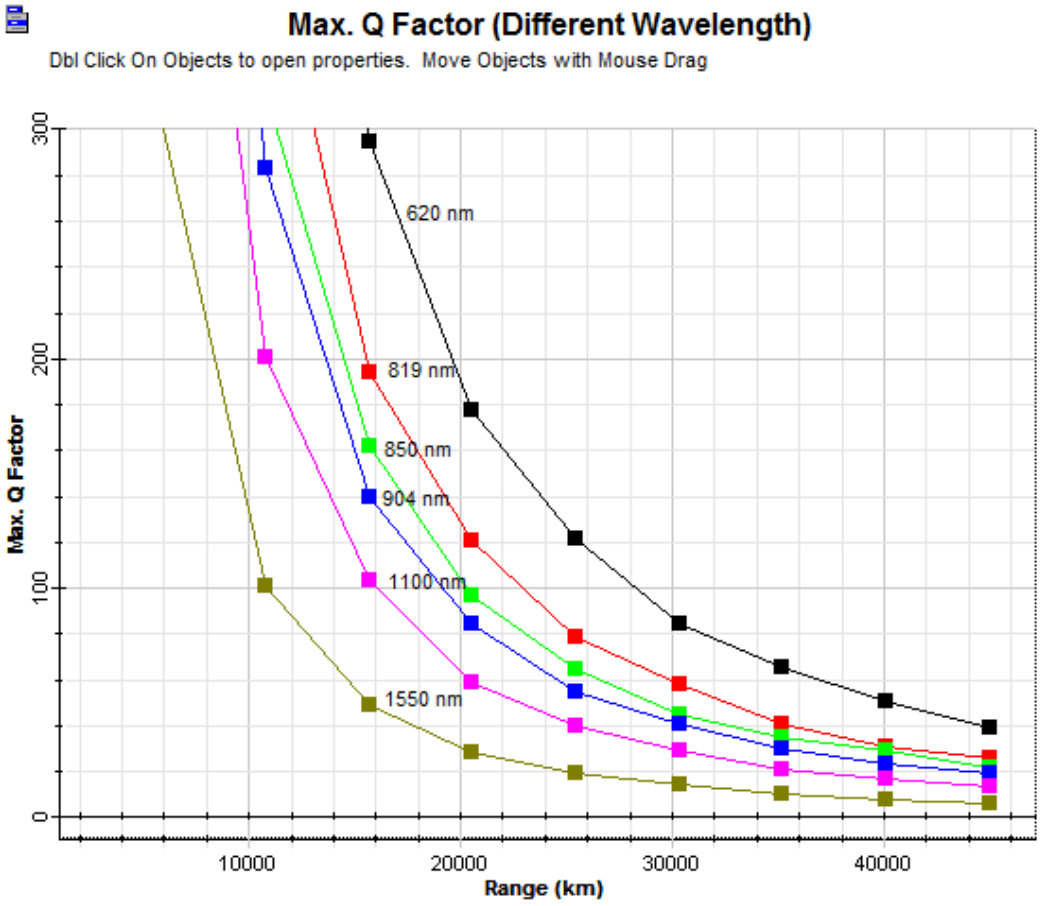

Figure 3.62 Q factor diagram of FSO links at various distances and various wavelengths.

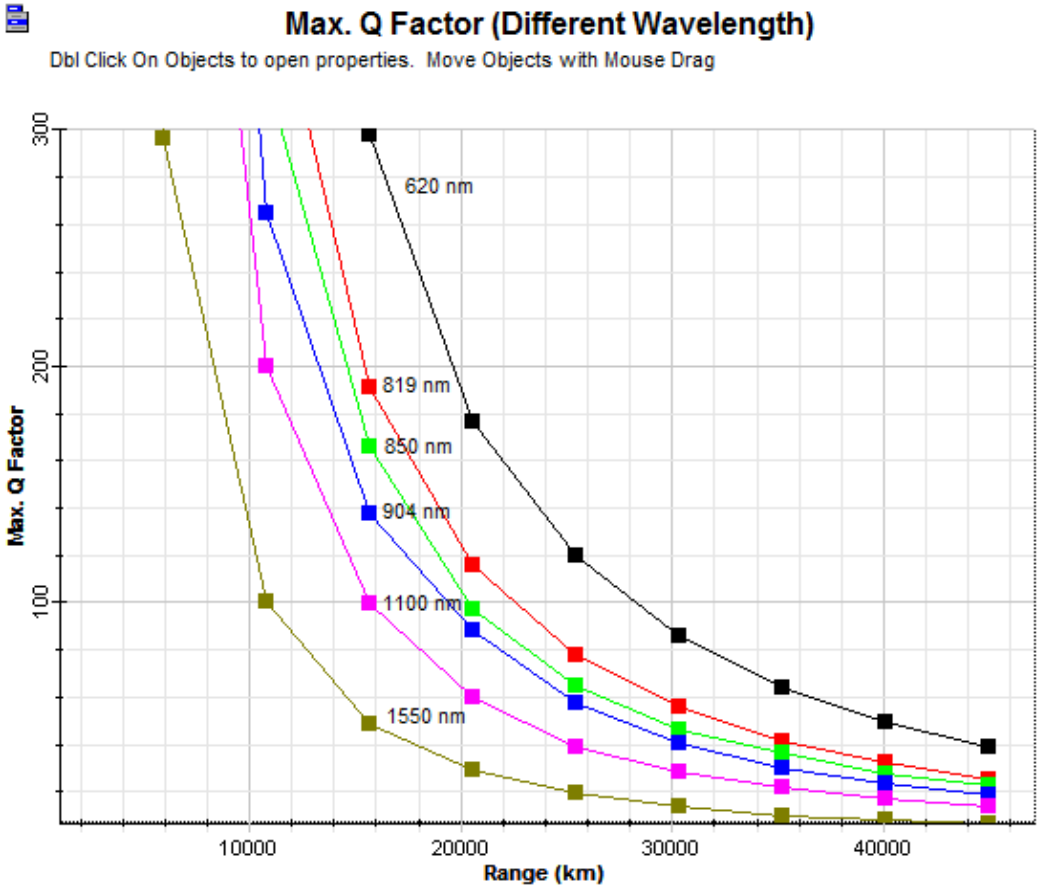

Figure 3.63 Q factor diagram of FSO links at various distances and various wavelengths.

3.3 Relationship between Q Factor, Telescope Diameter and Range

The transmit power, wavelength, range and data rate have been set at a constant value of 23 dBm, 850 nm, 45.000 km, 50 Mbps, respectively. Telescope diameter has been set at 6 levels which are 15 cm, 20 cm, 25 cm, 30 cm, 35 cm and 40 cm.

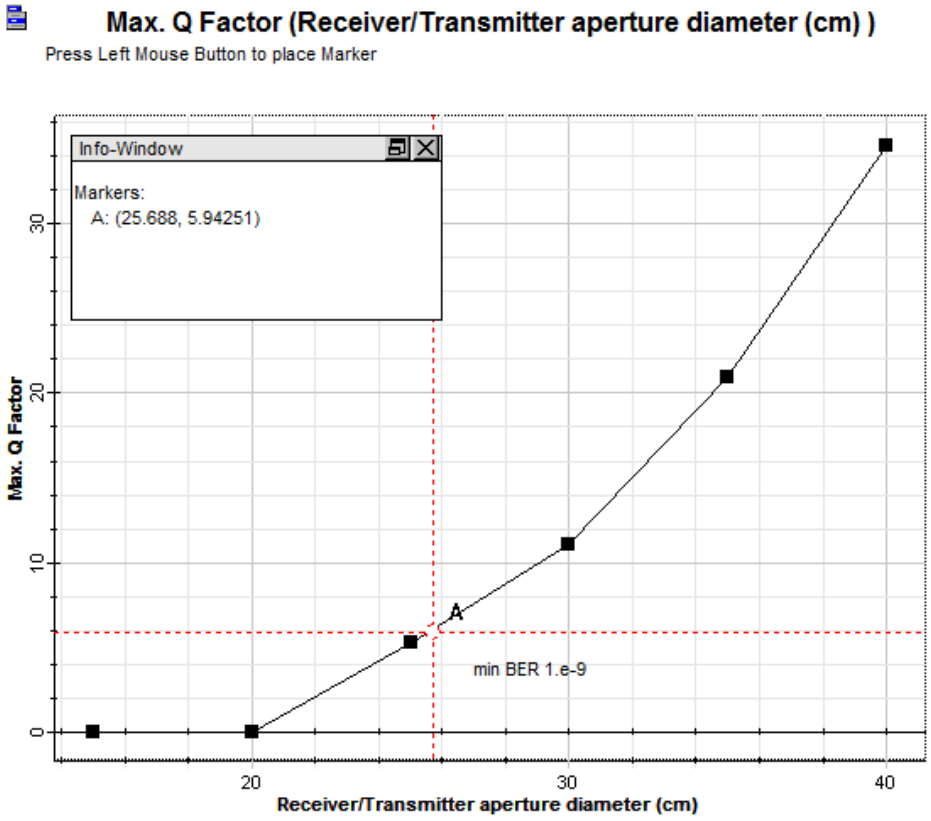

Figure 3.64 Q factor versus telescope diameter diagram at 850 nm wavelength.

As can be seen in Figure 3.64, at least 25.688 cm telescope should be used to achieve 10^{-9} BER performance for this configuration.

Eye diagrams have been plotted for each telescope shown in figures from 3.65 to 3.70. As can be seen in figures, when the telescope diameter increases the eye diagram consist of less jitter and the opening of eye increases.

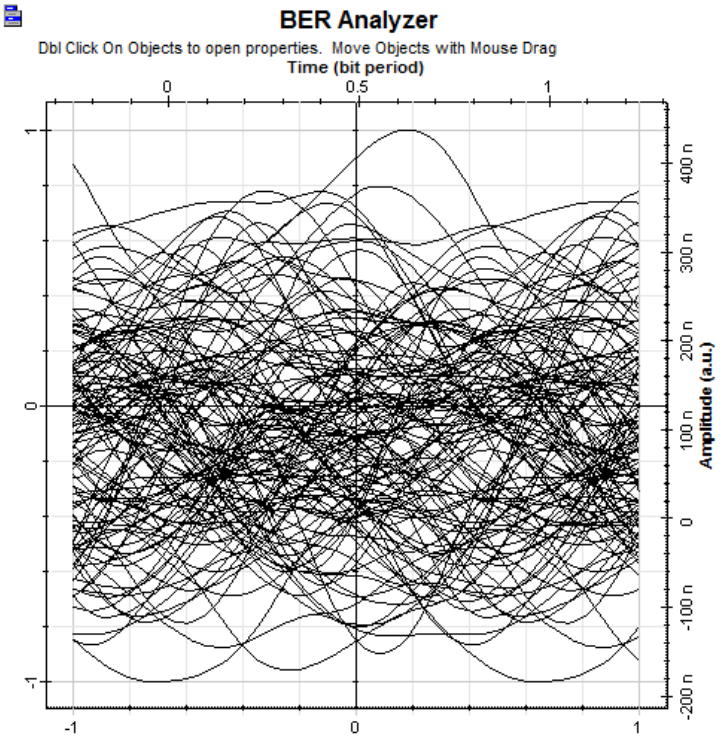

Figure 3.65 Eye diagram for 15 cm telescope.

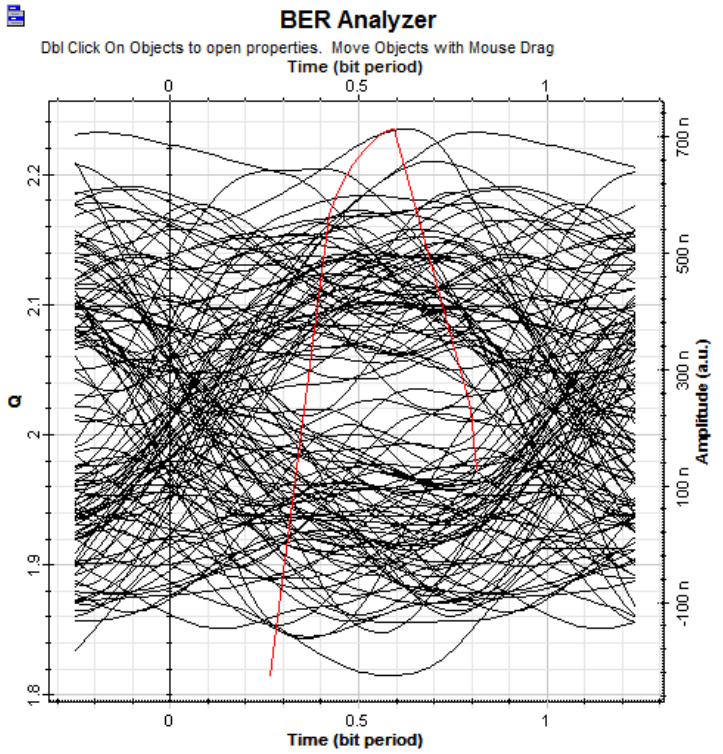

Figure 3.66 Eye diagram for 20 cm telescope.

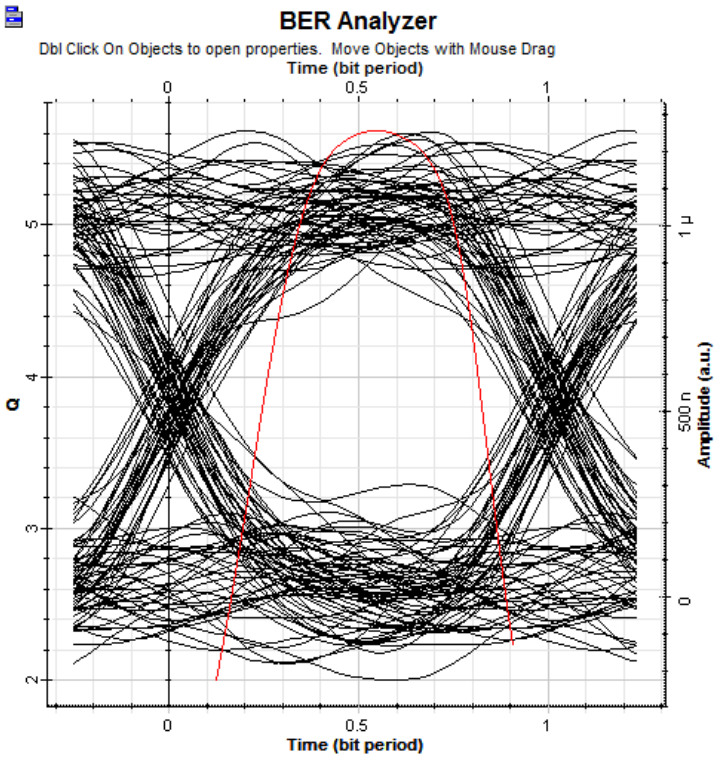

Figure 3.67 Eye diagram for 25 cm telescope.

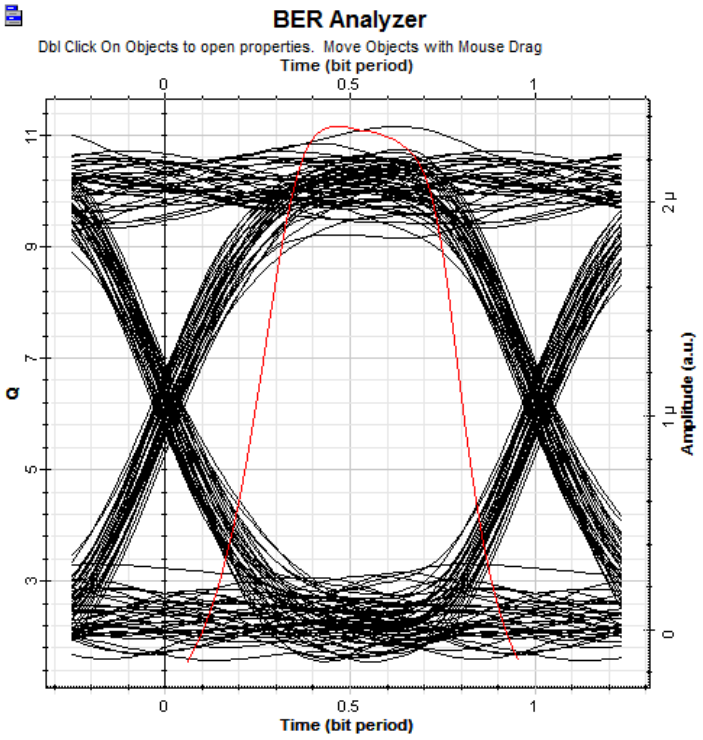

Figure 3.68 Eye diagram for 30 cm telescope.

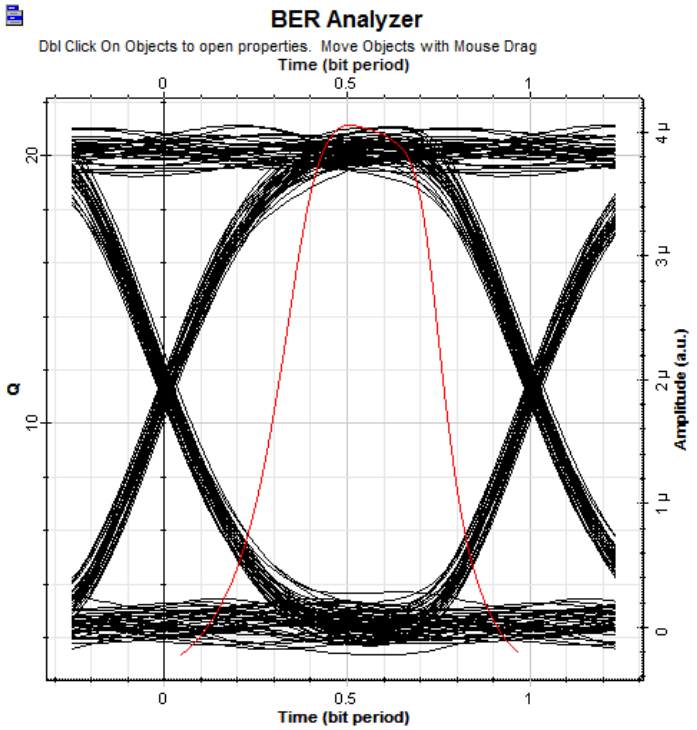

Figure 3.69 Eye diagram for 35 cm telescope.

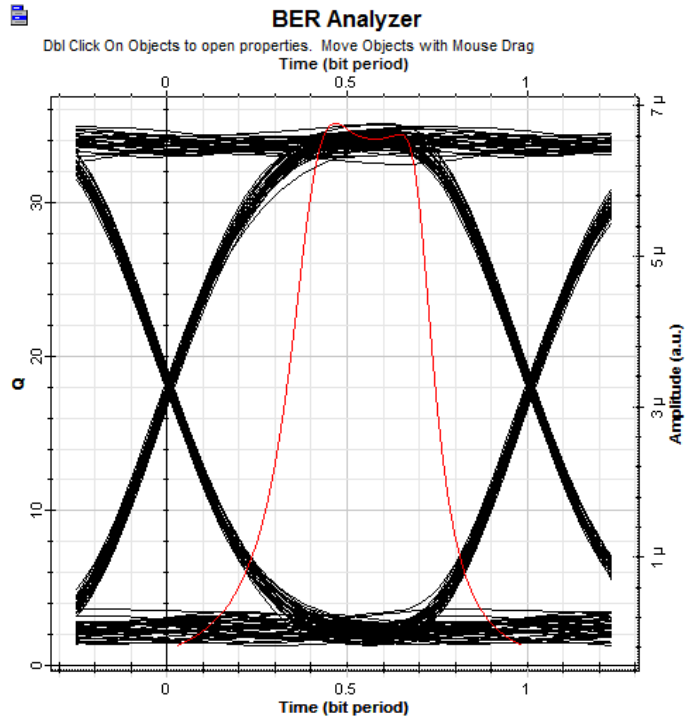

Figure 3.70 Eye diagram for 40 cm telescope.

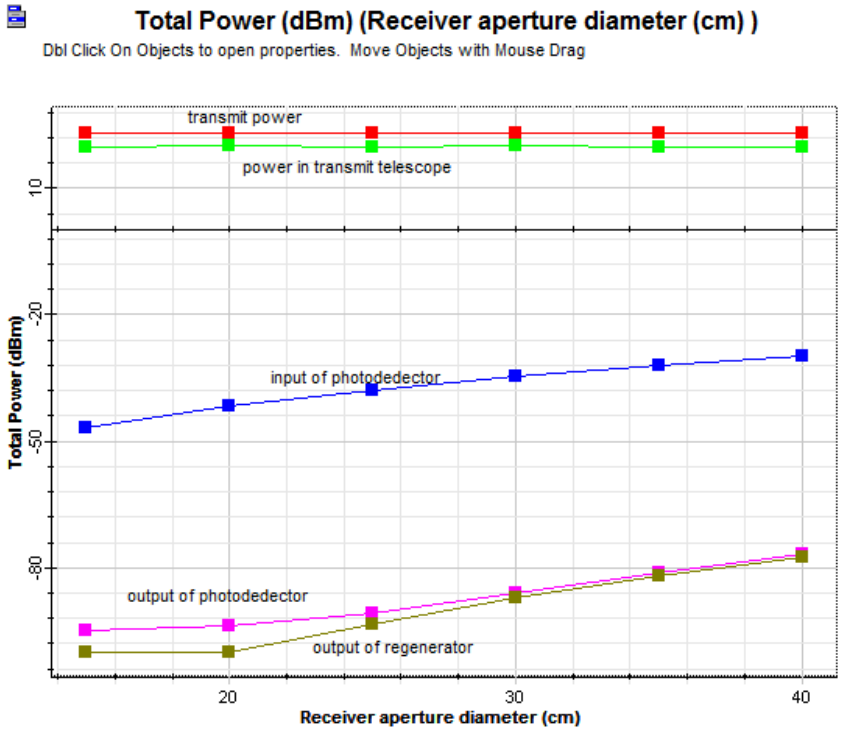

Figure 3.71 Received power for respective telescope diameter at 45.000 km distance and transmit power of 23 dBm.

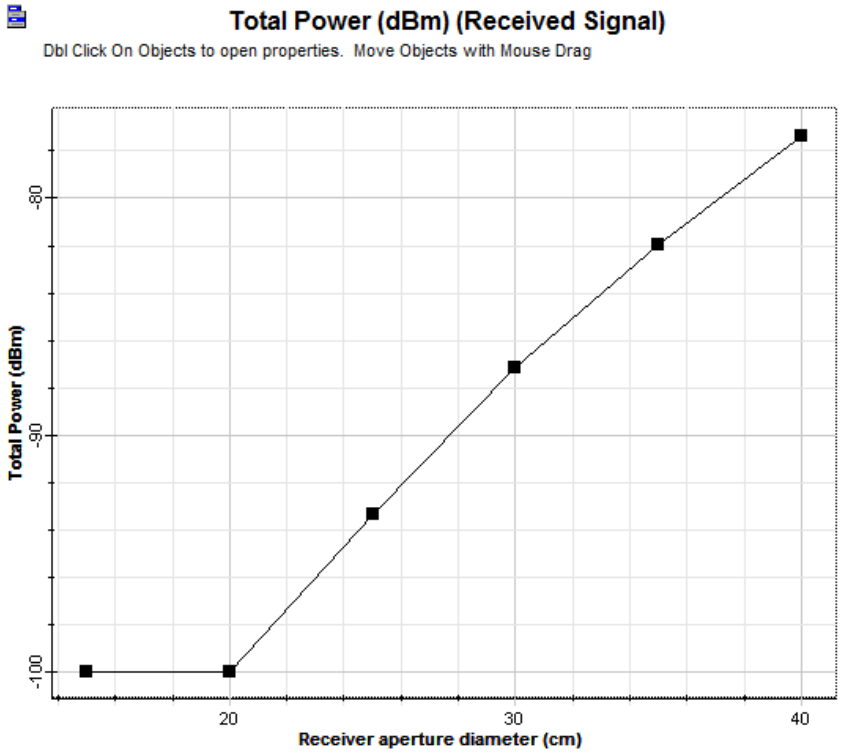

Figure 3.72 Power at the output of regenerator for respective telescope diameter at 45.000 km distance and transmit power of 23 dBm.

Figure 3.71 and Figure 3.72 shows that using bigger telescopes causes an increase in received power and Q factor.

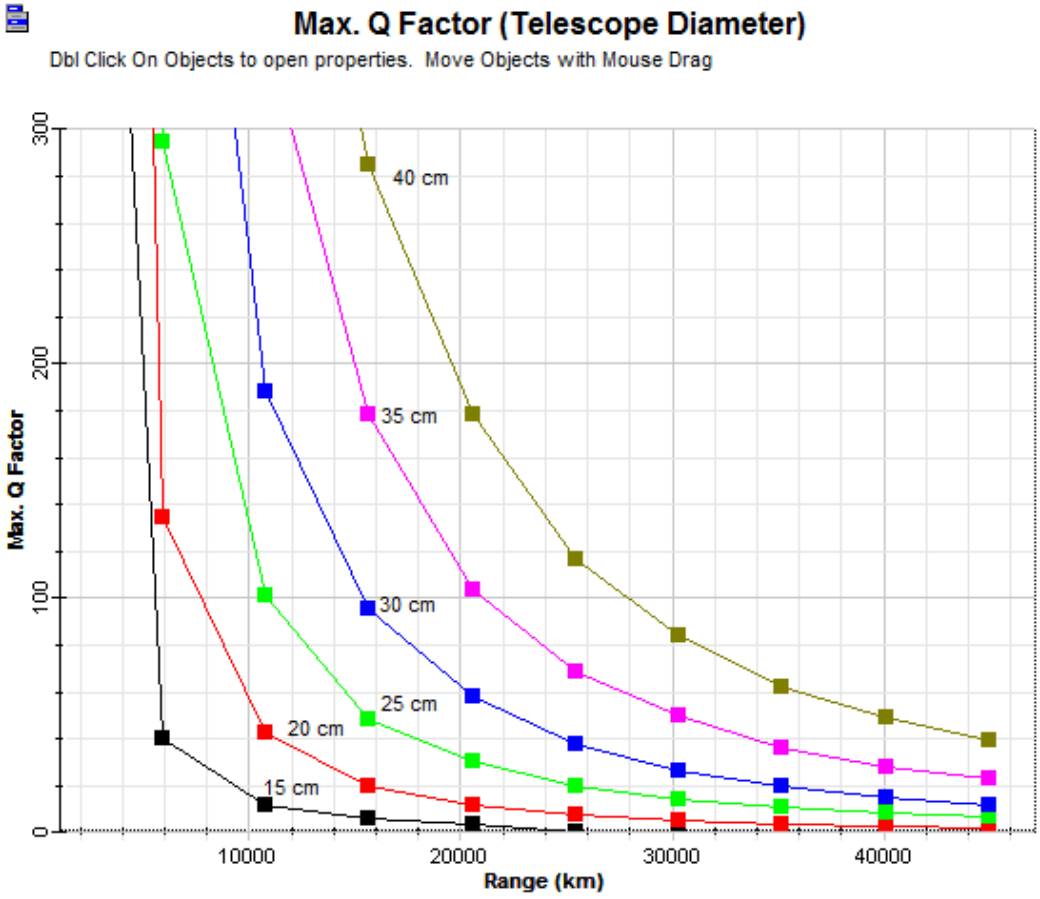

Figure 3.73 Relationship between Q factor, range and telescope diameter.

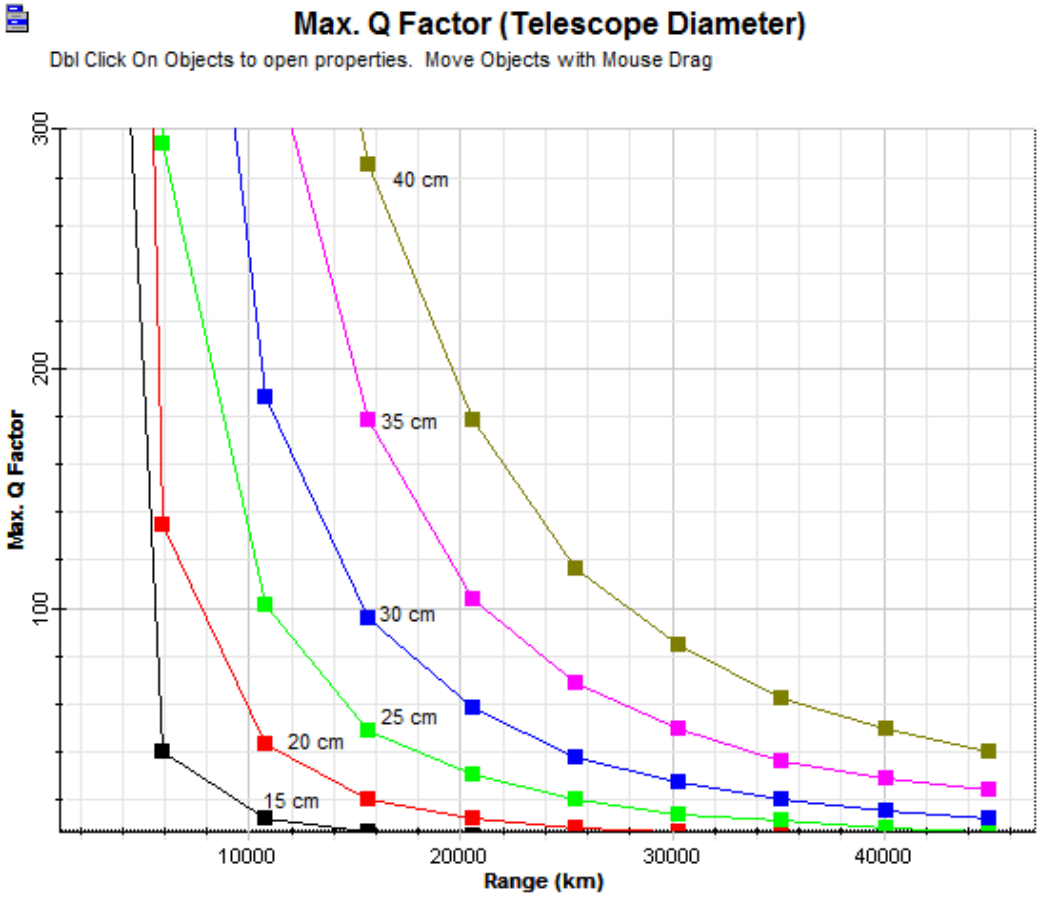

Figure 3.74 Relationship between Q factor, range and telescope diameter.

Relationship between Q factor, range and telescope diameter is shown in Figure 3.73 and 3.74. In figure 3.74, max Q factor scale has been started 6 which indicates 10^{-9} BER in order to understand graphic more clearly. Increasing the distance between satellites reduce the received power. As a result of it, Q factor decreases. Bigger telescope should be used for long distances to achieve intended BER value.

3.4 Relationship between Q Factor, Data Rate and Range

In this section for simulation, the range has been set from 0 km up to 8000 km which is the maximum distance for LEO-LEO Inter Satellite Link (ISL) and the input power and telescope diameter have been set at a constant value of 30 dBm and 12.5 cm, respectively. Signal wavelength has been selected at 850 nm. The bit rate has been set at 5 levels which are 50 Mbps, 100 Mbps, 500 Mbps, 1 Gbps, 5 Gbps. By varying the bit rate and the distance between the satellites, the system performance in terms of Q-factor has been obtained and plotted in Figure 3.75. In addition, in Figure 3.76, max Q factor scale has been started 6 which indicates 10^{-9} BER and range has been started 4000 km in order to understand graphic more clearly.

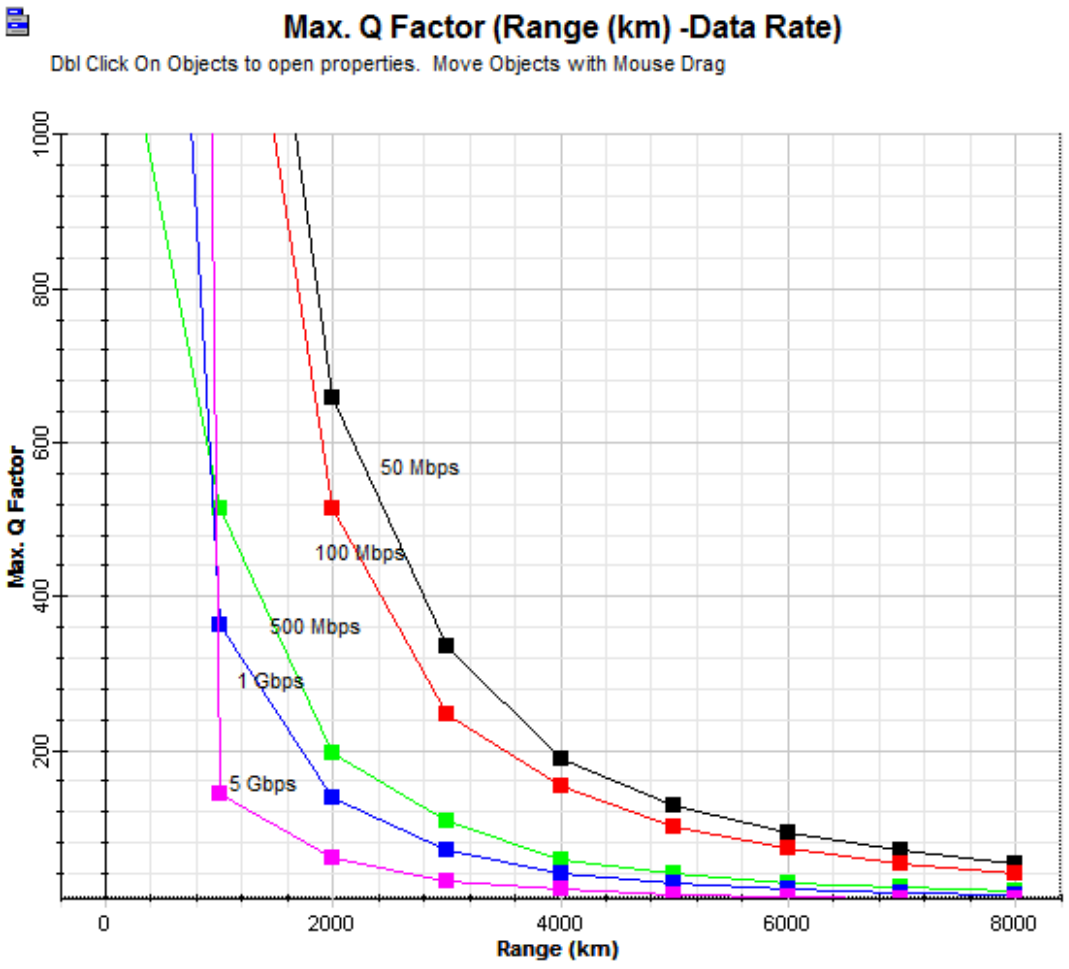

Figure 3.75 Maximum Q factor for variable distance at 850 nm wavelength for 50 Mbps, 100 Mbps, 500 Mbps, 1 Gbps, 5 Gbps data rate.

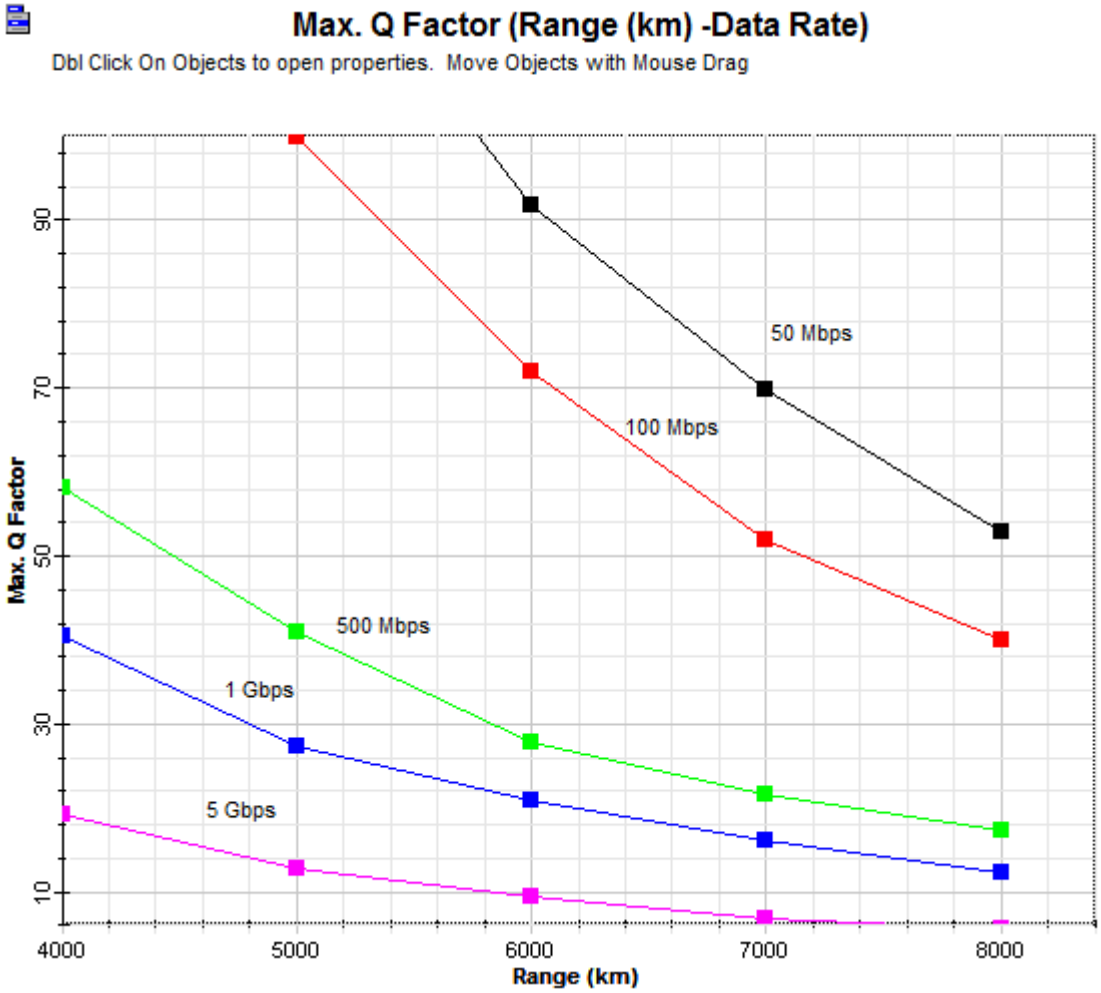

Figure 3.76 Maximum Q factor for variable distance at 850 nm wavelength for 50 Mbps, 100 Mbps, 500 Mbps, 1 Gbps, 5 Gbps data rate.

It can be understood from the graph that at longer range Q-factor of the system decreases. This means that BER of the signal increases as the distance increases. The graph also indicates that with higher bit rate, maximum Q-factor is reduced. At the distance of 8000 km, 5 Gbps link can not be achieved with 10^{-9} BER.

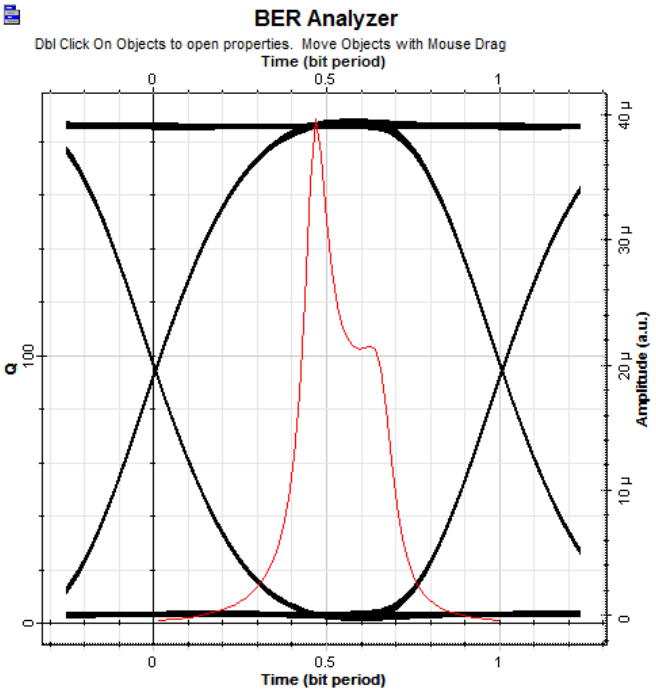

Figure 3.77 Eye diagram for 4000 km distance and 50 Mbps data rate.

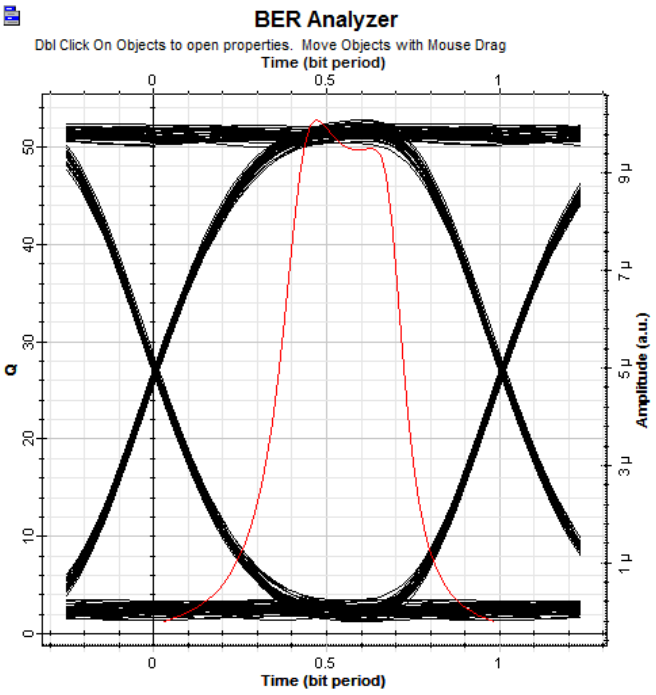

Figure 3.78 Eye diagram for 8000 km distance and 50 Mbps data rate.

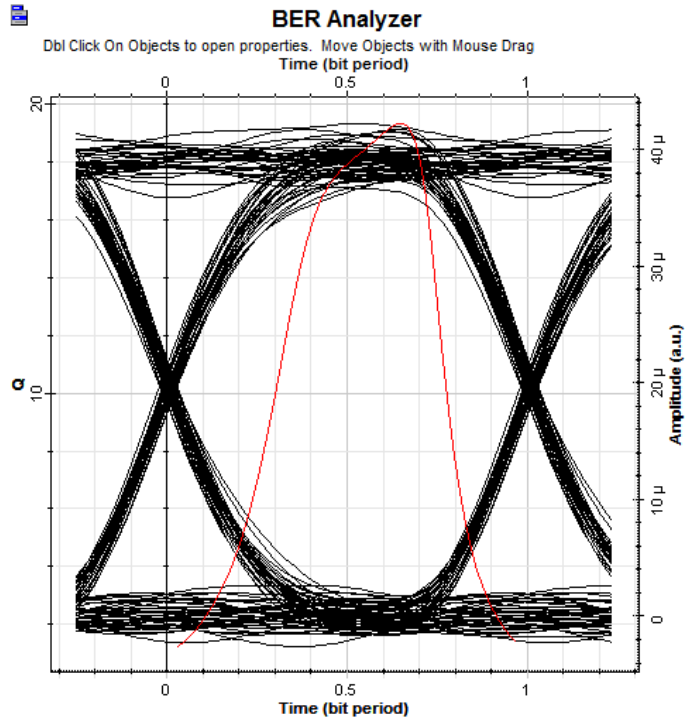

Figure 3.79 Eye diagram for 4000 km distance and 5 Gbps data rate.

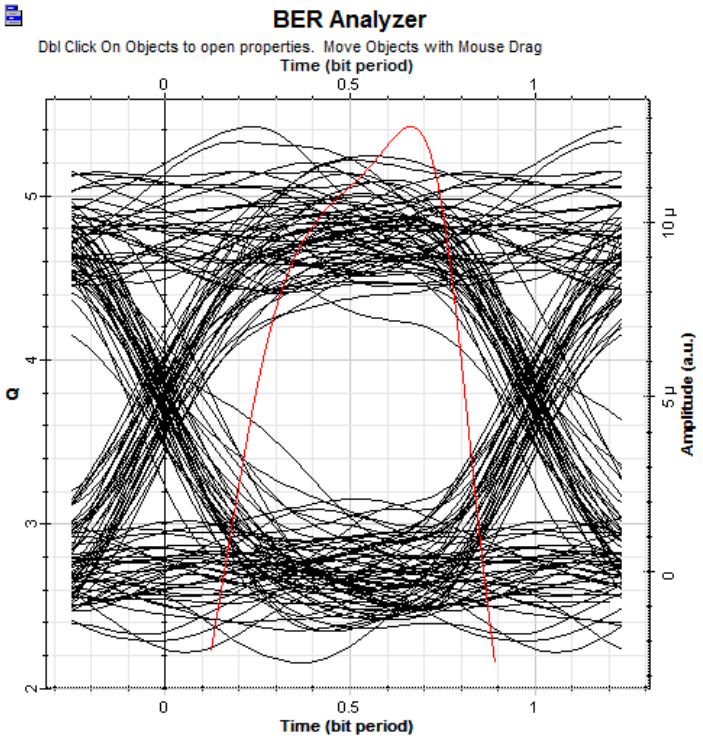

Figure 3.80 Eye diagram for 8000 km distance and 5 Gbps data rate.

Figure 3.77 shows the eye diagram of the link where the distance is 4000 km that is the typical LEO-LEO inter satellite link and data rate is 50 Mbps. Recorded Q factor is 188.541. When the distance is increased to 8000 km that is the maximum LEO-LEO inter satellite link with the same data rate, the eye diagram consists of more jitter and the opening of the eye decreases. But as can be seen in Figure 3.78, maximum Q factor is 52.78 and link quality is still perfect.

When the data rate is increased to 5 Gbps, Q factor recorded 19.30 for 4000 km distance and 5.41 for the 8000 km distance. Figure 3.79 and 3.80 shows the eye diagrams for these situations. As can be seen in Figure 3.80, BER is still over the desired value of 10^{-9} but link quality is not perfect enough.

3.5 APD Type and PIN Type Photodetector Comparison

In this section APD type and PIN type photodetector comparison has been done. For simulation, transmit power has been adjusted to 23 dBm, range has been set to a constant value of 45.000 km and telescope diameter has been set to a constant value of 25 cm. Furthermore, wavelength and data rate have been adjusted to 850 nm and 50 Mbps, respectively. In this configuration “fork” copies the input signal into two output signals. One of them is directed to the APD photodetector and the other is directed to the PIN photodetector. System design model is shown in Figure 3.81.

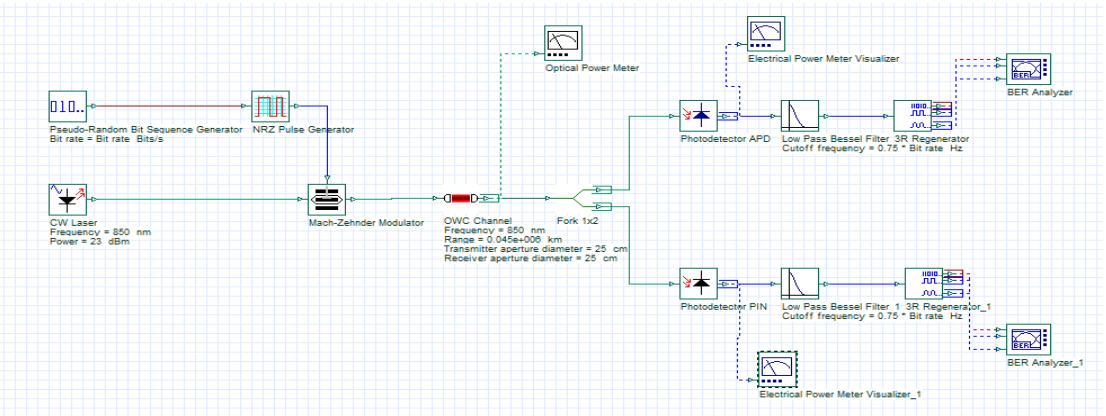

Figure 3.81 System design model for APD type and PIN type photodetector comparison.

As can be seen in figures from 3.82 to 3.85, it is possible to achieve 10^{-9} BER with APD photodetector, recorded Q factor value is 5.7892. On the other hand, for PIN configuration Q factor is 2.024, which corresponds to 0.0215 BER.

It has been recorded that power at the input of photodetectors is -37.981 dBm. Power at the output of APD photodetector is -90.858 dBm while power at the output of PIN photodetector is -94.163 dBm. It means that APD type photodetector has approximately 4 dB better performance than PIN type photodetector.

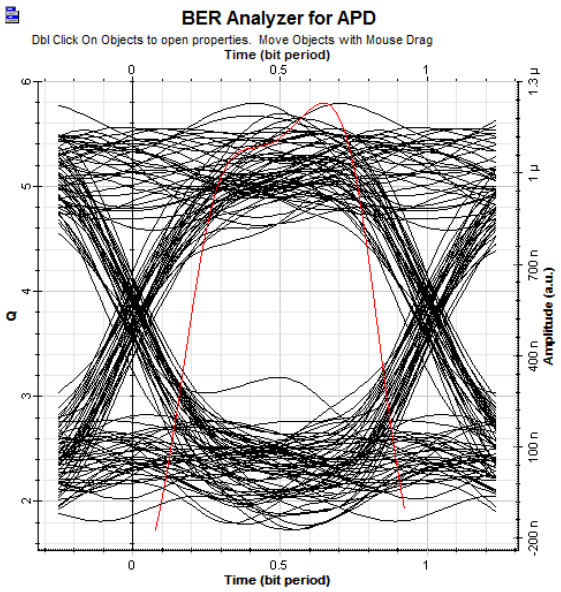

Figure 3.82 Eye diagram for APD type photodetector at 23 dBm transmit power.

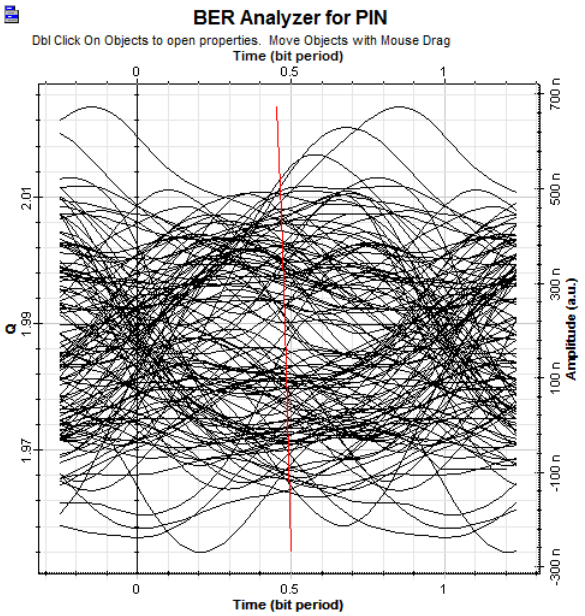

Figure 3.83 Eye diagram for PIN type photodetector at 23 dBm transmit power

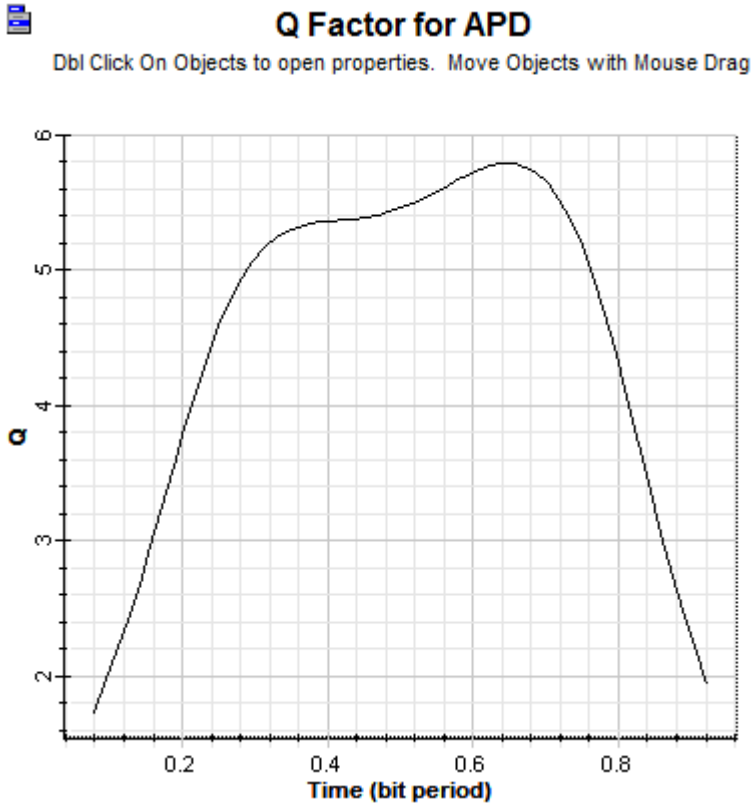

Figure 3.84 Q factor for APD type photodetector at 23 dBm transmit power.

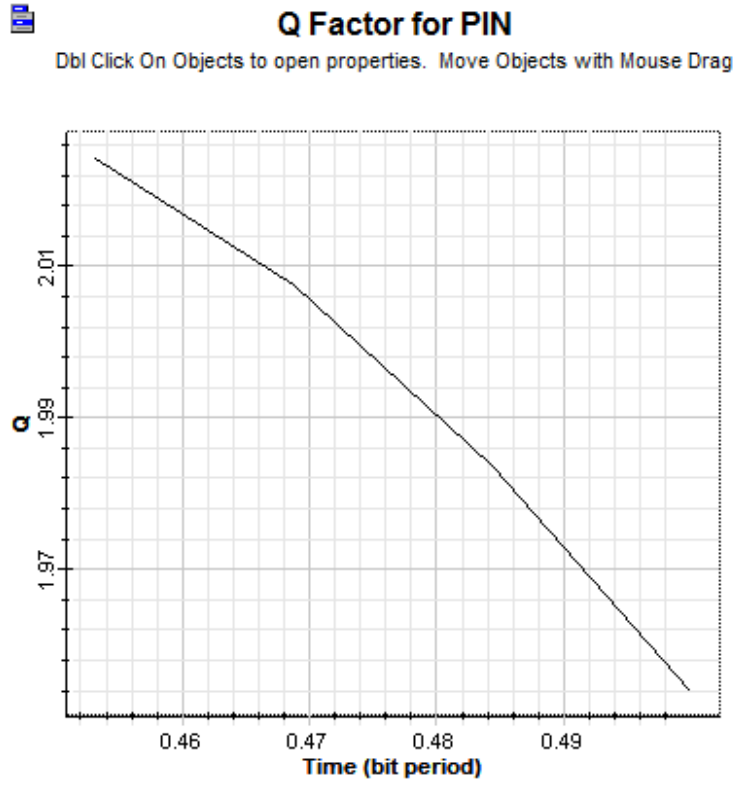

Figure 3.85 Q factor for PIN type photodetector at 23 dBm transmit power.

When the transmit power has been changed to 28 dBm, which is essential value to achieve 10^{-9} BER for PIN photodetector, it has been recorded that power at the input of photodetectors is -32.912 dBm. Power at the output of APD photodetector is -82.973 dBm while power at the output of PIN photodetector is -90.633 dBm. In this situation, APD has approximately 8 dB better performance than PIN. Eye diagrams and Q Factor diagrams for this case are shown in Figure 3.86 to 3.89.

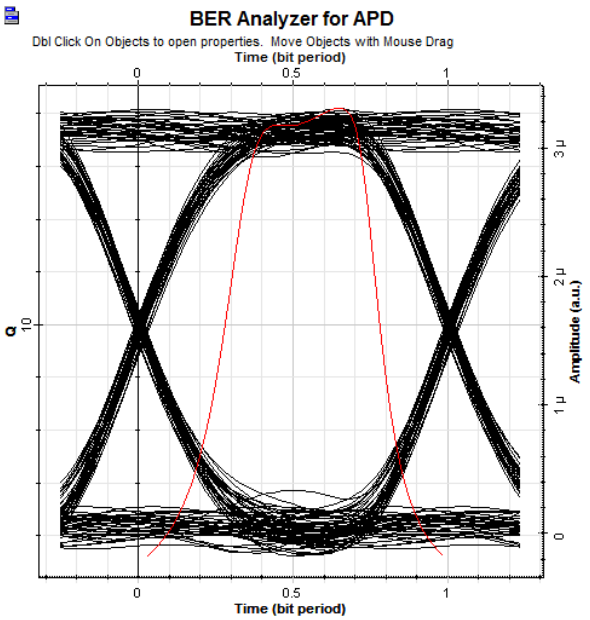

Figure 3.86 Eye diagram for APD type photodetector at 28 dBm transmit power.

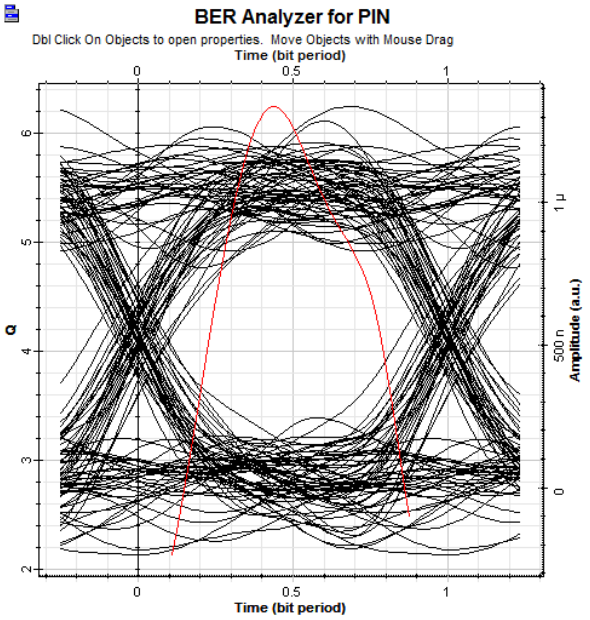

Figure 3.87 Eye diagram for PIN type photodetector at 28 dBm transmit power.

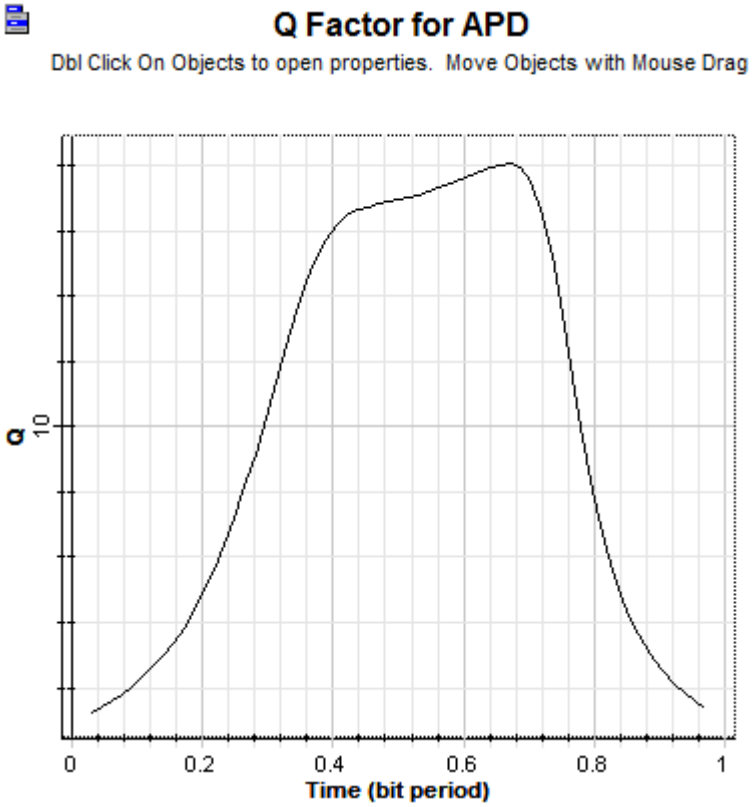

Figure 3.88 Q factor for APD type photodetector at 28 dBm transmit power.

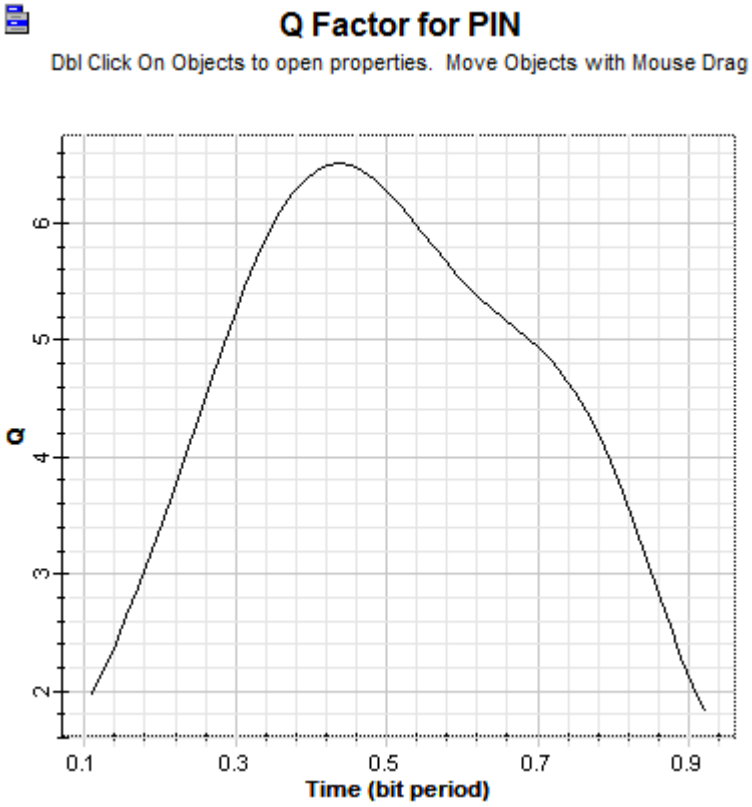

Figure 3.89 Q factor for APD type photodetector at 28 dBm transmit power.

3.6 Conventional System and EDFA System Comparison

With the advent of Erbium Doped Fiber Amplifier (EDFA), high capacity free space optical communication become increasingly practical compared to conventional FSO communication system [50].

In section 3.1, it has been concluded that transmit power should be at least 29 dBm with 25 cm telescope to obtain 10^{-9} BER for the inter orbit link whose data rate and range are 50 Mbps and 45.000 km, respectively.

In this section Erbium Doped Fiber Amplifier (EDFA) has been used for the same link to recognize its effect on the link quality.

Figure 3.90 shows the system design model for conventional system and EDFA system comparison. In this model "fork" copies the input signal into two output signals. One of them is directed to the conventional system and the other is directed to the EDFA system. In this configuration, high power EDFA whose length is 5 meters is used at the transmitter as booster amplifier and low power EDFA whose length is 2 meters as low noise receiver preamplifier is used at the receiver. Both EDFA's pump powers and pump wavelengths are 20 dBm and 980 nm, respectively. An optical band-pass filter is used to reduce the broadband Amplified Spontaneous Emission (ASE) generated by the EDFA.

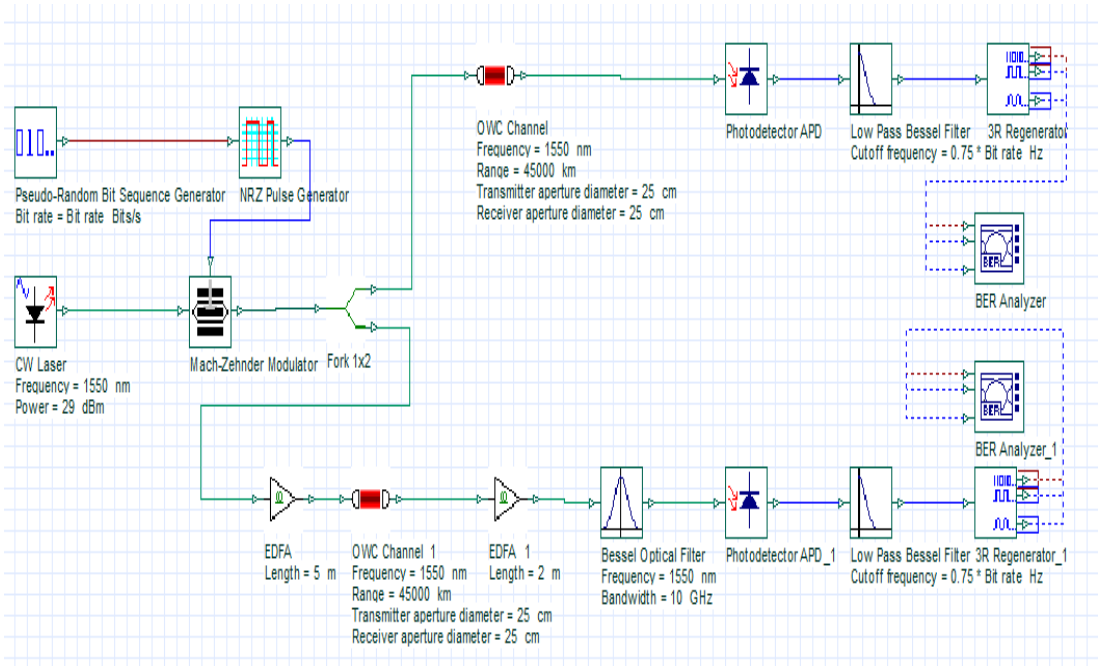

Figure 3.90 System design model for conventional system and EDFA system comparison.

Eye, maximum Q factor and minimum BER diagrams have been plotted for each system and shown in figures from 3.91 to 3.96.

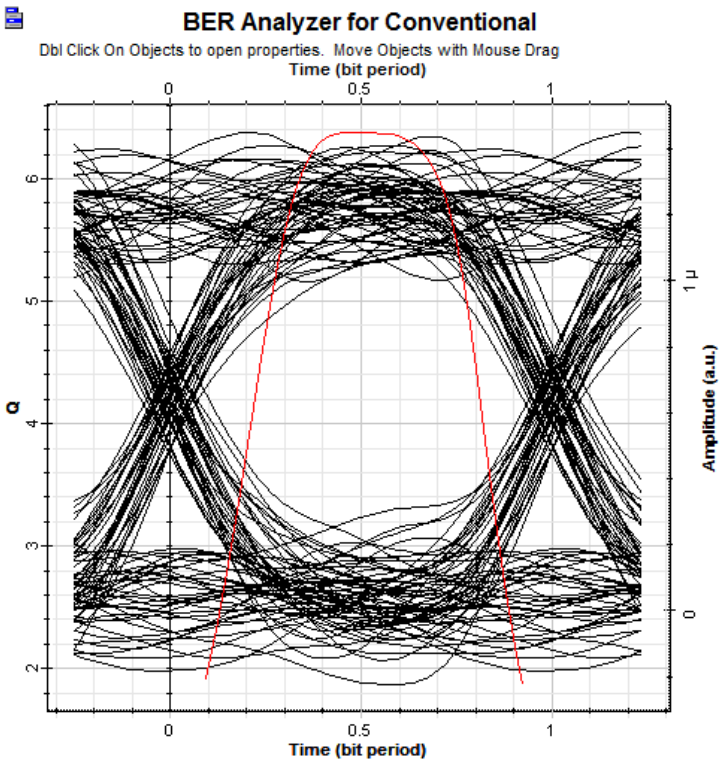

Figure 3.91 Eye diagram for conventional system.

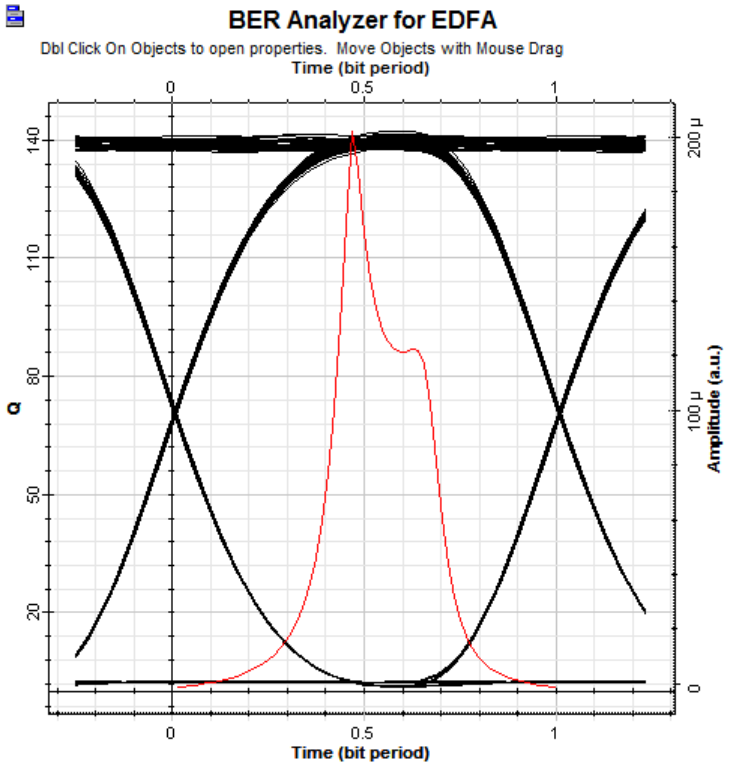

Figure 3.92 Eye diagram for EDFA system.

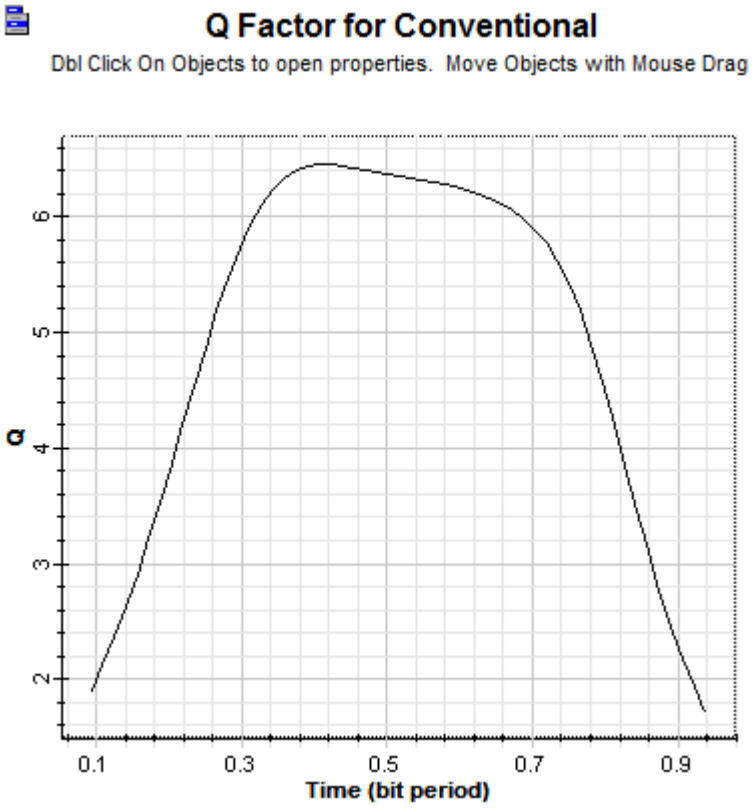

Figure 3.93 Maximum Q factor diagram for conventional system.

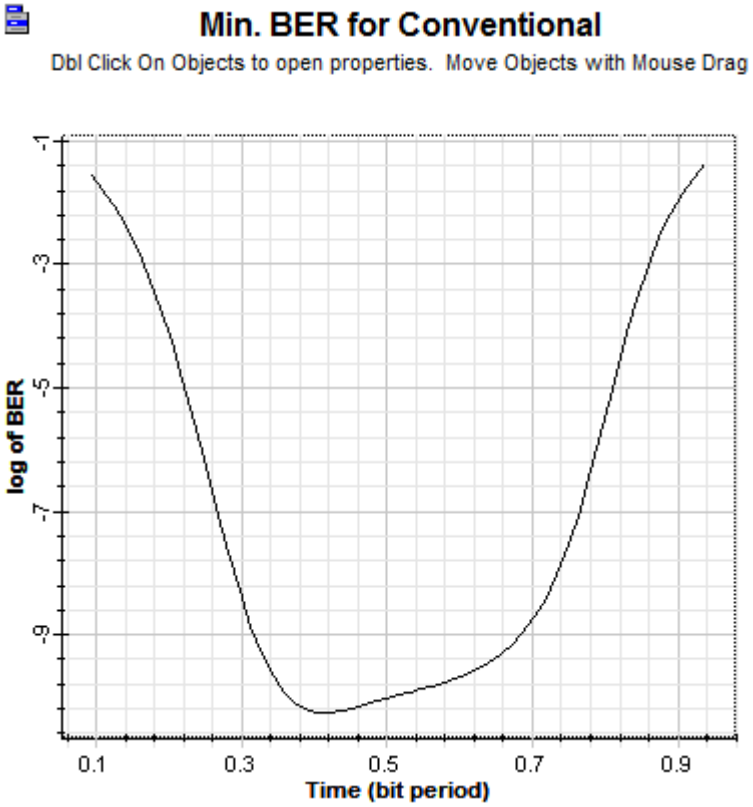

Figure 3.94 Minimum BER diagram for conventional system.

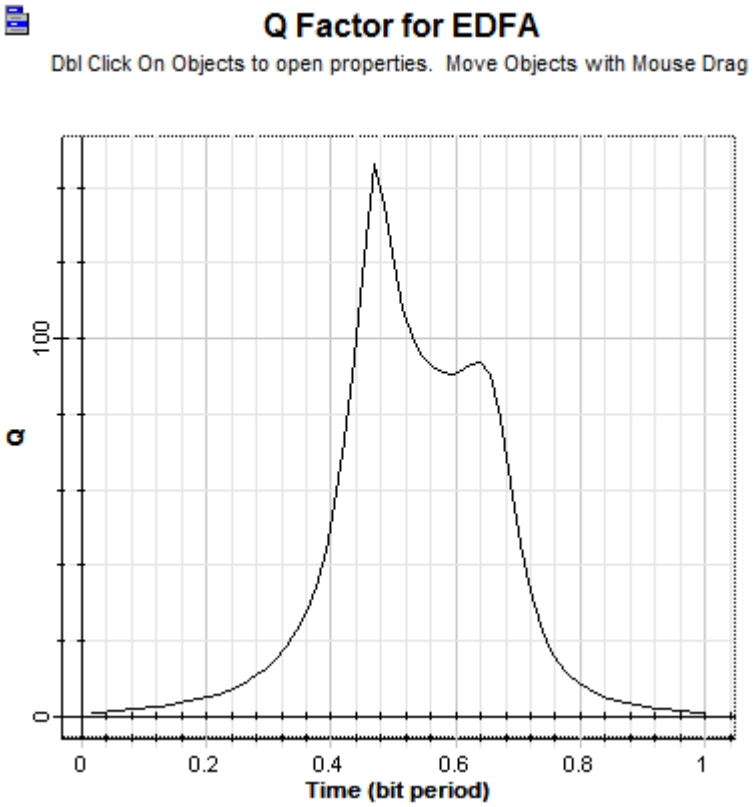

Figure 3.95 Maximum Q factor diagram for EDFA system.

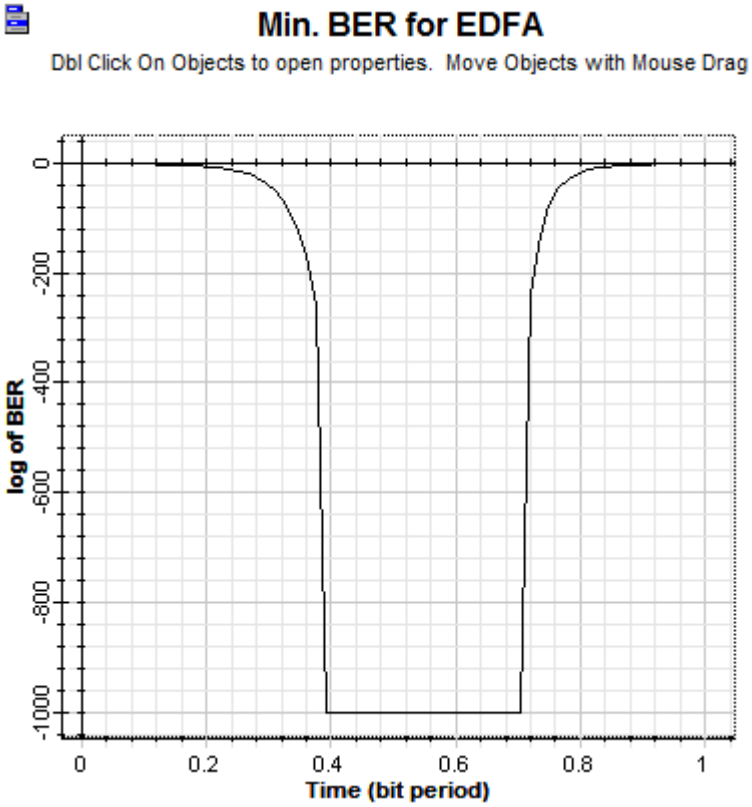

Figure 3.96 Minimum BER diagram for EDFA system.

As can be seen in figures, the eye diagram for EDFA system consists of less jitter and the opening of eye excessively increases. Moreover, Q factor for EDFA is 142.216, while Q factor of conventional system is only 6.378 as can be seen in Figure 3.93 and Figure 3.95.

The following figure shows the power at the input of photodetector according to the transmit power. As can be seen in Figure 3.97, power at the input of photodetector for EDFA system is -14.888 dBm (-2.773 dBm power at the input of optical filter), while power at the input of photodetector for conventional system is -37.199 dBm. Received power at EDFA system is 22.311 dBm better than conventional system for this configuration.

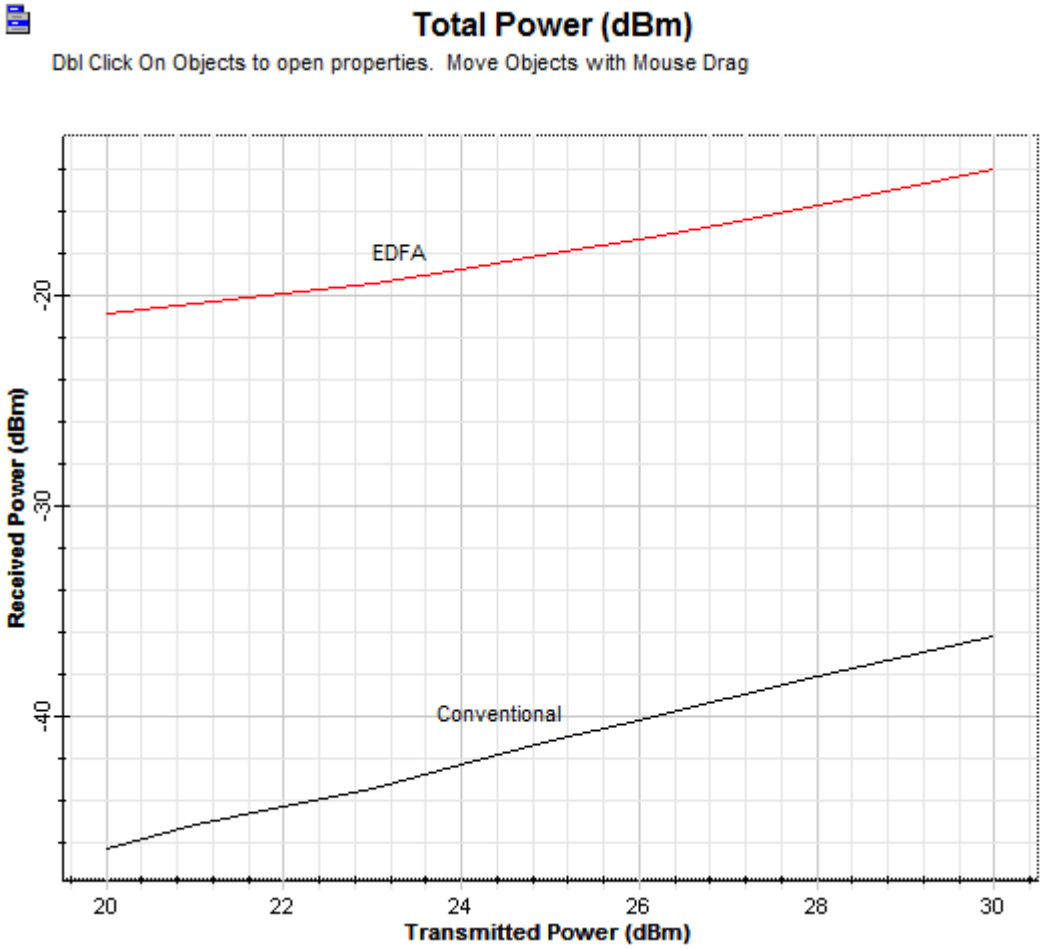

Figure 3.97 Transmit power versus power at the input of photodetector.

In order to determine the performance comparison between conventional and EDFA system in terms of range, distance has been varied from 0 km to 45.000 km and the following figure has been drawn. As can be seen in figures below, performance of EDFA system is better at the distances greater than 8800 km for this configuration.

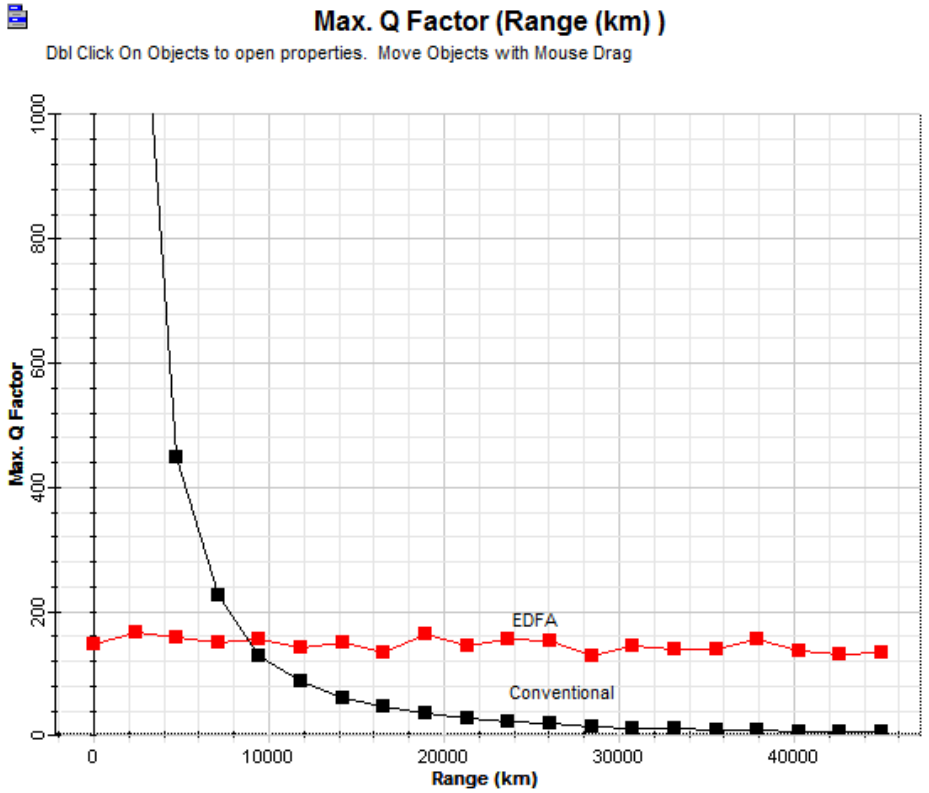

Figure 3.98 Range versus Q factor diagram for conventional and EDFA system.

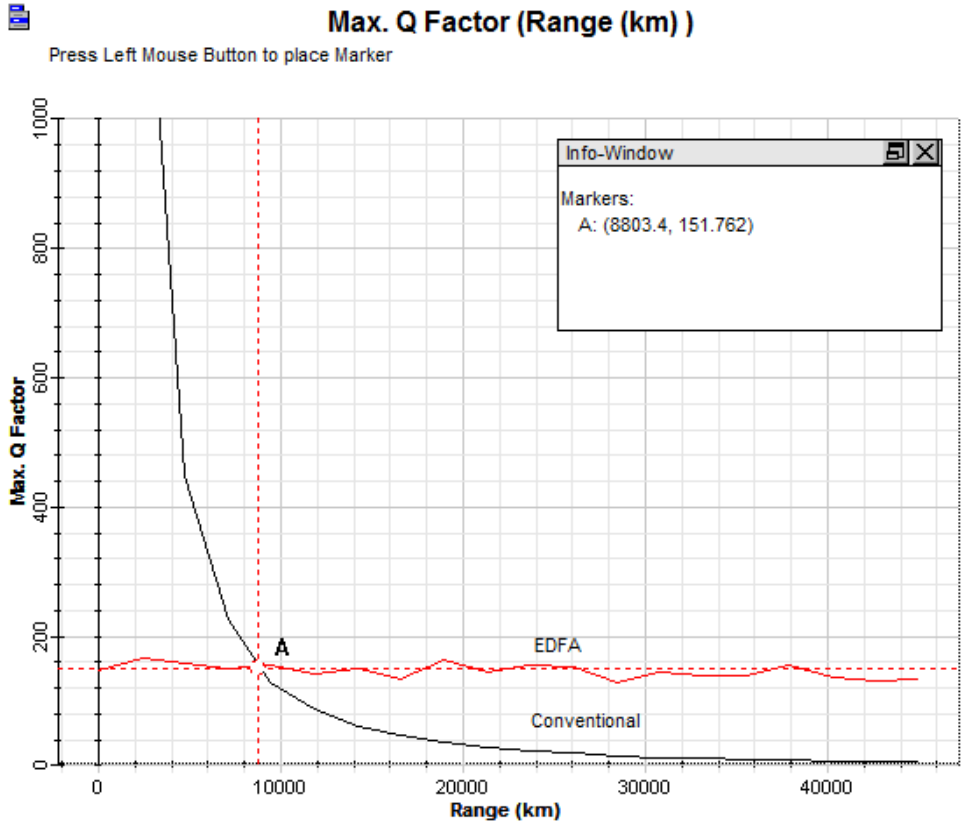

Figure 3.99 Range versus Q factor diagram with marker for conventional and EDFA system.

The layout in Figure 3.100 enables evaluating the amplifier performance as a function of the signal input power. The signal input power is swept from small signal to large signal regime, i.e. -50 dBm to 30 dBm in order to evaluate the amplifier performance. The amplifier performance given by output power and noise power, respectively are shown in Figure 3.101 and Figure 3.102.

As can be seen in Figure 3.101, gain is larger at the small signal regime, while it is smaller at the large signal regime. Output power is smaller than input power at the point of the 29 dBm due to the gain saturation. On account of this, booster EDFA is not useful for this configuration, until small input power such as less than -10 dBm is supplied.

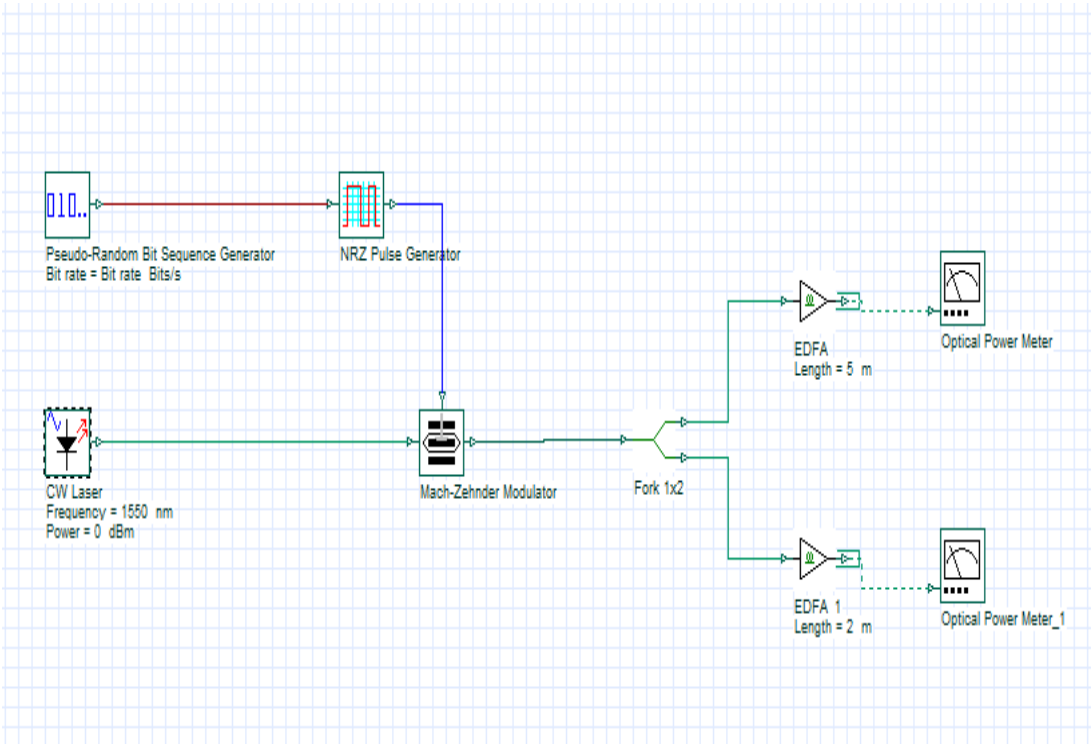

Figure 3.100 System design model for evaluating the amplifier performance.

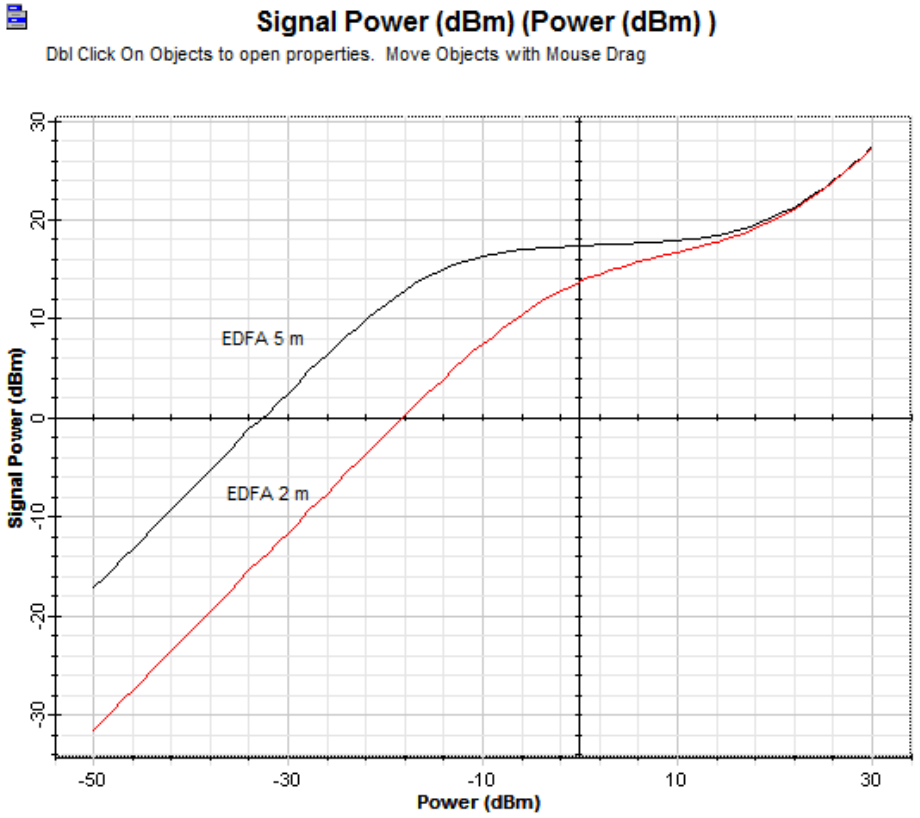

Figure 3.101 Input power versus output power for 2 m length EDFA and 5 m length EDFA.

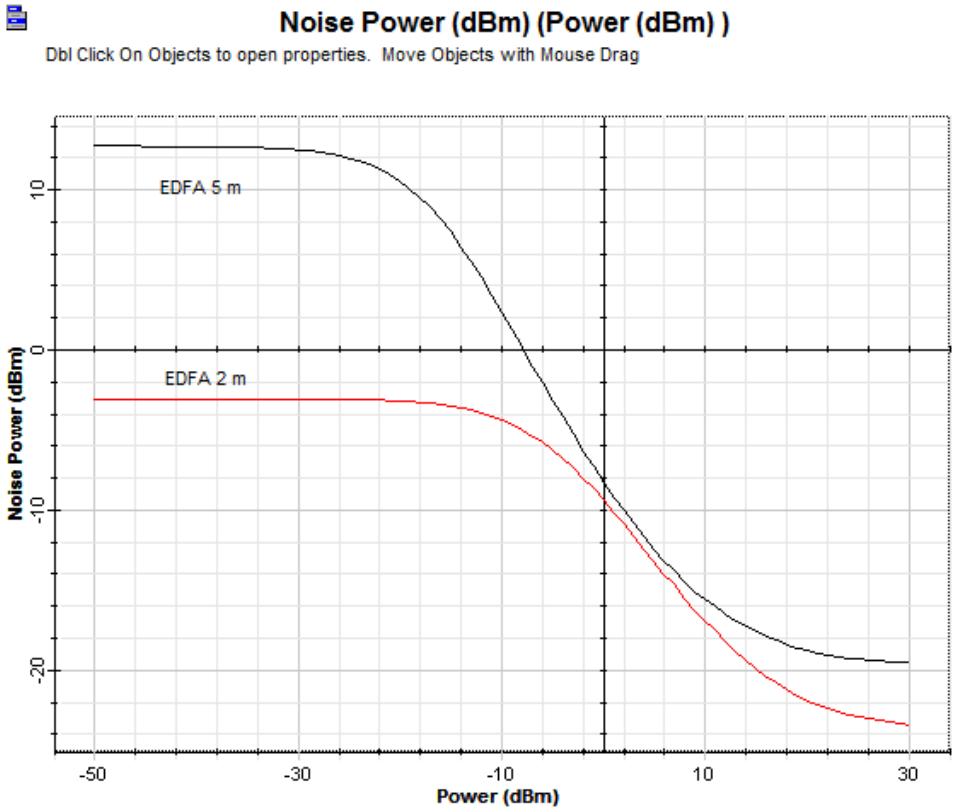

Figure 3.102 Input power versus noise power for 2 m length EDFA and 5 m length EDFA.

CHAPTER FOUR

CONCLUSION

Free Space Optical (FSO) Communication Systems are alternatives to Radio Frequency (RF) communication systems because of the high data rate, high bandwidth capacity, smaller size and weight, less power consumption, high security, resistance to interference and etc. As the number of manufactured satellites increases every year and consequently inter-satellite communication requirements are increasing. It is possible to send several Gbps data to thousands kilometers distances with laser communication. This caused to adapt optical wireless communication technology into space technology.

In this thesis, the inter-satellite link has been modeled and simulated for the various inter-satellite links by using Optiwave Software and the system performance (BER/Q-Factor) has been analyzed in terms of each basic parameter such as transmitted power, wavelength, data rate, range and telescope diameter in order to achieve minimum BER.

Link power budget is done by calculating the power received by the system. Equation 2.14 is used to calculate the received power in an OWC system

$$P_R = P_T \eta_T \eta_R \left(\frac{\lambda}{4\pi Z}\right)^2 G_T G_R L_T L_R \quad \textbf{(2.14)}$$

As can be figured out from Equation 2.14, FSO link performances can be determined by several parameters such as;

P_T : Transmitter optical power

η_T : Optics efficiency of the transmitter

η_R : Optics efficiency of the receiver

λ : Wavelength

Z : Distance between the transmitter and the receiver (Range)

G_T : Transmitter telescope gain

G_R : Receiver telescope gain

L_T : Transmitter pointing loss factor

L_R : Receiver pointing loss factor

Transmitted power is one of the most important parameter for the inter satellite link. As can be seen in figurers below, more powerful lasers should be used in order to establish link at the desired distance and desired quality.

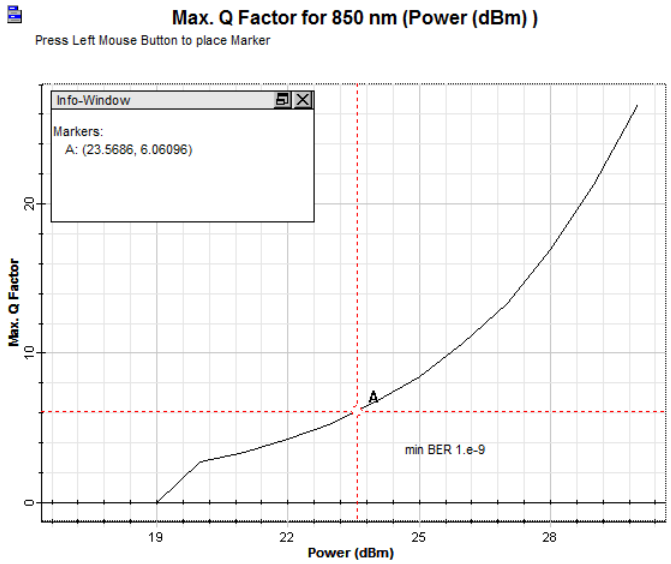

Figure 3.23 Q factor versus transmit power diagram at 850 nm wavelength.

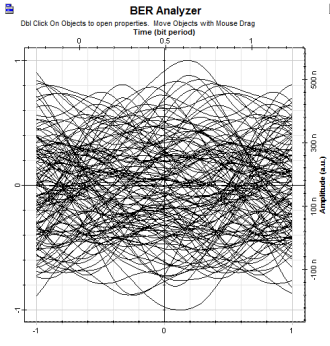

Figure 3.26 Eye diagram for 17 dBm transmit power.

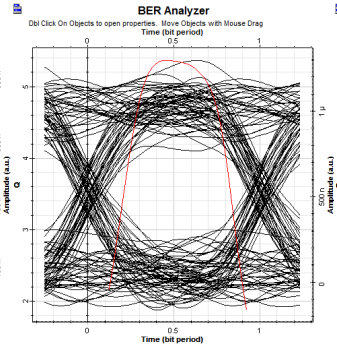

Figure 3.32 Eye diagram for 23 dBm transmit power.

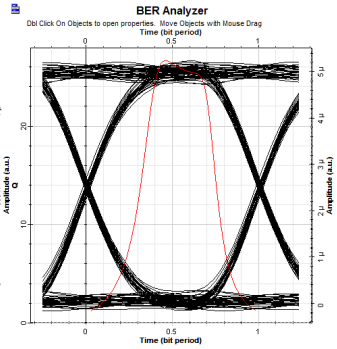

Figure 3.39 Eye diagram for 30 dBm transmit power.

Wavelength is another important parameter in FSO. It can be concluded from the figures below that signal qualities are better at shorter wavelengths due to bigger value of Q-factor.

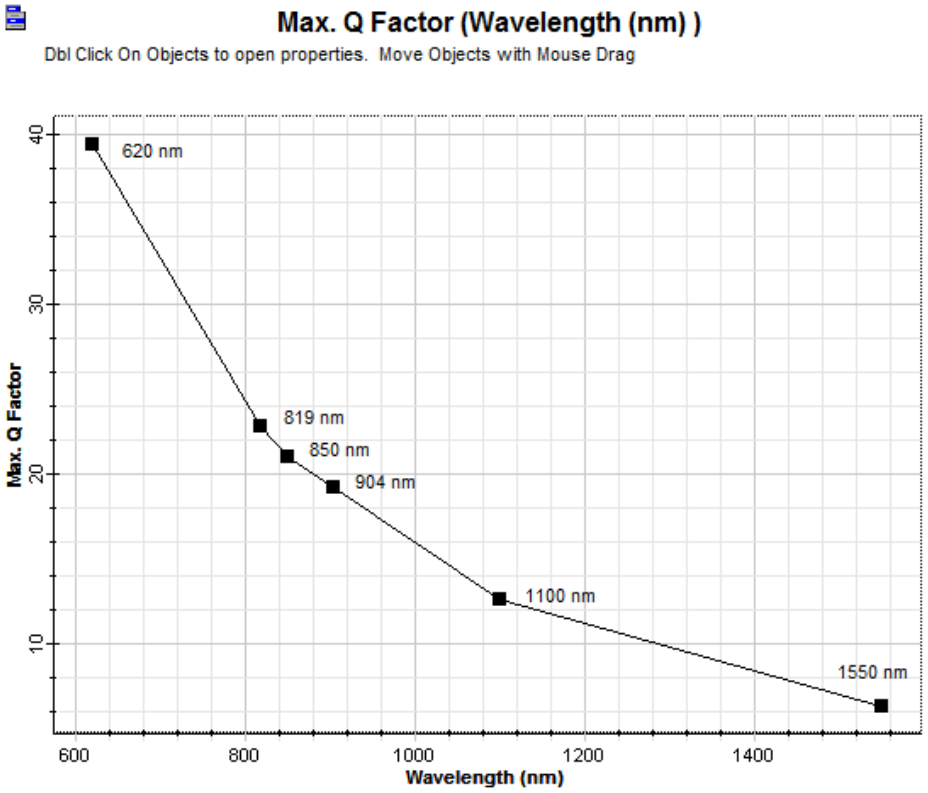

Figure 3.40 Q factor diagram at 620 nm, 819 nm, 850 nm, 904 nm, 1100 nm and 1550 nm wavelength.

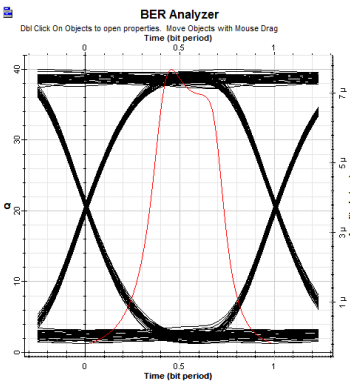

Figure 3.43 Eye diagram for 620 nm wavelength.

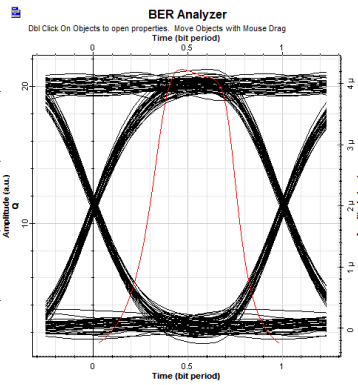

Figure 3.45 Eye diagram for 850 nm wavelength.

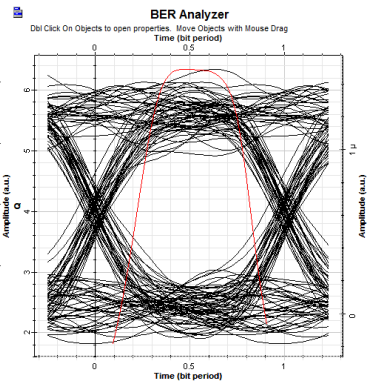

Figure 3.48 Eye diagram for 1550nm wavelength.

As can be seen in figures below, received error increases as the distance between satellites increases since laser beam emitted by transmitter is expanding with increasing distance. In order to reduce the power loss due to the distance, it is obligatory to use a much narrower beam angle. Additionally, attenuation has been examined according to the distance and various wavelengths and concluded that attenuation is less in shorter wavelengths.

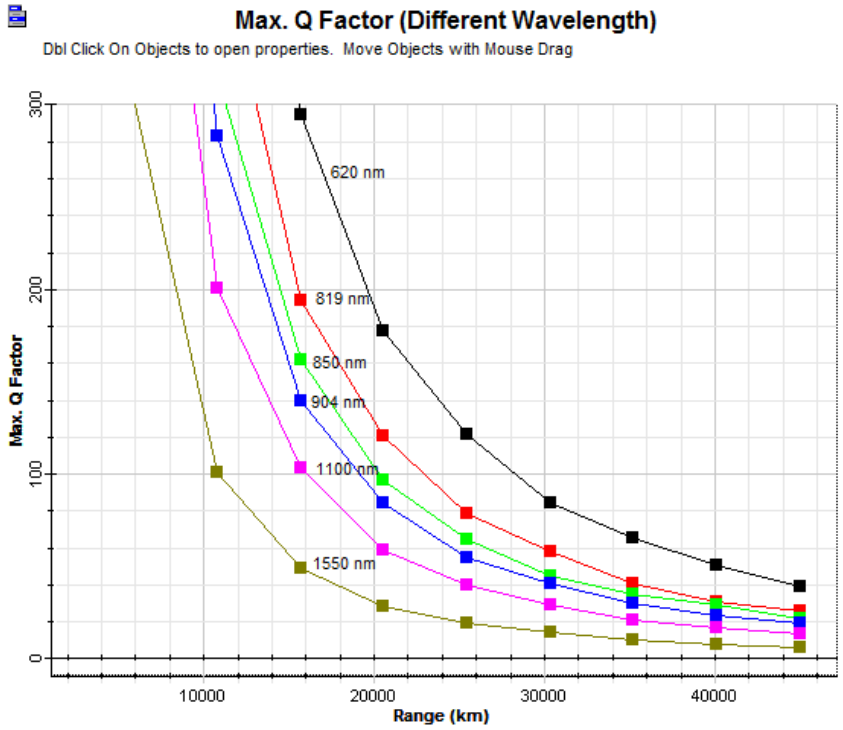

Figure 3.62 Q factor diagram of FSO links at various distances and various wavelengths.

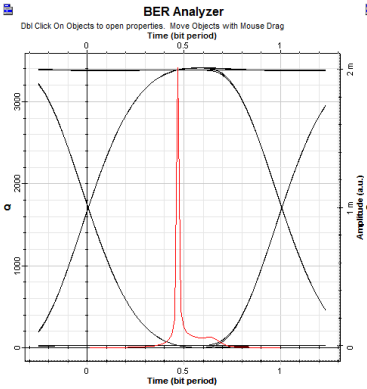

Figure 3.52 Eye diagram for 1000 km distance.

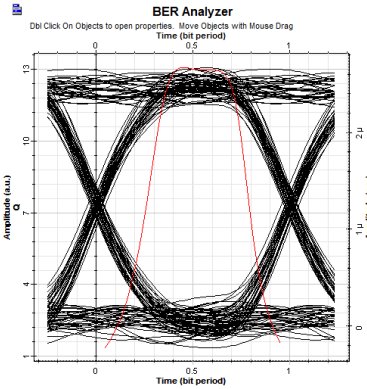

Figure 3.55 Eye diagram for 28667 km distance.

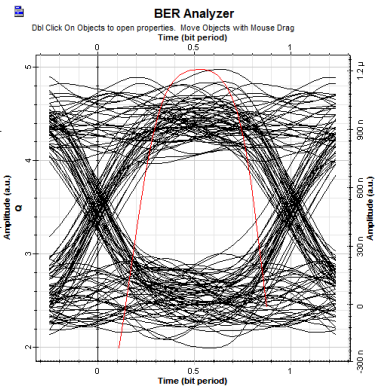

Figure 3.57 Eye diagram for 47111 km distance.

Telescope diameter is another important parameter in FSO. Geometrical gain can be expressed by:

$$G_T \approx (\frac{\pi D_T}{\lambda})^2 \quad \textbf{(2.15)}$$

D_T is the transmitter telescope diameter. Similarly, the receiver telescope gain that can be expressed by:

$$G_R \approx (\frac{\pi D_R}{\lambda})^2 \quad \textbf{(2.16)}$$

D_R is the receiver telescope diameter.

As can be seen in figures below, when the telescope diameter increases, link quality is also increases.

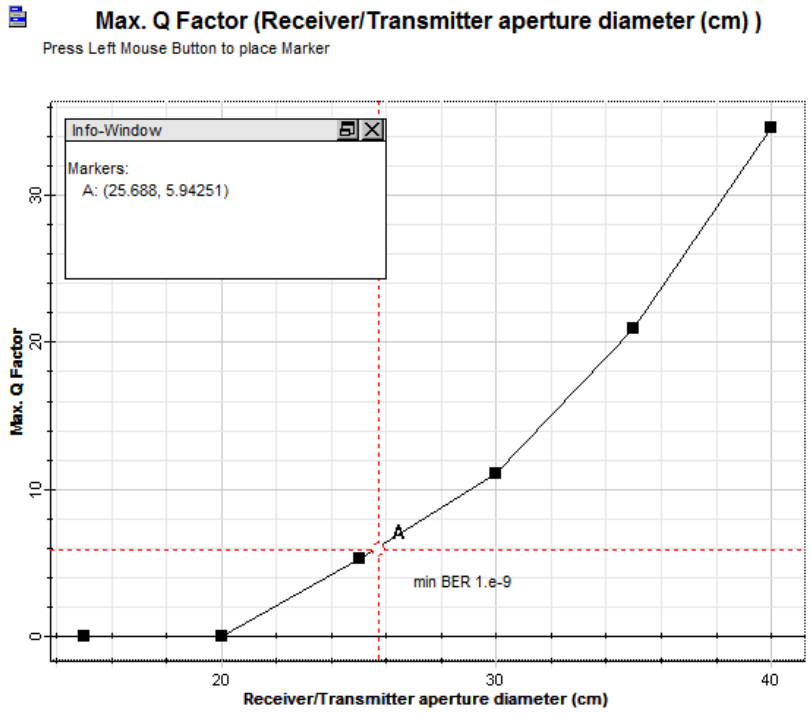

Figure 3.64 Q factor versus telescope diameter diagram at 850 nm wavelength.

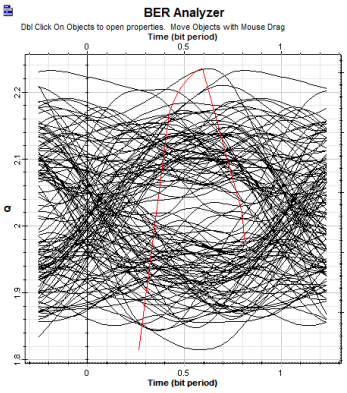

Figure 3.66 Eye diagram for 20 cm telescope.

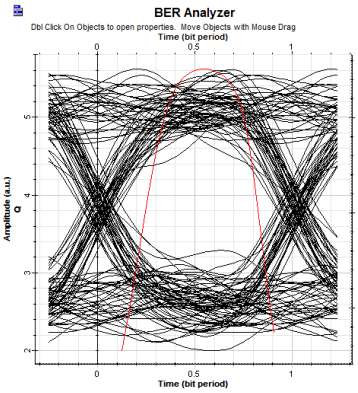

Figure 3.67 Eye diagram for 25 cm telescope.

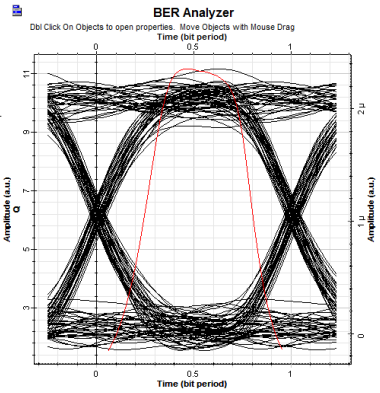

Figure 3.68 Eye diagram for 30 cm telescope.

Receiver telescope diameter is an important parameter in order to gather sufficient number of photons to achieve desired BER. As can be seen in figure below, increasing the telescope diameter causes increase in received power.

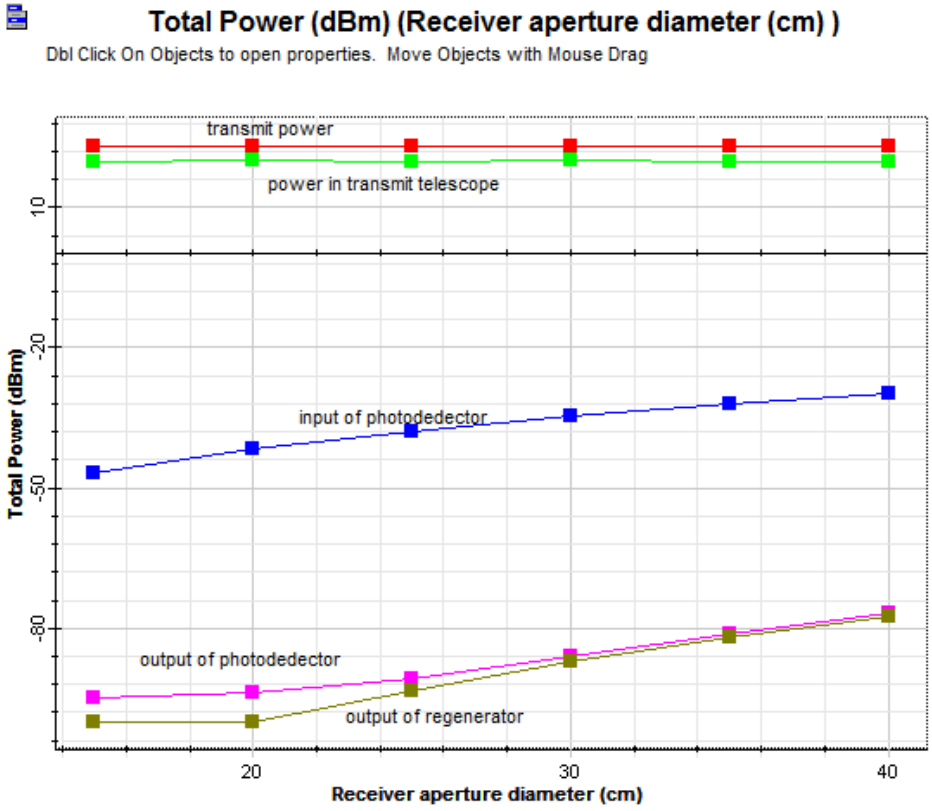

Figure 3.71 Received power for respective telescope diameter at 45.000 km distance and transmit power of 23 dBm.

It’s concluded from the figure below that; bigger telescope should be used for long distances to achieve intended BER value.

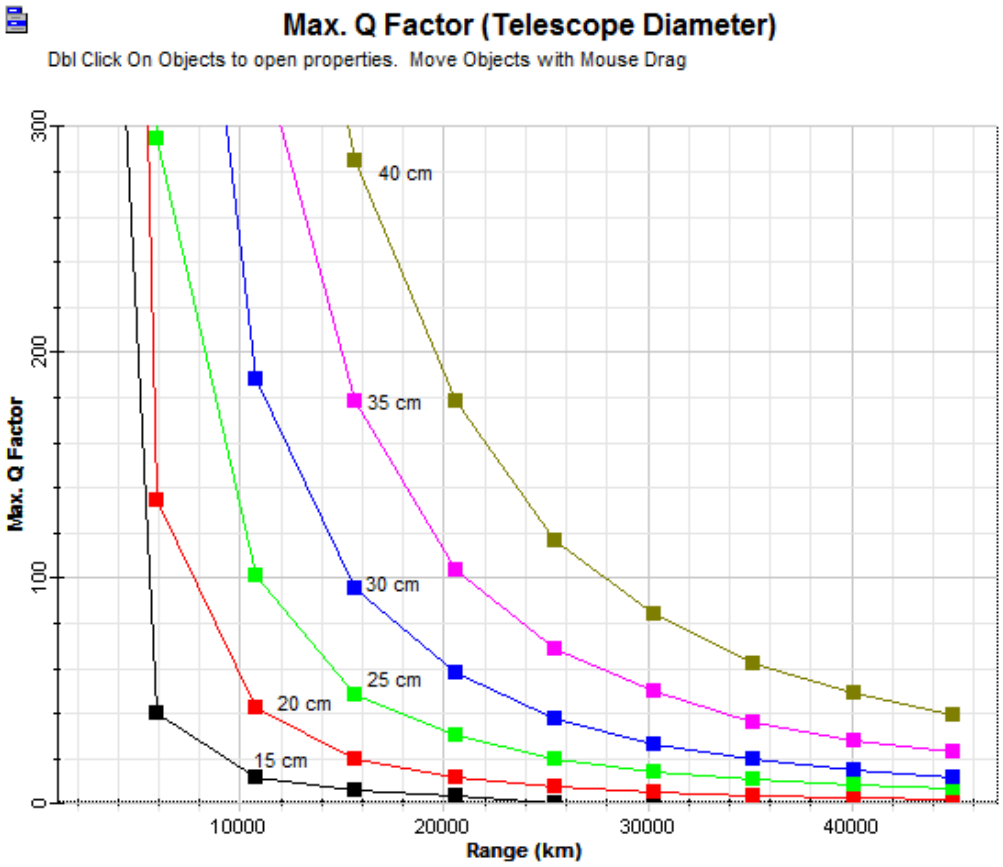

Figure 3.73 Relationship between Q factor, range and telescope diameter.

From figure below, it can be concluded that Q factor is inversely proportional to data rate. At the same distance signal with lower data rate produces higher Q-factor compared to signals of higher data rate. It can also be concluded that signal at lower data rate can travel further at the same input transmit power.

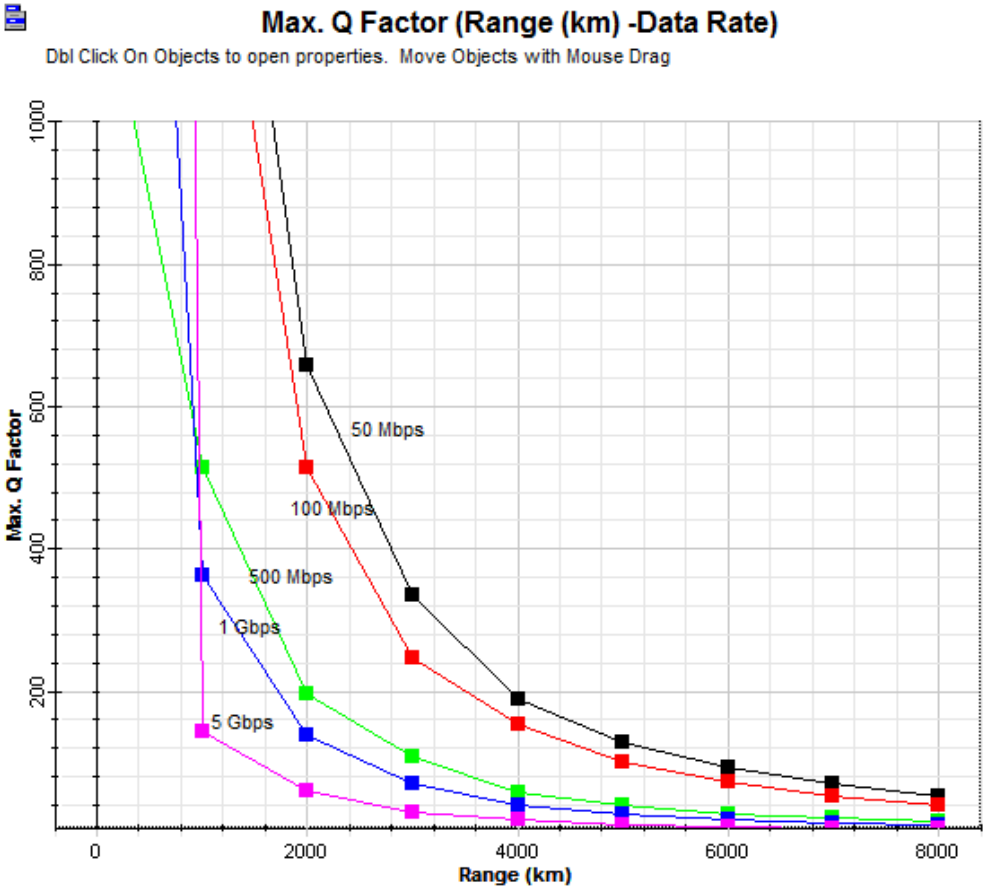

Figure 3.75 Maximum Q factor for variable distance at 850 nm wavelength for 50 Mbps, 100 Mbps, 500 Mbps, 1 Gbps, 5 Gbps data rate.

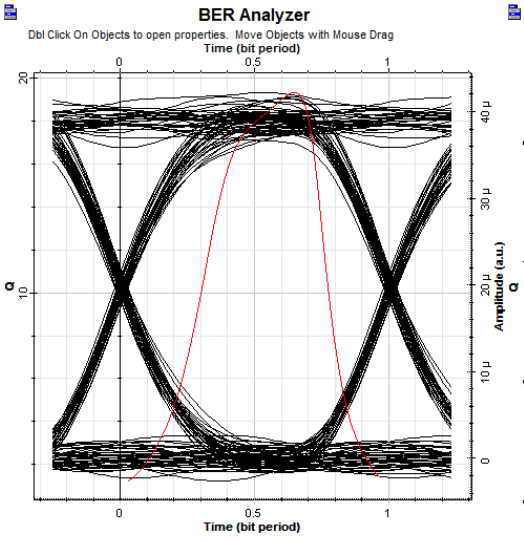

Figure 3.78 Eye diagram for 4000 km distance and 5 Gbps data rate.

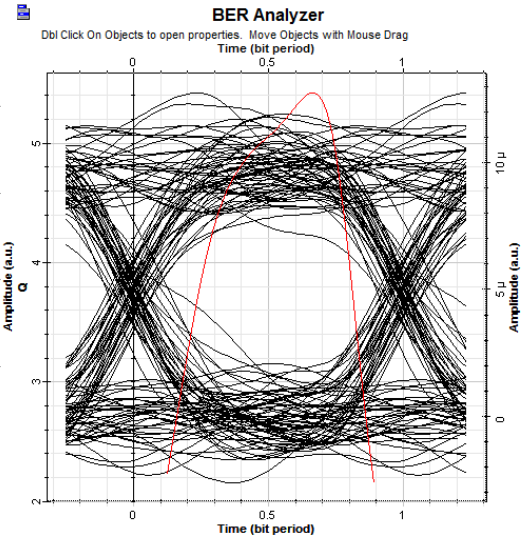

Figure 3.79 Eye diagram for 8000 km distance and 5 Gbps data rate.

As can be seen in figure below, it's concluded that, APD generates a higher Q-factor than the PIN at the same transmit power. This improvement in the signal quality is due to the APD internal gain. APD provides a gain in the generated photocurrent while PIN generates the most one electron-hole pair per photon. The gain of the APD, which results in higher Q factor, has made it more suitable for long haul inter-satellite communications.

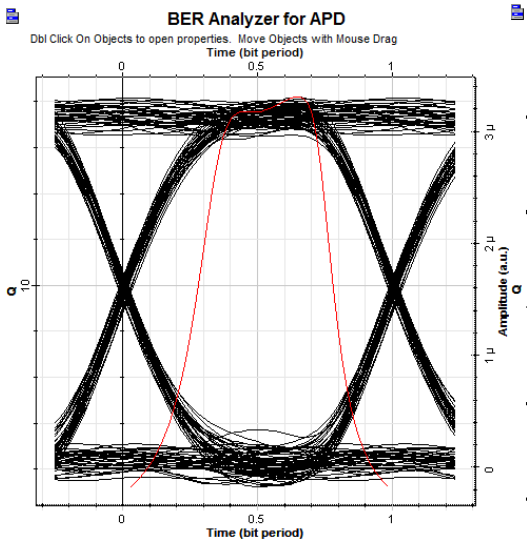

Figure 3.86 Eye diagram for APD type photodetector at 28 dBm transmit power.

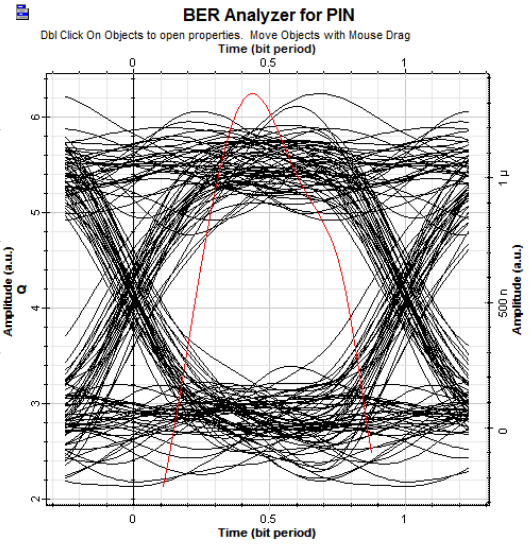

Figure 3.87 Eye diagram for PIN type photodetector at 28 dBm transmit power.

From the figures below, it can also be concluded that the inter-satellite laser communication system can perform better by having an EDFA to travel further.

If transmit power is in low level, EDFA can be used at the transmitter as booster amplifier to optically amplify input power. However, booster EDFA is not useful if the optical power at the input of EDFA is in high level.

Increasing the level of the signal power at the receiver, improving the performance of a APD type photodiode direct detection receiver and decreasing the losses effects, EDFA can be used as preamplifier at the receiver for long distance and high data rate inter- satellite laser communications.

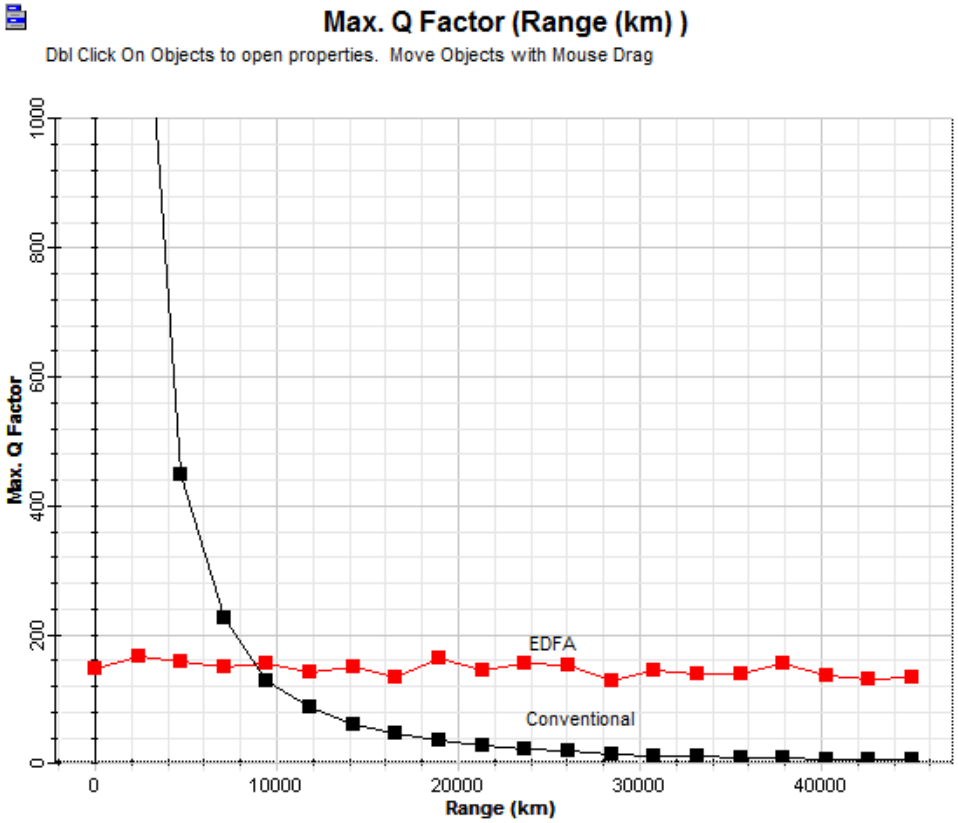

Figure 3.98 Range versus Q factor diagram for conventional and EDFA system.

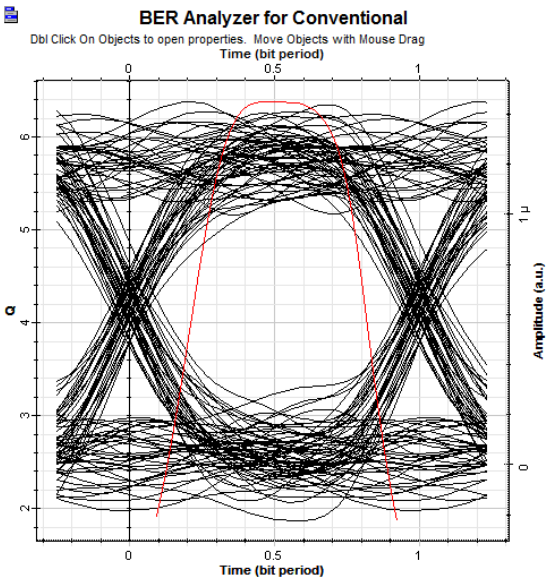

Figure 3.91 Eye diagram for conventional system.

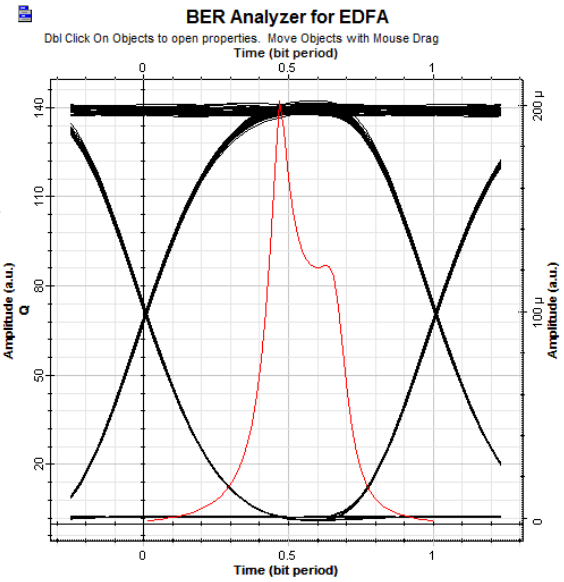

Figure 3.92 Eye diagram for EDFA system.

The following topics are recommended for the inter-satellite laser communication system improvements;

- Analyzing the different types of modulation's effect on link quality,
- Pointing, Acquisition, and Tracking Systems analysis for Free-Space Optical Communication Links.

REFERENCES

[1] Sun, Z., *Satellite Networking - Principles and Protocols*, John Wiley & Sons, UK, 2005.

[2] Chan, S., *Architectures of the space based information network with shared on orbir processing*, Thesis (PhD), Massachusetts Institute of Technology, 2005.

[3] Hashim, A. H., & Mahad, F. D., *Modeling and Performance Study of InterSatellite Optical Wireless Communication System*, 1st International Conference On Photonics, 5-7 July 2010 Malaysia: IEEE, ICP2010-64, 1-4, 2010.

[4] Araki, K. & Suziki, Y., *Inter-Satellite Link by Lightwave*, Page 221-224, Microwave Photonics 1996 MWP '96 Technical Digest 1996 Internatonal Topical Meeting 5-5 Dec. 1996 Japan, USA: WE4-2, 221-224, 1996.

[5] Frenzel, L., *Understanding Solutions For The Crowded Electromagnetic Frequency Spectrum* [online], http:// electronicdesign.com /communications/ understanding-solutions-crowded-helectromagnetic-frequency-spectrum, [Viziting Date : 10 January 2014].

[6] Agraval, G. P., *Fiber-Optic Communication System*, John Wiley & Sons, UK, 2002.

[7] Vishal Sharma, & Kaur, Amandeep, *Optimization of Inter-satellite Link (ISL) in Hybrid OFDM-IsOWC Transmission System*, Proc. of Int. Conf. on Advances in Communication Network and Computing 2013, 22- 23 Feb 2013 India: ACEEE, 25-28, 2013.

[8] Riebeek, Holli, *Catalog of Earth Satellite Orbit* [online], http://earthobservatory.nasa.gov/Features/OrbitsCatalog/page1.php, [Visiting Date : 10 January 2014].

[9] Maral, Gerard & Bausquet Michel, *Satellite Communications Systems, Systems, Techniques and Technology*, John Wiley & Sons, UK, 2009.

[10] Baister, G. & Lewis, J., *Applications for optical free space links in inter-satellite and intra-satellite communications*, Optical Free Space Communication Links, IEE Colloquium on, 19 Feb 1996 UK, London: IEE, 9/1-9/6,1996

[11] Sánchez, J.D. & Arturo, A., *Trends of the Optical Wireless Communications*, intech, USA, 2011

[12] John Wilson, J. F. B. Hawkes, *Optoelectronics: an introduction*, Prentice Hall, Europe, 1998

[13] Akbulut, A., P*roject Design for Ground to Satellite two-way Link Using Laser*, Thesis (Ph.D), Ankara University,2006.

[14] Marshalek, R. G., *Prime power, and volume estimates for reliable optical intersatellite link payloads*, Comsat Technical Review, Volume 18 Number 2, 191-239, 1988.

[15] Mulholland, J.E. & Cadogan, S.A., *Intersatellite Laser Crosslinks*, IEEE Transactions On Aerospace And Electronic Systems Vol. 32, No. 3 July 1996, 1011-1020, 1996.

[16] Henniger, H. & Wilfert, O., *An Introduction To Free-Space Optical Communications*, 2011 International Conference on Devices and Communications (ICDeCom), 24-25 Feb. 2011 India, USA: IEEE, 203-212, 2011

[17] Singh, M.K. & Kapoor, V., *Bit Error Rate Analysis of Free Space Optical Link using Different Optical Windows*, 2011 International Conference on Devices and Communications (ICDeCom), 24-25 Feb. 2011 India, USA: IEEE, 978-1-4244-9190-2/11, 2011

[18] Singh, M.K. & Kapoor, V., *Power Budget Performances of Free Space Optical Link using Direct Line of Sight Propagation,* Special Issue of International Journal of Computer Applications (0975 – 8887) on Electronics, Information and Communication Engineering - ICEICE No.3, Dec 2011, USA, 12-14, 2011

[19] Sasaki, T. & Toyoshima, M., *Digital Coherent Optical Receiver for Satellite Laser Communication*, 2011 International Conference on Space Optical Systems and Applications May 11-13 2011 California, USA: IEEE, 245-247, 2011

[20] Özek, F., *Optoelektronik*, AÜFF, Türkiye, 1995.

[21] Hranilovic, S., *Wireless Optical Communication Systems*, Springer Science Business Media, Inc., USA, 2005.

[22] Oorschot, M. & Vanstone, S., *Handbook of Applied Cryptography*, CRC Press, USA, 2001

[23] Flannery, W. H., & , Teukolsky, B. P., *Numerical Recipes in C*, Cambridge University Press, UK, 1991.

[24] Carlson, A. B., *Communication System*, McGraw-Hill, Singapore, 1986.

[25] Kartalopoulos, S., *Introduction to DWDM Technology: Data in a Rainbow*, Wiley-IEEE Press, UK, 2000.

[26] Meno, P.V., & Detemple, T., *Rate-Equation-Based Laser Models with a Single Solution Regime*, Journal of Lightwave Tech. Vol. 15 No 4; 717-730, 1997.

[27] Hansen, K., Schlachetzki, A., *Transferred-electron Device as a Large-Signal Laser Driver*, IEEE J. Quantum Electron Vol. 27 No 3; 423-427, 1991.

[28] Optical Society of America, (Author), Michael Bass (Editor), *Handbook of Optics Volume II Devices Measurements and Properties,* Mcgraw-Hill Inc, US, 1995

[29] Polishuk, A. & Arnon, S., *Optimization of A Laser Satellite Communication System with An Optical Preamplifier*, Journal Optical Society of America Vol 21, No 7, 1307-1315, 2004.

[30] Ramirez-Iniguez, R., Idrus, S.M. & Sun, Z., *Optical Wireless Communication: IR for Wireless Connectivity*, CRC Press, USA, 2008.

[31] Mazalkova, M., *The Laser Satellites Communications and Laser Noises*, WSEAS Transactions On Communications Issue 8 Volume 7, 872-881, 2008.

[32] Leeb, W., *Space Laser Communications: Systems, Technologies, and Applications*, The Review of Laser Engineering, vol. 28 2000 no 12; 804-808, 2000.

[33] Noor, N. & Naji, A., *Performance Analysis of a Free Space Optics Link With Multiple Transmitters/Receivers*, IIUM Engineering Journal Vol 13 No 1, 49-58, 2012

[34] Mazálková, M., *The premises of laser inter-satellite communication system*, ELECTRO'06 Proceedings of the 4th WSEAS Int. Conference on Electromagnetics Wireless and Optical Communications November 20-22 2006, Venice Italy, USA: ACM, 32-36, 2006

[35] Zhou, L. & Wen, C., *Optical system in laser inter-satellites communication*, International Conference on Computer Science and Information Technology 2008 Chine, USA: IEEE, 903-906, 2008

[36] Mazálková, M., *The system transfering between laser-satellites*, WSEAS Transactions on Communications Issue 3 Volume 7 ISSN: 1109-2742, 152-159, 2008

[37] Arnon, S. & Rotman, S.R., *Bandwidth Maximization for Satellite Laser Communication*, IEEE Transactions on Aerospace and Electronic Systems Vol. 35 No. 2, 675-682, 1999.

[38] Zhao, Z & Liao, R, *Impacts of Laser Beam Diverging Angle on Free-Space Optical Communications*, Aerospace Conference 2011 IEEE 5-12 March 2011 USA, USA: IEEE, 1 – 10, 2011

[39] Karki, J., *Active Low-Pass Filter Design*, Application Report SLOA049B -, Texas instruments, 2002

[40] Kumar A., &.Verma, A.K., *Compact Low Pass Bessel Filter Using Microstrip DGS Structure*, Proceedings of Asia-Pacific Microwave Conference 2010 Japan, USA: IEICE, 1189-1192, 2010

[41] Susan, D. & Jayalalitha, S., *Bessel Filters Using Simulated Inductor*, 2011 International Conference on Recent Advancements in Electrical, Electronics and Control Engineering 2011 India, USA: IEEE, 268-271, 2011

[42] Foster, E.J., *Active Low Pass Filter Design*, IEEE Transaction on Audio Vol. 13 No. 5, 104-111, 1965.

[43] Paarmann, L.D., *Design and Analysis of Analog Filters a Signal Processing Perspective*, Kluwer Academic Publishers, US, 2001

[44] Gumaste, A. & Antony, T., *DWDM Network Designs and Engineering Solutions*, Ciscopress, USA, 2002.

[45] Elbert, R.L., *The Satellite Communication Applications Handbook*, Artech House Publishers, London, 1997.

[46] F. Heine, H. Kämpfner, R. Lange, *Optical Inter-Satellite Communication Operational*, MILCOM 2010 Military Communications Conference Oct 31-Nov 3 2010 California USA, USA: IEEE, 1583-1587, 2010

[47] Behera, D. & Varshney, S., *Eye Diagram Basics: Reading and applying eye diagrams*, Freescale Semiconductor, USA, 2011

[48] Gary Breed, *Analyzing Signals Using the Eye Diagram*, November 2005 High Frequency Electronics, 2005 Summit Technical Media, 50-53, 2005

[49] Zoran Sodnik, Z. & Furch, B., *Optical Intersatellite Communication*, IEEE Journal Of Selected Topics In Quantum Electronics, Vol. 16, No. 5, page1051-1057, 2010.

[50] Song, D.Y. & Suk Hurh, Y.K., *4 X 10 Gb/s Terrestrial Optical Free Space Transmission Over 1.2 Km Using an EDFA Preamplifier with 100 GHz Channel Spacing*, Optics Express, Vol. 7 Issue 8, 280-284,2000.

BIOGRAPHY

Mustafa PANCAR was born in Ankara, in 1975. He received the B.Sc. degree in Electronics Engineering from Ankara University and commissioned as a second lieutenant in the Turkish Air Force, in 1999. He is currently a chief of system support section at the Turkish General Staff SATCOM Center in Ankara. Prior positions were held at the Turkish General Staff SATCOM Center as a project officer, chief of Ku-Band Satellite Communication System, and chief of X-Band Satellite Communication System, respectively. He worked in various satellite projects and received award for the contribution to Processed Extremely High Frequency (EHF) Transponder Project from Bilkent University Space Technologies Research Center (BilUzay) & ASELSAN, in 2008.